Chang Liu

Stimuli-Responsive Porous Nanomaterials for Controlled Drug Delivery and Gene Therapy

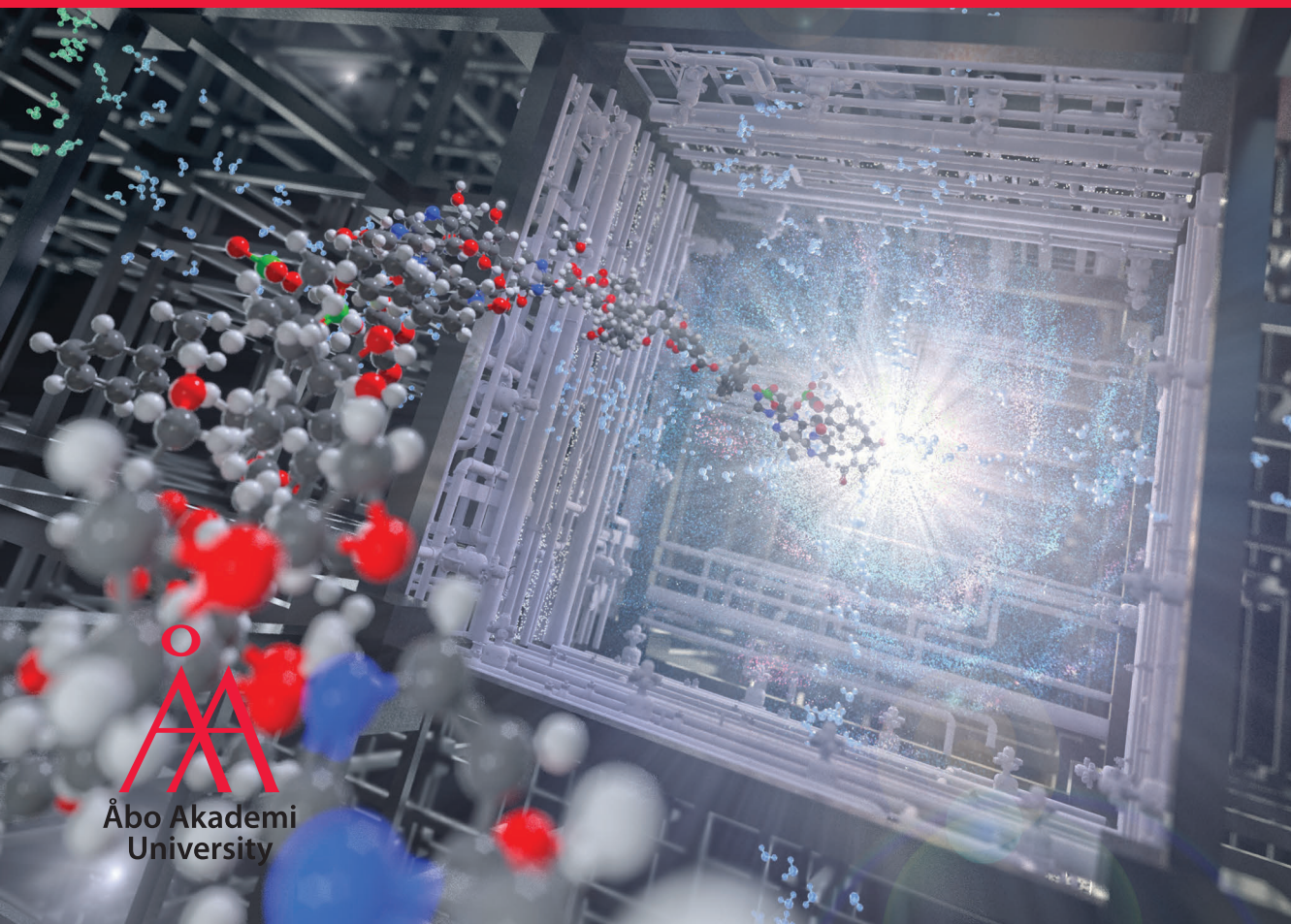

Åbo Akademi University

Chang Liu

Born 1990, Shandong, China

Previous Studies and Degrees

Master of Science in Inorganic Chemistry, Tongji University, 2016

Bachelor of Science in Applied Chemistry, Shandong Agricultural University, 2013

Stimuli-Responsive Porous Nanomaterials for Controlled Drug Delivery and Gene Therapy

Chang Liu

Pharmaceutical Sciences Laboratory
Faculty of Science and Engineering
Åbo Akademi University
Åbo, Finland, 2022

Supervisors:

Associate Professor Hongbo Zhang
Pharmaceutical Sciences Laboratory
Åbo Akademi University
Finland

Turku Bioscience Centre
University of Turku and Åbo Akademi University
Finland

Professor Jessica Rosenholm
Pharmaceutical Sciences Laboratory
Åbo Akademi University
Finland

Reviewers:

Senior Lecturer Ciro Chiappini
Faculty of Dentistry, Oral & Craniofacial Sciences
King's College London
United Kingdom

Tenured Associate Professor Jixi Zhang
College of Bioengineering
Chongqing University
China

Opponent:

Senior Lecturer Ciro Chiappini
Faculty of Dentistry, Oral & Craniofacial Sciences
King's College London
United Kingdom

ISBN 978-952-12-4144-4 (printed)
ISBN 978-952-12-4145-1 (electronic)
Painosalama Oy, Turku, Finland 2022
Cover: Functionalization Chemistry of Porous Materials (*Copyright 2020, John Wiley and Sons*)

To Xiaoyu
To my family

Abstract

Stimuli-responsive drug delivery systems have become increasingly fascinating and vital in nanomedicine because they can change the drugs pharmacokinetics, significantly improve the drugs utilization efficiency, provide on-demand local drug delivery, and reduce toxic side effects. As a typical representative, porous nanomaterials have unique physicochemical properties, such as rich pore structure, low density, high surface area, and tunable porous size. They show great promise not only in industrial catalysis, gas adsorption, linear optics, and electromagnetic materials, but also in stimuli-responsive delivery system for the diagnosis and treatment of diseases. This thesis mainly focuses on some important scientific issues such as seeking new release and targeting mechanisms, broadening their biomedical applications, developing multifunctional drug delivery systems, exploring biomimetic encapsulation strategies, and further improving the loading diversity of nanocarriers. Here, we have designed different drug/biomolecule delivery systems based on porous nanomaterials, which are listed as follows:

First, mesoporous silica nanoparticle (MSNs)-based drug delivery system with *in vivo* endothelial targeting was prepared for the inhibition of antibody-mediated rejection after allograft kidney transplantation. The photothermal sensitive copper sulphide (CuS) nanoparticles were encapsulated in biocompatible MSNs, followed by multi-step surface engineering to form the anti-inflammatory drug-loaded theragnostic nanoparticles. Non-invasive targeting imaging, and near-infrared (NIR) triggered photothermal responsive drug release investigations demonstrated this system can reduce systemic inflammation, downregulate innate immune responses and promote recovery of the injured endothelium. Intracellular delivery of CRISPR/Cas9 plasmids via MSNs was subsequently explored for homology-directed repair through gene editing. By microfluidic-assisted electrostatic nanoprecipitation, polymer was coated onto plasmid-loaded MSNs to prevent biomolecule denaturation by EcoRV restriction enzymes as well as premature release. The pH-responsive breakdown of the polymer enabled controlled intracellular release of the plasmid and knock-in of the paxillin gene sequence. However, due to the low encapsulation efficiency and complex assembly process, there is a need to develop new porous vectors that can be easily prepared, have better drug and biomolecular loading capacity, and have better biocompatibility and biodegradability.

Therefore, metal-organic frameworks (MOFs) with good biocompatibility are used for drug delivery. By post-synthetic modification with disulfide anhydride and folic acid, MOFs with redox-responsive and tumor-targeting properties were constructed as a dual-drug carrier, exhibiting synergistic enhanced anticancer effects. However, pre-prepared MOFs have the same problems as MSNs in delivering biomolecules, and the encapsulation of MOFs with postsynthetic modification provides limited protection for biomolecules. Biomimetic mineralisation technique, which has been extensively studied for

inorganic systems, was applied to the synthesis of MOFs to wrap and protect biomolecules, such as the encapsulation of CRISPR-Cas9 plasmids into MOFs, where controlled nanostructures were synthesised in situ through a biomolecule-mediated strategy. The structure-function relationship studies showed that the nanostructures of the MOF coatings greatly influence the biological properties of the contained biomolecules through different embedding structures. With the help of the superior ZIF-8 vector, the GFP-tagged paxillin genomic sequence was successfully knocked in a cancer cell line with high transfection potency. In addition, microfluidic-assisted biomineralization strategy for MOFs was utilised for efficient delivery and remote regulation of CRISPR-Cas9 ribonucleic acid protein (RNP)-based gene editing. By tuning different microfluidic parameters, well-defined and comparable RNP-encapsulated nanocarriers were obtained with high delivery efficiency, significant protection and NIR-responsive release, endosomal escape and precise gene knock-down capabilities.

Keywords

drug delivery, mesoporous silica nanoparticles, immune inhibition, stimuli-responsive, photothermal conversion, metal-organic frameworks, tumor targeting, biomimetic mineralization, microfluidic

Sammanfattning

Stimuli-responsiva system för läkemedelstillförsel har blivit alltmer fascinerande och viktiga inom nanomedicin eftersom de kan förändra läkemedlens farmakokinetik, avsevärt förbättra läkemedelsutnyttjandet, tillhandahålla lokal läkemedelstillförsel på begäran och minska toxiska biverkningar. Som en typisk representant har porösa nanomaterial unika fysikalisk-kemiska egenskaper, t.ex. rik porstruktur, låg densitet, hög yta och justerbar porstorlek. De är mycket lovande inte bara inom industriell katalys, gasadsorption, linjär optik och elektromagnetiska material, utan även inom stimulansresponsiva leveranssystem för diagnos och behandling av sjukdomar. Denna avhandling fokuserar huvudsakligen på några viktiga vetenskapliga frågor, t.ex. att söka nya frisättnings- och målinriktningsmekanismer, bredda deras biomedicinska tillämpningar, utveckla multifunktionella system för läkemedelstillförsel, utforska biomimetiska inkapslingsstrategier och ytterligare förbättra laddningsmångfalden hos nanodragare. Här har vi konstruerat olika system för att leverera läkemedel/biomolekyler baserade på porösa nanomaterial, som listas nedan:

För det första framställdes ett mesoporöst kiseldioxidnanopartikelsystem (MSN) baserat på läkemedelsleveranser med in vivo endotelmålsättning för att hämma antikroppsmedierad avstötning efter en njurtransplantation med allograft. De fototermiskt känsliga kopparsulfidnanopartiklarna (CuS) kapslades in i biokompatibla MSN, följt av en ytkonstruktion i flera steg för att bilda antiinflammatoriska nanopartiklar laddade med teragnostiska läkemedel. Undersökningar av icke-invasiv målbildsanalys och NIR-utlöst fototermisk responsiv läkemedelsfrisättning visade att detta system kan minska systemisk inflammation, nedreglera det medfödda immunförsvaret och främja återhämtning av skadat endotel. Intracellulär leverans av CRISPR/Cas9-plasmider via MSN:er undersöktes därefter för homologiskt riktad reparation genom genredigering. Genom elektrostatisk nanoprecipitering med hjälp av mikrofluidik har polymeren belagts på plasmidladdade MSN:er för att förhindra denaturering av biomolekylerna med hjälp av EcoRV-restriktionsenzymerna och för tidig frisättning. Den pH-responsiva nedbrytningen av polymeren möjliggjorde en kontrollerad intracellulär frisättning av plasmidet och knock-in av paxillin-gensekvensen. På grund av den låga inkapslingseffektiviteten och den komplexa monteringsprocessen finns det dock ett behov av att utveckla nya porösa vektorer som lätt kan framställas, som har bättre laddningskapacitet för läkemedel och biomolekyler och som har bättre biokompatibilitet och biologisk nedbrytbarhet.

Därför används metallorganiska ramverk (MOF) med god biokompatibilitet för läkemedelsleveranser. Genom postsyntetisk modifiering med disulfidanhydrid och folsyra konstruerades MOF:er med redoxresponsiva och tumörmålande egenskaper som en dubbel läkemedelsbärare som uppvisar

synergistiska förbättrade cancerbekämpande effekter. Förberedda MOF:er har dock samma problem som MSN:er när det gäller att leverera biomolekyler, och inkapsling av MOF:er med postsyntetisk modifiering ger ett begränsat skydd för biomolekyler. Den biomimetiska mineraliseringstekniken, som har studerats ingående för oorganiska system, tillämpades på syntesen av MOF:er för att omsluta och skydda biomolekyler, t.ex. inkapsling av CRISPR-Cas9-plasmider i MOF:er, där kontrollerade nanostrukturer syntetiserades in situ genom en biomolekylmedierad strategi. Studierna av struktur-funktionsförhållandet visade att MOF-beläggningarnas nanostrukturer i hög grad påverkar de biologiska egenskaperna hos de ingående biomolekylerna genom olika inbäddningsstrukturer. Med hjälp av den överlägsna ZIF-8-vektorn lyckades man framgångsrikt slå ut den GFP-märkta genomsekvensen av paxillin i en cancercelllinje med hög transfektionsförmåga. Dessutom utnyttjades en mikrofluidiskt assisterad biomineraliseringsstrategi för MOFs för effektiv leverans och fjärrreglering av CRISPR-Cas9 ribonukleinsyreprotein (RNP)-baserad genredigering. Genom att ställa in olika mikrofluidiska parametrar erhölls väldefinierade och jämförbara RNP-inkapslade nanodragare med hög leveranseffektivitet, betydande skydd och NIR-responsiv frisättning, endosomal flykt och exakta möjligheter att slå ner gener.

Nyckelord

läkemedelstillförsel, mesoporösa kiselnanopartiklar, immunhämning, stimulerande, fototermisk omvandling, metallorganiska ramar, tumörmålsättning, biomimetisk mineralisering, mikrofluidisk

TABLE OF CONTENTS

List of original publications

1. *In vivo* kidney allograft endothelial specific scavengers for on-site inflammation reduction under antibody-mediated rejection

Chang Liu, Pengpeng Yan, Xiaoyu Xu, Wenhui Zhou, Dhayakumar Rajan Prakash, Shuqi Wang, Junnian Zhou, Rending Wang, Hongfeng Huang, Jianghua Chen, Hongbo Zhang* and Jia Shen*. *Small* **2022**.

2. Effective delivery of the CRISPR-Cas9 system enabled by functionalized mesoporous silica nanoparticles for GFP-Tagged paxillin knock-in

Xiaoyu Xu, Oliver Koivisto, **Chang Liu**, Junnian Zhou, Mitro Miihkinen, Guillaume Jacquemet, Daqi Wang, Jessica M. Rosenholm*, Yilai Shu*, and Hongbo Zhang*. *Advanced Therapeutics* **2021**; 4 (1): 2000072.

3. Redox-responsive tumor targeted dual-drug loaded biocompatible metal–organic frameworks nanoparticles for enhancing anticancer effects

Chang Liu, Xiaoyu Xu, Junnian Zhou, Jiaqi Yan, Dongqing Wang and Hongbo Zhang*. *BMC Materials* **2020**; 2 (1): 1-11.

4. Improving the knock-in efficiency of MOF-encapsulated CRISPR-Cas9 system through controllable embedding structures

Chang Liu, Xiaoyu Xu, Oliver Koivisto, Wenhui Zhou, Jessica M. Rosenholm and Hongbo Zhang*. *Nanoscale* **2021**; 13: 16525-16532

5. Microfluidic-assisted biomineralization of CRISPR-Cas9 in near-infrared responsive metal-organic frameworks for programmable gene-editing (manuscript)

Xiaoyu Xu, **Chang Liu**, Junnian Zhou, Oliver Koivisto, Yilai Shu* and Hongbo Zhang*.

This work was carried out at the Pharmaceutical Sciences Laboratory during the years of 2018-2021 under the supervision of Associate Professor Hongbo Zhang and Professor Jessica Rosenholm at Åbo Akademi University. Part of the work was carried out at First Affiliate Hospital, Zhejiang University, Zhejiang, China.

Contribution of the author

1. In PAPER I, the author was responsible for all the sample preparations, surface functionalization, characterizations and writing of the first draft. The author performed *in vitro* and *in vivo* experiments and analyzed the data. P. Yan contributed to the *in vivo* biodistribution and histology experiments. D. Prakash helped in the visualization. X. Xu and W. Zhou performed the data analysis.

2. In PAPER II, the author prepared microfluidic chips and optimized the parameters of polymer coating deposition in the drug encapsulation experiments. The author contributed to material characterization and draft writing. X. Xu was responsible for the synthesis and modification of samples, characterization and the first draft writing. O. Koivisto performed *in vitro* experiments and data analysis.

3. In PAPER III, the author was responsible for all the sample preparations, surface modifications, characterization and writing of the first draft. The author evaluated the anticancer effects of samples in different cell lines. X. Xu and J. Zhou contributed to the *in vitro* experiments, cell imaging and draft writing.

4. In PAPER IV, the author was responsible for all the sample preparations, characterization and writing of the first draft. X. Xu performed *in vitro* experiments, data analysis and contributed to the writing of the draft. O. Koivisto and W. Zhou performed the plasmids amplification and purity identification. W. Zhou performed western blot to detect the gene editing efficiency.

5. In PAPER V, the author performed synthesis and characterization of some samples and data analysis. The author contributed to the draft writing. X. Xu was responsible for the sample preparations, surface modifications, and their characterizations and writing of the first draft.

Supplementary publications

1. Encapsulated biomolecules for intracellular delivery

Hongbo Zhang, **Chang Liu,** Xiaoyu Xu. Finnish Patent Application No. 20215856, *Finnish Patent and Registration Office* **2021**.

2. Encapsulated bioactive mitochondria

Hongbo Zhang, Junian Zhou, **Chang Liu,** Yong Guo. Finnish Patent Application No. 20215857, *Finnish Patent and Registration Office* **2021**.

3. Helper T Cell ($CD4^+$) Targeted Nanorobotics Mediated the Precise Suppression of Allogeneic Humoral Immunity

Jia Shen, **Chang Liu**, Pengpeng Yan, Hongfeng Huang, Meifang Wang, Luying Guo, Shuaihui Liu, Jianghua Chen, Rending Wang, Hongbo Zhang*. *Proceedings of the National Academy of Sciences of the United States of America* **2022**; Submitted manuscript. (Co-first author)

4. Metal-organic framework (MOF)-based biomaterials in bone tissue engineering

Chang Liu, Xiaoyu Xu, Wenguo Cui, Hongbo Zhang*. *Engineered Regeneration* **2021**; 2: 105-108.

5. Nanotechnology-based delivery of CRISPR-Cas9 for cancer treatment

Xiaoyu Xu, **Chang Liu**, Yonghui Wang, Oliver Koivisto, Junnian Zhou, Hongbo Zhang*. *Advanced Drug Delivery Reviews* **2021;** 176: 113891. (Co-first author)

6. Mineralization of pH-sensitive doxorubicin prodrug in ZIF-8 to enable targeted delivery to solid tumors

Jiaqi Yan, **Chang Liu**, Qiwei Wu, Junnian Zhou, Xiaoyu Xu, Lirong Zhang, Dongqing Wang*, Fan Yang*, and Hongbo Zhang*. *Analytical chemistry* **2020**; 92(16): 11453-11461. (Co-first author)

7. Delivery of protein kinase A by CRISPRMAX and its effects on breast cancer stem-like properties

Jun-Nian Zhou, Tzu-Chen Rautio, **Chang Liu**, Xiao-Yu Xu, Dong-Qing Wang, Yong Guo*, John Eriksson*, and Hongbo Zhang*. *Pharmaceutics* **2021;** 13(1): 11.

8. Fabrication of a pH/redox-triggered mesoporous silica-based nanoparticle with microfluidics for anticancer drugs doxorubicin and paclitaxel codelivery

Yan, Jiaqi, Xiaoyu Xu, Junnian Zhou, **Chang Liu**, Lirong Zhang, Dongqing Wang, Fan Yang*, and Hongbo Zhang*. *ACS Applied Bio Materials* **2020;** 3(2): 1216-1225.

9. Hybrid Nanoparticles for Haloperidol Encapsulation: Quid Est Optimum?

Sergey K. Filippov*, Ramil R. Khusnutdinov, Wali Inham, **Chang Liu**, Christopher J. Garvey, Dmitry O. Nikitin, Irina I. Semina, Shamil F. Nasibullin, Vitaliy V. Khutoryanskiy, Hongbo Zhang, Rouslan I. Moustafine*. *Polymers* **2021**; 13: 4189.

Abbreviations

2-MIM	2-methylimidazole
5-FU	5-fluorouracil
ABMR	antibody-mediated rejection
APTEOS	(3-aminopropyl)triethoxysilane
ATP	adenosine triphosphate
AuNRs	gold nanopaticles
C4d	complement component 4d
Cas9	CRISPR-associated protein 9
CCM	curcumin
CdS	cadmium sulfide
CLSM	confocal laser scanning microscopy
COVID-19	coronavirus disease 2019
CRISPR	clustered regularly interspaced short palindromic repeats
CTAC	cetyltrimethylammonium chloride
CuS	copper sulfide nanoparticles
Cy5.5	Sulfo-Cyanine5.5 NHS ester
DAPI	4′,6-diamidino-2-phenylindole
DCA	dichloroacetic acid
DHA	dihydroartemisinin
DLS	dynamic light scattering
DMEM	Dulbecco's modified eagle's medium
DMF	N, N'-dimethylformamide
DOX	Doxorubicin
DSBs	DNA double-strand breaks
DTDPA	3,3′-dithiodipropionic acid anhydride
DTT	dithiothreitol
FA	folic acid
FBS	fetal bovine serum
FDA	U.S. Food and Drug Administration
Fe_3O_4	iron tetroxide
FT-IR	Fourier-transform infrared spectroscopy
GFP	green fluorescent protein
GOx	glucose oxidase
GSH	glutathione
GSH-Px	glutathione peroxidase
GST	glutathione S-transferase
H_2O_2	hydrogen peroxide
HDR	homologous directed repair
LCST	low critical solution temperature
ME	mercaptoethanol
MFI	mean fluorescent intensity
MOF	metal organic framework
MP	Methylprednisolone

MSN	mesoporous silica nanoparticle
NADPH	nicotinamide adenine dinucleotide phosphate
NHEJ	non-homologous end joining
NMR	nuclear magnetic resonance spectroscopy
KT	kidney transplantation
P1	GFP-Cas9-paxillin_gRNA
P2	AICSDP-1: PXN-EGFP
PAS	Periodic acid-Schiff
PBMC	peripheral blood mononuclear cells
PBS	phosphate-buffered saline
PCC	pearson correlation coefficient
PDA	polydopamine
PEG	polyethylene glycol
PLA	polylactic acid
PLGA	poly(lactic-co-glycolic acid)
PNcM	poly(N-isopropylacrylamide-co-methacrylic acid)
PNIPAM	poly(N-isopropylacrylamide)
PSM	post-synthetic modification
PXRD	powder X-ray diffraction
ROS	reactive oxygen species
RNS	reactive nitrogen species
sgRNA	single guide RNA
SOD	superoxide dismutase
TEM	transmission electron microscopy
TEOS	tetraethoxysilane
TRX	thioredoxin
WST-1	cell proliferation assay Roche diagnostics reagent
ZIF	zeolitic imidazolate framework

1. Introduction

With the rapid development of intersection of nanotechnology and biomedical science, nanomedicine has emerged. In recent years, nanomedicine has made great research progress in the diagnosis and treatment of various diseases, especially cancer. Nanomaterials have shown great application prospects in the construction of novel disease treatment systems due to their unique advantages of many multifunctional nanomaterials with good biocompatibility. For example, in oncology treatment, the high toxic side effects of chemotherapeutic drugs caused by non-targeted distribution throughout the body have been a critical problem to be solved. Compared with the non-targeted feature of most conventional anticancer drugs, this new nano-drug delivery system, which is built by loading small molecule drugs into nanomaterials, can preferentially accumulate in the tumor area through the high permeability and retention (EPR) effect. At the same time, the nano-drug delivery system can overcome the inherent defects of small molecule drugs and has the advantages of improving the solubility of insoluble drugs, increasing the drug utilization, reducing the toxic side effects during chemotherapeutic drug transport, prolonging their blood circulation time, and enhancing their targeting to tumor cells, which will greatly promote the application of chemotherapeutic drugs in tumor treatment.

In recent years, delivery carriers based on porous silica nanomaterials (MSN) have the advantages of high drug loading efficiency, adjustable structure, easy surface modification and good biocompatibility, which have been used in the loading of anticancer drugs, targeted delivery of bioimaging and tumor therapy. However, silica nanomaterials still have the problems of poor stability and difficult degradation. To better solve the above problems, we introduced another class of porous material metal-organic frameworks (MOFs) to replace silica to carry out the above research work. MOFs are crystalline materials with a periodic network structure assembled by the coordination of metal ions or clusters as nodes and organic ligands as linking units, and they have been a key research topic in the field of new materials in recent years. MOFs materials are easy to be synthesized and functionalized, and a variety of MOFs-based stimuli-responsive drug carriers have been developed, which are constructed mainly by embedding responsive components in MOFs structures or modifying responsive molecules on the surface of MOFs materials, and MOFs themselves can also be used as stimuli-responsive drug carriers. The design of stimuli-responsive nano-drug carriers can achieve targeted and efficient drug delivery while reducing the toxic side effects on healthy tissues, and realize efficient tumor therapy by combining the characteristics of tumor microenvironment, such as lower pH, redox, hypoxia, or external field stimuli response, such as light, heat, ultrasound, magnetic field, etc.

The second part of this thesis mainly includes a review of the types of nanocarriers, internal and external stimuli responsive mechanisms, the construction of the stimuli responsive nanosystems and their applications in

drug delivery. The fifth part of this thesis firstly constructs a near-infrared light-responsive MSN drug delivery system for alleviating rejection after kidney transplantation, followed by the elaboration of an MSN nanoparticle with charge reversal properties triggered by acidic tumor microenvironment for biomolecule delivery; after that a GSH-responsive release of dual drug nanocapsules based on MOF material is designed for synergistic enhancement of anticancer effect, followed by the study of gene editing with the assistance of biomimetic mineralization and microfluidic technology for synthesizing MOF-encapsulated biomolecules. The above work is summarized in the sixth part of this thesis. The research results of this thesis provide an important scientific basis and ideas for the research of MSN and MOF-based stimuli-responsive multifunctional nanocarriers in drug delivery, tumor therapy and gene editing and other related fields, and laying the foundation for the implementation of precision treatment of diseases.

2. Review of literature

2.1. Nanomedicine

With the continuous advances in materials science and biomedicine, researchers expect to be able to control and manipulate the arrangement of atoms to assemble molecules into nanoparticles (or nanostructures) and make them carry a variety of diagnostic and therapeutic molecules to detect the occurrence, progression, and regression of diseases at the molecular, cellular, and overall levels, and ultimately leading to personalized and precise treatment for diseases. Nanomedicine is one of the key research directions in the field of nanobiotechnology because of their unique features and advantages such as changing drug metabolism kinetics, improving drug utilization, achieving on-demand drug delivery at the focal sites, regulating drug release rate, reducing drug toxic side effects (Bourzac 2012; Chen et al., 2016; Li et al., 2019; Li et al., 2012; Liu et al., 2020; Peer et al., 2007; Pham et al., 2020; Sun and Davis 2021). Among them, nanomaterial-based drug carriers, especially stimuli-responsive nano-drug vectors, have attracted high attention from the scientific community and pharmaceutical industry. So far, various carrier materials with excellent structures and properties, including nanoparticles, nanocapsules, nanomicrospheres and nanogels, have been developed for the delivery of therapeutic agents such as nucleic acids, peptides, proteins, small molecule drugs, photosensitizers (Crucho 2015; Lu et al., 2014; Zhang et al., 2019; Zhou et al., 2018). In particular, porous nanomaterials, due to their excellent physicochemical properties, such as diverse nanopore structures, low density, high specific surface area and adjustable pore size, have demonstrated promising applications and economic value in scientific and technological fields like industrial catalysis, gas adsorption, analytical detection, linear optics and electromagnetic materials, especially in drug delivery (Cai et al., 2019; Feng et al., 2021; Guimaraes et al., 2020; Shim and Kwon 2012; Song et al., 2017; Vallet-Regi et al., 2007).

This section first provides an overview of the evolution of nano-drug carriers, their advantages in drug delivery over conventional molecular drugs, the classification of nanocarriers especially porous materials, introduces the different stimuli-responsive release mechanisms and the practical applications of porous nanomaterials in the field of stimuli-responsive nano-drug carriers, in view of which the main research topics of this thesis is presented.

2.2. Nano-drug delivery

Nanotechnology is the high point of scientific and technological development in the 21st century and is the leading technology of the new industrial revolution. The study has shown that nanotechnology can be applied to medicine, pharmacy, biology, chemistry, and information technology, and play a key role in advances in each of these fields. As a "small but powerful" drug carrier, it is one of the important applications of nanotechnology. Nanomedicine carriers are a kind of drug delivery system belonging to the nanoscale microscopic category, which

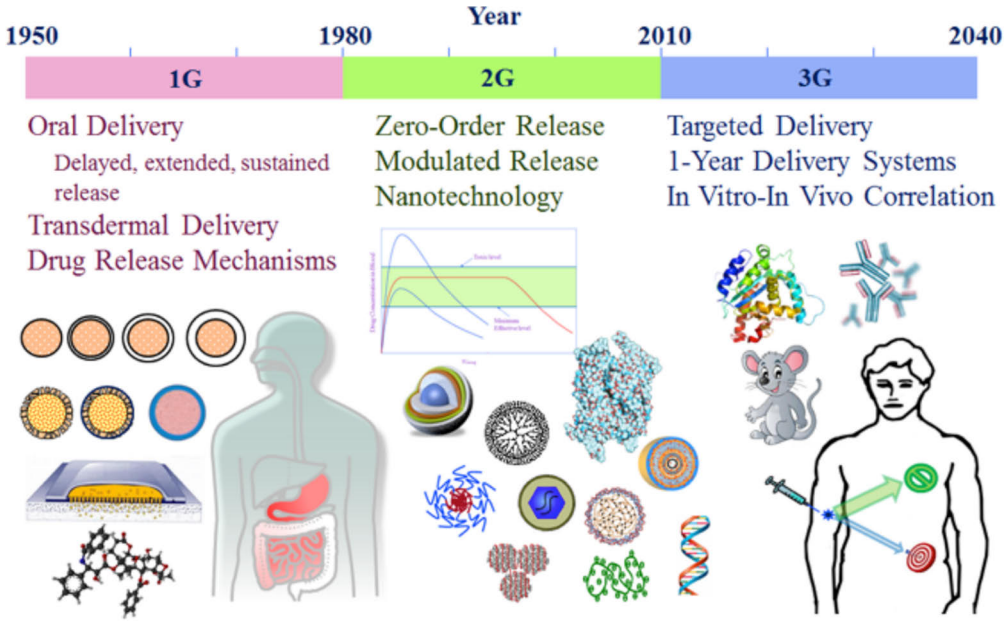

Figure 1. *Evolution of controlled drug delivery systems. (Copyright 2013, American Chemical Society)*

mainly encapsulates drugs in nanoparticles by chemical bonding, physical adsorption, molecular self-assembly or wrapping, constituting a controlled drug delivery platform. The development of the controlled drug delivery systems has gone through three main stages (Figure 1) (Park 2013): the first stage was from 1950 to 1980, during which the basic principles of sustained drug release were established (Dokoumetzidis and Macheras 2006). Many oral and transdermal delivery nano-formulations were developed that could be maintained in the body for extended periods ranging from twelve hours to one week. Several oral nano-formulations were productized and entered the clinic. In the second phase, from 1980 to 2010, the focus of nano-drug delivery development was primarily on zero-order drug release technology, which maintains a constant rate over the release cycle. At the same time, there was a spurt in research on nano-formulations and a wide variety of drug carriers were developed. As of 2006, more than a dozen nanomaterials and about 240 nanomedicines have entered the process of drug development and drug products. Another research focus on this period was the exploitation of stimuli-responsive nano-drug carriers, which could adjust the release rate of drugs according to the actual condition of the lesion site and realize intelligent self-feedback drug delivery. The third phase is after 2010, whose main development direction is the design and construction of targeted and multifunctional nano-drug delivery system, as well as the performance validation of nano-drug carriers from *in vitro* to *in vivo*.

2.2.1. Advantages of nano-drug carriers

The advantages of nano-drug carriers over conventional molecular drugs are:
(1) Nano-drug carriers can increase drug solubility, improve drug stability, reduce drug dosage, and enhance drug efficacy.

The nanocarriers themselves can have a wide variety of morphologies and can be designed and tailored to the desired properties. This allows for the encapsulation of hydrophilic/hydrophobic drug molecules as needed for efficient solubilization. For example, oil-in-water drug carriers can be designed to enhance the solubility of hydrophobic drugs by encapsulating them in their hydrophobic cavities through hydrophobic-hydrophobic interactions. In addition, nanomaterial drug carriers can provide a stable and hidden storage space for drug molecules, which can effectively avoid the degradation and deactivation of drugs under the action of human physiological environment during drug delivery, thus maintaining the drug activity (Hasan et al., 2007). Nanomaterials have a high specific surface area and can load large amounts of drugs, which facilitates to increase the drug concentration when accumulated at the site of the lesion, reducing the number of doses, and improving the therapeutic effect. At the same time, the same nano-drug carrier can be loaded with two or more drugs, thus effectively reducing the chance of "drug resistance" in cells and achieving synergistic treatment.

(2) Nano-drug carriers can enable precision therapy through active/passive targeting.

Nano-drug carriers change the biological absorption, distribution, and metabolic pathways of molecular drugs, and deliver the drugs to the pathogenic parts of human body, thus reducing the damage of drugs to normal organs or tissues. For tumor treatment, solid tumor tissues are characterized by large amount of vascular proliferation, lack of smooth muscle layer, defective vascular

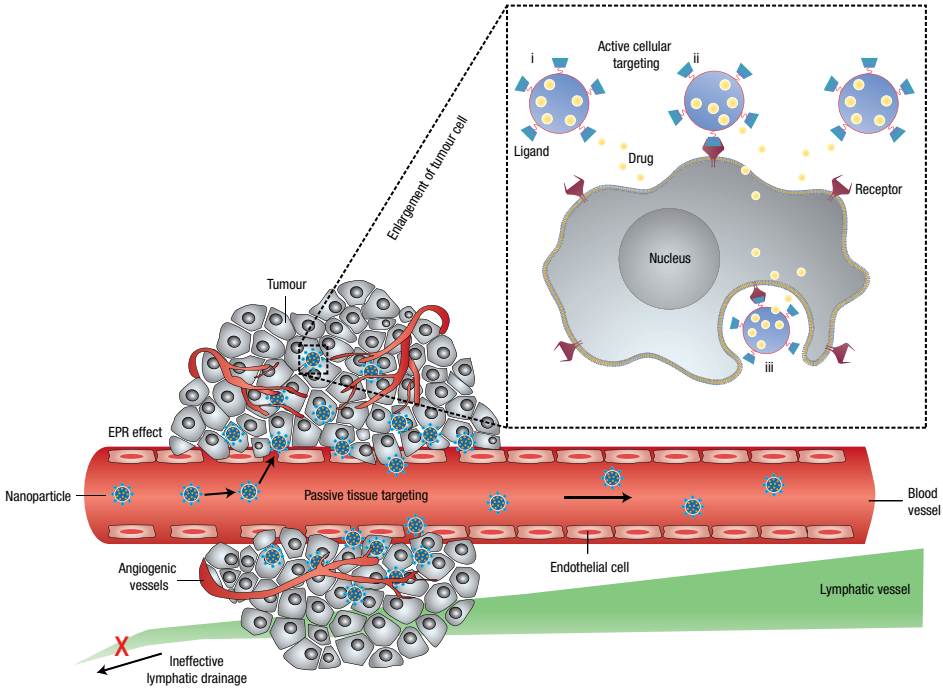

Figure 2. *Scheme of nanoparticle accumulation at the tumour site through the EPR effect. (Copyright 1969, Springer Nature)*

system, weak lymphatic system clearance and slow venous blood return, resulting in "leakage" of new blood vessels (Figure 2). This is the high permeability and retention effect of solid tumor tissues, which is known as the EPR effect (Maeda et al., 2000; Peer et al., 2007; Torchilin 2011). When nanocarriers convey drugs into the tumor tissues, the local drug concentration in tumor can reach several times of the normal plasma concentration due to the EPR effect, thus realizing the targeted drug delivery to solid tumors (Golombek et al., 2018; Maeda et al., 2001). In addition, some cells have specific receptors on their surface, and specific ligands with strong affinity for the receptors can be modified on the surface of nanocarriers to allow them to actively target the lesion site (Brannon-Peppas and Blanchette 2004). Currently, the mechanisms with specific recognition are lectin-carbohydrate interaction (Nicolas et al., 2013), interaction between transferrin and its receptor (Ferris et al., 2011; Xu et al., 2021), interaction between folate receptor and folate (Dong et al., 2018; Rosenholm et al., 2010; Rosenholm et al., 2009), antibody-related targets (Tsai et al., 2009) (such as tumor growth factor, matrix metalloproteinases, integrins, vascular growth factor, epidermal growth factor receptors), nucleic acid aptamers (Liu et al., 2018; Wu et al., 2011; Zhu et al., 2009) and peptide chains (Dong et al., 2019; Fang et al., 2012; Jain and Stylianopoulos 2010) (e.g., tumor cells or neovascularization can specifically express certain integrin RGD peptides). At the same time, physicochemical targeting and targeted traction strategies can assist in drug delivery to specific sites of the patient and reduce drug-induced side effects. For example, drug-loaded magnetic nanoparticles are enriched at focal sites under the effect of magnetic fields (Hao et al., 2010; Ke et al., 2011; Wu et al., 2014), and targeting is achieved by weakening the action of most mononuclear phagocytes, such as through macrophage inhibitors.

(3) Nano-drug carriers can reduce the blocking effect of the physiological barriers and increase the circulation time.

Functional protective barriers exist in the body, such as the blood barrier, the immune system, the blood-brain barrier, and the cellular barrier. They can quickly remove external substances such as bacteria, viruses, and drugs from the body and thus defend against their invasion. To effectively reach target tissues, cells and molecules, drugs need to overcome multiple physiopathological barriers (Figure 3), such as the blood barrier, tissue barrier, cellular barrier and intracellular transport barrier (Blanco et al., 2015). Each barrier has a direct impact on the final therapeutic effect. Nanocarriers can effectively penetrate these biological barriers and deliver drugs to focal areas because of their small and tunable size and the ease of modification of " stealth" or targeting moieties. For example, when a nano-drug delivery system is administered intravenously into the circulation, the reticulocytes of organs such as the liver and spleen and the endothelial cells of blood vessels can engulf foreign bodies in the body with the help of pseudopods. Sometimes, to accommodate the removal of larger foreign bodies, some tissue cells unite to form a system of mononuclear phagocytes with extremely high phagocytic capacity, which is known as the reticuloendothelial system (RES) (Longmire et al., 2011). Numerous studies have

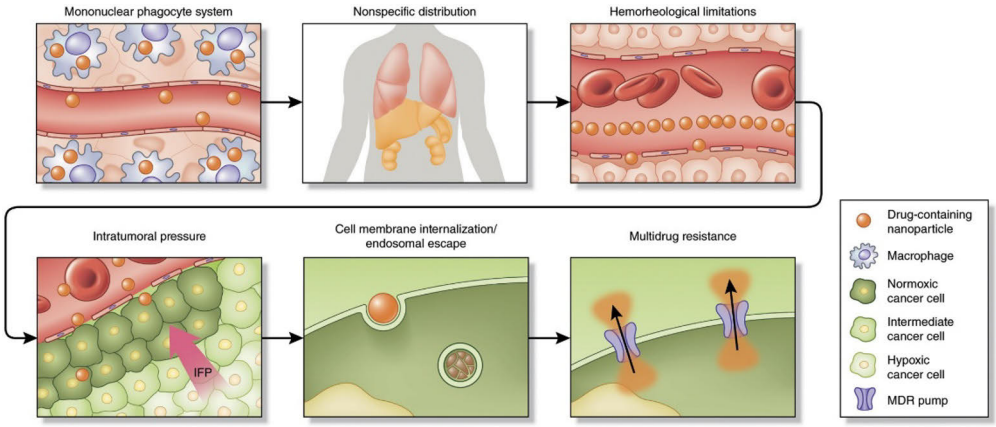

Figure 3. *Physiological barriers encountered by nano-drug carriers in vivo. (Copyright 2015, Springer Nature)*

shown that modification of the surface characteristics of nanoparticles, such as polyethylene glycol modification, biomimetic delivery systems, and live cells as drug carriers, can create "stealth" nanoparticles that impede the phagocytosis of the RES system and overcome this barrier (Harris and Chess 2003; Villa et al., 2016). In turn, when the nano-delivery system reaches the pathogenic tissue, there is a trans-cellular barrier to its entry into the cell. The nano-drug carriers are generally between 10-1000 nm in size, like biological macromolecules such as proteins and nucleic acids, which being much smaller than cells and various organelles, making it easier to bring a variety of biomolecules or drugs into cells or organelles (Bae et al., 2011).

In addition, many experimental results have demonstrated that many kinds of nanoparticles are more easily endocytosed by cells than small molecules or microparticles. Meanwhile, the surface modification of nanoparticles with targeting groups can change the uptake methods of nanoparticles by cells and improve the uptake efficiency. When nano-drug carriers enter the diseased cells through the endocytosis pathway, they are mainly localized in endo/lysosomes. For drugs whose targets are in the nucleus, the endo/lysosomes are the most important barrier to intracellular delivery because of the acidic environment and various enzymes existed in endo/lysosomes that tend to degrade or inactivate the drugs. To address this environment, nanocarriers can be functionalized to disrupt, destabilize, or fuse lysosomal membranes through the proton sponge effect, to achieve endo/lysosomal escape of carriers and drugs (Ashley et al., 2011). In addition, modification of positively charged cell-penetrating peptides on the particle surface can also assist nanocarriers to enter cells and break the lysosomal barrier.

(4) Nano-drug carriers provide an opportunity to develop smart nano-drug delivery systems with stimulus responsiveness.

Due to the diversity of the structure and composition of nanomaterials themselves and their easy modification, it is possible to design and construct stimuli-responsive nanomaterials according to some special physicochemical characteristics of the lesion site to achieve the purpose of avoiding drug leakage

and releasing drugs on demand after reaching the target site (Torchilin 2014). There are two main ways to design stimuli-responsive nano-drug carriers: one is the stimuli-responsive nanocarriers themselves, such as pH-responsive polymeric nanoparticles and protease-degradable nanogels, which produce physical or chemical changes in molecular chain structure, swelling, solubility, and dissociation behaviors upon stimulation by external signals to release drugs. The other is to modify stimuli-responsive groups or molecules on the inner and outer surfaces of nanoparticles and use the reversible binding between the modified groups and the drug or set up "gating" molecules on the particles to confer a controlled effect of drug release on-demand or switch on/off under different stimulation conditions. These stimulation signals mainly include chemical signals such as pH, oxygen partial pressure, biological endogenous substances, and some physical signals like temperature, light, magnetic and electric fields (Aznar et al., 2016). By constructing stimuli-responsive smart nano-drug carriers, premature drug release can be effectively avoided, which greatly reduces the toxic side effects caused by early drug leakage during transportation.

(5) Nano-drug carriers can realize multi-functionalization and integration of diagnosis and treatment.

On the one hand, the fundamental physical effects of nanoparticles, such as quantum effect, small size effect and surface effect, give nanocarriers unique properties, like light, heat and magnetism, which enable the nanocarriers themselves to be used as probes for disease diagnosis. On the other hand (Figure 4), the high surface energy and surface reactivity of nanomaterials make them easy to achieve multifunctional integration and assembly, and they can combine many other different functions in one while serving as drug carriers, which can not only be directly used to detect the occurrence, development and naturalization of diseases, monitor the drug efficacy in real time, and provide doctors with rich location, size and shape information for timely adjustment and optimization of treatment plans, but also can integrate multiple therapeutic means to achieve efficient treatment of diseases (Lim et al., 2015; Sanvicens and Marco 2008).

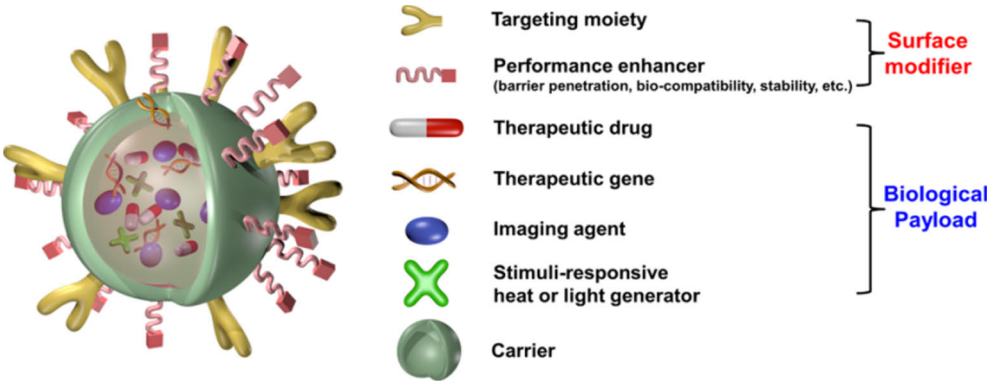

Figure 4. *Scheme of a multifunctional nanocomposite. (Copyright 2015, American Chemical Society)*

2.2.2. Types of nano-drug carriers

The advances in nanotechnology have turned nanomaterials promising carriers for targeted drug delivery systems. Nanoparticles are typically defined as particles with a diameter of approximately 10-1000 nm, and when used as nano-drug carriers, they can extend the half-life of a drug, improve the solubility of hydrophobic drugs and enhance efficacy by releasing the drug in a controlled or sustained mode. Stimuli-responsive nanoparticles can also help reduce biotoxicity and enable controlled release of drugs. Liposomes were used as carriers for drugs and proteins in 1964, and were the first nano-drug delivery systems to be developed (Gregoriadis and Ryman 1971). Since then, an increasing number of materials have been made into nanoparticles and used as nano-drug delivery systems (Shi et al., 2017). There were 51 nanoparticles approved by the U.S. Food and Drug Administration (FDA) and 77 other nanoproducts are in clinical trials in 2016 (Bobo et al., 2016).

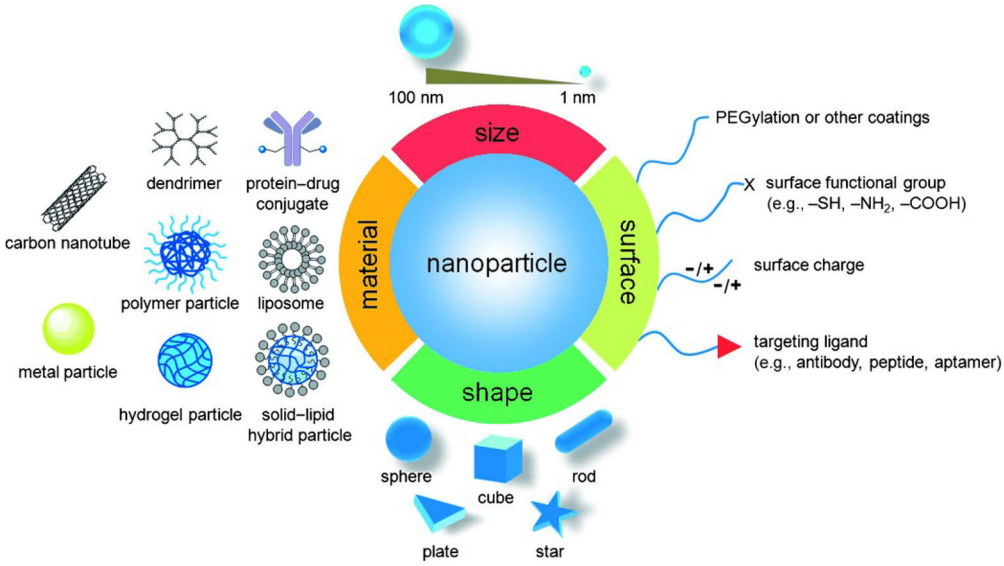

Figure 5. *Nanomaterials for drug delivery and their functionalized modifications. (Copyright 2014, John Wiley and Sons)*

The types of nanomedicine carriers are quite extensive (Figure 5), and according to the components of nanomaterials can be divided into lipids nanocarriers (e.g., solid lipid nanoparticles, liposomes), polymer nanoparticles (e.g., micelles, dendrimers, hydrogels), porous nanomaterials (mesoporous silica nanoparticles, metal-organic frameworks), and other inorganic nanocarriers (e.g., metal nanoparticles, carbon nanomaterials) (Allen and Cullis 2013; Chen et al., 2014; Chen et al., 2013; Connor et al., 2005; Gomes et al., 2021; Graf and Lippard 2012; Li et al., 2003; Nasongkla et al., 2006; Siepmann and Peppas 2001; Sun et al., 2014; Xu et al., 2021). Several of the most common nano-drug carriers and their general delivery mechanisms are described as follows:

(1) Lipid nanocarrier: usually composed of natural phospholipids or synthetic lipids as the raw material vesicular structures that are biocompatible and can be loaded with hydrophilic or hydrophobic drugs.

Liposome nano carriers are formed by wrapping drug molecules with nanoscale vesicles formed by phospholipid bilayer membranes. Since phospholipid molecules have a hydrophilic head and a hydrophobic tail, when forming liposomes, the hydrophilic head is located outside the bilayer, while the hydrophobic tail faces the middle of the bilayer (Bozzuto and Molinari 2015; Wang et al., 2013). This special structure allows the loading of both lipid soluble drugs and water-soluble drugs, where the lipid soluble drugs can be loaded in the lipid bilayer while the water-soluble drugs are loaded inside the particles. Since their lipid bilayer structure is like biological membranes which can be absorbed and fused to cell membranes on the cell surface, liposomes have good biocompatibility with low immune response from organisms. Also, there are many ways to modify the surface of liposome membranes, either by grafting desirable targeting molecules onto the liposomes surface or by adjusting the surface charge of liposomes to improve drug delivery efficiency according to the needs. Compared with conventional liposomes, nanoliposomes demonstrate significant improvements in encapsulation rate, stability, specific targeting, drug-controlled release, and reduced reticuloendothelial uptake. Research on liposomes has become increasingly sophisticated, and several liposomal drug delivery systems have been approved for clinical use (Zhang et al., 2008). Sequus Pharmaceuticals has developed a nanoliposome-encapsulated Doxil, which was first approved by the FDA in 1995 (Frenkel et al., 2006), and especially the lipid nanoparticle–mRNA vaccines are now being used against coronavirus disease 2019 (COVID-19) (Hou et al., 2021). Liposomal drug carriers also have some disadvantages, which are easily cleared by the reticuloendothelial system when injected intravenously, very unstable in the blood stream and can be disassembled, resulting in early release of the drug.

(2) Polymer drug carriers: they are some natural polymers such as chitosan (Li et al., 2011), dextran (Peng et al., 2011), or synthetic polymers like polylactic acid (PLA) (Huang et al., 2007), poly(lactic-co-glycolic acid) (PLGA) (Kim et al., 2008), which are loaded with drug molecules by agglomerating into micro and nano-sized particles.

Micelles are usually composed of amphiphilic molecules with hydrophilic heads and hydrophobic tails assembled in aqueous solution to form core-shell structures that act as nano-drug carriers. The hydrophobic drugs can be non-covalently embedded in the hydrophobic core of the micelles or covalently attached to the polymer. Under the stimulation of some external signals, the conformation of polymeric backbone changes, causing the micelles to disintegrate or inducing the breakage of the attached drug molecules, resulting in drug release. The size and morphology of polymeric micelles can be regulated by adjusting the length and ratio of hydrophilic/hydrophobic fragments (Yang and Alexandridis 2000). The hydrophobic core of polymeric

micelles can increase the solubility of hydrophobic drugs, while the hydrophilic shell can form many hydrogen bonds with water molecules in solution, forming a tight protective shell on the outside of the micelles, reducing protein adsorption and cell adhesion and enhancing the circulation time of the micelles in the blood (Kooijmans et al., 2016; Oerlemans et al., 2010).

Dendrimers are highly branched nanopolymeric materials with many branches irradiating from the center to form a three-dimensional structures (Klajnert and Bryszewska 2001). Its core has some sub-nanometer pores that can be used to load drug molecules, and its surface extends a variety of functional groups, such as amine groups and carboxyl groups, which ensure the stability of dendrimers in water, and can be used to modify a variety of targeting molecules and contrast molecules, and even drug molecules (Lukowiak et al., 2015). The use of dendrimers for drug transport can improve the pharmacokinetics of drugs and enable targeting of labeled tissues to control drug release. Also, due to their extremely small size (<5 nm), dendrimers can be excreted from the body via blood vessels and from the kidneys with very low physiological toxicity. However, the complex design and synthesis process, as well as the high cost, are the main reasons why dendrimers are difficult to be used in clinical applications (Morgan et al., 2006).

Hydrogels are soft materials with a three-dimensional network structure and are widely used as substrates for cell culture, templates for tissue engineering, and carriers for drug and cell delivery due to their excellent biological properties (Wu and Xu 2018). Hydrogels were initially limited in their application for drug delivery because of their poor mechanical properties that prevented them from maintaining the stability and controlled release of the loaded drugs. Recently, the development and improvement of hydrogel-based nanocarriers by researchers has greatly increased their potential for drug delivery (Sun et al., 2020). Smart hydrogels can intelligently respond to environmental changes to provide remotely controlled, highly targeted delivery and on-demand release. More precisely, hydrogels can undergo degradation or conformational changes in response to temperature, light, pH, redox potential, magnetic field, and ultrasound stimuli and can be used to achieve high drug delivery efficiency for in situ cancer therapy.

Altogether, liposomes, polymeric micelles, dendrimers, and hydrogel nanoparticles formed by self-assembly of several organic molecules, these organic carriers are designed with simple principles and can achieve controlled release of the loaded drugs through their own deformation or degradation. However, the disadvantages of organic nanoparticles, such as poor stability in living organisms, easy clearance by the reticuloendothelial system, high toxicity of their own organic molecular components, difficulty in manipulating molecular weight and size, and unstable drug release kinetics, have greatly limited their application scope. Compared with organic nanocarriers, inorganic nanoparticles can be endowed with potential synergistic therapeutic and targeted tracer imaging functions due to their uniform size control, good stability, large specific surface area and easy surface functionalization, as well

as the unique photothermal and electromagnetic properties of inorganic nanoparticles themselves. Therefore, the application of inorganic materials such as porous silicon, gold nanoparticles, carbon nanotubes and quantum dots as nanocarrier has received widespread attention and emphasis (Rotello 2008). For example, gold nanoparticles (AuNPs) with a very large specific surface area can be used to attach various biomolecules (Peng et al., 2019). AuNPs modified with positively charged polymers can attach negatively charged drugs, such as siRNA and plasmid, to their surfaces by electrostatic interactions or covalent bonds (Zhang et al., 2020). In addition, conjugation of cell-specific targeting components onto AuNPs can promote active cancer-specific drug delivery and EPR effects. However, for inorganic carriers, on the one hand, the degradation properties of the carriers themselves need to be improved to further reduce the biotoxicity. On the other hand, to achieve good biocompatibility, the carrier surface modification is also important, for example, the modification of PEG can enhance the dispersion and stability of inorganic nanoparticles in blood, prolong the circulation time of particles, and promote their entry into tumor tissues through EPR effect; or modify the targeting molecules to facilitate the specific and efficient entry of inorganic nanoparticles into tumor cells.

In recent years, porous nanomaterials, especially mesoporous silica nanoparticles (MSNs) and metal-organic frameworks (MOFs), have attracted increasing attention in drug delivery, tumor synergistic treatment, optical imaging and magnetic resonance because of their good biocompatibility, adjustable pore size, functionalized modification of surface groups, and high drug loading capacity (Chen et al., 2012; Gao et al., 2019; Guillet-Nicolas et al., 2013; Ke et al., 2011; Lee et al., 2009; Li et al., 2018; Wang et al., 2015; Wu and Yang 2017; Zhang et al., 2015).

2.3. Porous nanomaterials

Porous nanomaterials are multiphase materials composed of solid-phase nanoparticles and many pores, which have the dual characteristics of both porous materials and nanomaterials and have become one of the focal points of research in the field of nanoscience and technology. Because porous nanomaterials have many unique structural and physicochemical properties such as high specific surface area and porosity, tunable pore size, low material density, high permeability and adsorption, and assembly, they have broad application prospects in high-tech fields such as catalytic carriers, gas adsorption and separation, drug delivery, photoelectromagnetic materials, nanoreactors and chemical sensors. The most important feature of porous nanomaterials is their rich nanopore structure. The size, shape, orientation, and dimension of pore channels as well as the composition and properties of pore walls are the basic parameters affecting their performance. Porous nanomaterials can be divided into two categories according to the regularity of their nanopore structure, namely those with irregular pore structure and those with regular pore structure. Porous nanomaterials with irregular pore structure, represented by organic macromolecules and polymers, cannot

accurately control the release rate of drugs due to the lack of a well-defined porosity. Porous nanomaterials with regular pore structure have better application prospects and economic value in controlled drug release because of their uniform and adjustable pore size, stable skeleton structure, and easily modified internal and external surfaces. According to the definition of the International Union of Pure and Applied Chemistry (IUPAC), porous nanomaterials can be divided into the following three categories according to the pore size (Sumiya et al., 2001): 1. Those with pore size range below 2 nm are called microporous materials, such as zeolites, metal-organic frameworks and microporous molecular sieves; 2. Those with pore size range between 2 nm and 50 nm are called mesoporous materials, such as mesoporous silicon dioxide and mesoporous carbon; 3. Those with pore size greater than 50 nm are called macroporous materials, such as porous glass and macroporous alumina. Currently, mesoporous silica is widely used in the field of stimulus response release due to its unique physicochemical properties and suitable pore structure. Recently, metal-organic frameworks with environmental sensitivity and multifunctional modifications are also emerging in this field.

2.3.1. Mesoporous silica nanomaterials for drug delivery

Mesoporous silica nanomaterials are porous nanostructured materials formed by using organic molecules (surfactants or amphiphilic block polymers) as templating agents and inorganic silica sources for interfacial reactions to form regular and ordered assemblies wrapped by silica, and then retaining the silica inorganic backbone after removing the templating agents by calcination or solvent extraction. Compared with other porous materials, mesoporous silica has unique advantages for controlled drug release: 1. simple preparation and the ability to synthesize nanoparticles of various sizes, morphologies and complex structures as needed (Figure 6), where nanomaterials such as ultra-small size mesoporous silica, mesoporous silica nanorods, hollow mesoporous

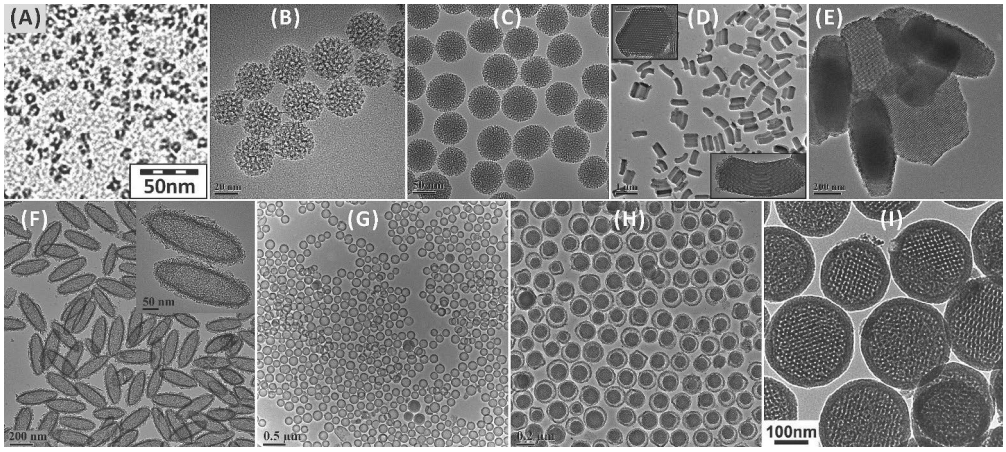

Figure 6. *MSNs with different particle sizes, morphologies, and nanostructures: (A)–(C) nanospheres, (D) nanorods, (E) nanoplates, (F)-(H) MSNs shell, (I) core-shell nanospheres. (Copyright 2013, John Wiley and Sons)*

silica, lamellar and shuttle mesoporous silica were successfully synthesized (He and Shi 2014); 2. good thermal and chemical stability, which prevents explosive drug release due to carrier decomposition; 3. homogeneous and adjustable pore size (2 to 30 nm), allowing the loading of drugs of different sizes and molecular weights (Wan and Zhao 2007); 4. easily modified external and pore cavities. By selectively modifying different functional groups and sealing them with a series of stimuli-responsive gates and switches, drug loading and controlled release can be achieved (Lin et al., 2012); 5. very large mesopore volume (0.9 $cm^{3} \cdot g^{-1}$) and high specific surface area (900 $m^{2} \cdot g^{-1}$.), which facilitates loading or adsorption of large amounts of drugs to increase the loading capacity (Trewyn et al., 2007); 6. Good biocompatibility and inhibition of reactive oxygen species (ROS) formation (Huang et al., 2010). Silicon dioxide is accepted by FDA as "generally recognized as safe and non-toxic"; 7. easy to assemble, mesoporous silica is easy to assemble and synthesize on a variety of functional nanomaterials and substrates to achieve the integration of multiple functions (Lee et al., 2011).

As early as 1968, Stöber prepared nonporous monodisperse silica microspheres in the ethanol-water-ammonia-ethyl orthosilicate system (Stöber et al., 1968). However, the pore structure of the synthesized mesoporous silica was poor because the earlier preparation methods such as aerosol method and aerogel method could not effectively and real-time regulate the process of mesoporous silica preparation. Until 1992, Mobil synthesized and reported the M41S series of ordered mesoporous materials with alkyl quaternary amine surfactants as the structural guide and silicates as the silica source (Beck et al., 1992), which made the rapid growth and wide application of mesoporous silica. In 2001, Vallet-Regi et al. first studied the filling efficiency and release properties of mesoporous silica nanoparticles as drug carriers (Vallet-Regi et al., 2007; Vallet-Regi et al., 2001). Their group then investigated the loading of drug ibuprofen by MSNs with two different pore sizes, and the results showed that MSNs have high drug loading capacity, as well as drug retardation, and the release rate of drug is accelerated with increasing pore size. In 2003, Tanaka et al. prepared a reversible photo-controlled release system based on MCM-41 mesoporous silica nanoparticles by designing coumarin derivatives and coumarin dimers as "double-gated organic nanoplug" molecular switches (Mal et al., 2003). The light-controlled and reversible intermolecular dimerization of coumarin derivatives attached to MCM-41 can modulate the uptake, storage, and release of organic molecules within the mesopores, achieving the first reversible release of light-controlled mesoporous silica. In the same year, Lin et al. used cadmium sulfide (CdS) quantum dots as gated blockers of mesopores to achieve the first gated system for controlled release of drugs under stimulated conditions (Lai et al., 2003). Since then, a series of different gated blockers (such as inorganic nanoparticles, nucleic acids, polymers, and supramolecular polymers) have been widely used for the blocking of MSNs, and numerous stimuli-responsive drug release mechanisms have been developed for tumor chemotherapy, which has greatly

promoted the application of chemotherapeutic drugs in tumor treatment (Liu et al., 2014).

2.3.2. Metal-organic frameworks for bioapplications

Although the development of mesoporous silica-based nanocarriers in the field of drug stimuli-responsive controlled release is becoming more and more mature and the mechanisms of stimulus response are becoming more and more numerous, however, these drug delivery systems also face disadvantages such as poor biocompatibility of blocking molecules and limited loading capacity. Metal-organic frameworks (MOFs), as novel nanomaterials, have received much attention and developed rapidly in recent years (Meek et al., 2011). They usually consist of metal ions or metal clusters interconnected with oxygen- and nitrogen-containing organic ligands through covalent or coordination bonds and self-assembled to form crystalline materials with periodic network structure (Zhou et al., 2012). MOFs were first proposed by Yaghi's group in *Nature* in 1995, and they prepared a two-dimensional material with metal ions as nodes and organic ligands as spacers (Yaghi et al., 1995). In 1999, the successful preparation of MOF-5 with a three-dimensional network structure gave a boost to the research and application of MOFs (Li et al., 1999). A series of MOFs have then been developed, such as HKUST-1 (Prestipino et al., 2006), MIL-101 (Latroche et al., 2006), UiO-66 (Kandiah et al., 2010) and ZIF-8 (Park et al., 2006).

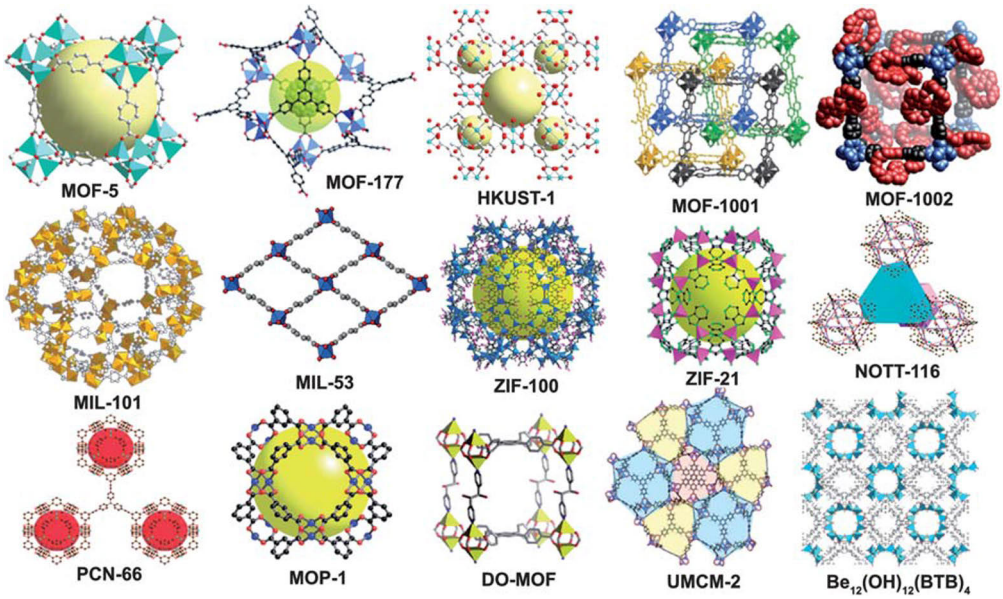

Figure 7. *The 3D structures of representative MOFs (MOF-5 (Li et al., 1999); MOF-177 (Chae et al., 2004); HKUST-1 (Prestipino et al., 2006); MOF-1001, 1002 (Li et al., 2009); MIL-101 (Ferey et al., 2005); MIL-53 (Serre et al., 2002); ZIF-100 (Wang et al., 2008); ZIF-21 (Banerjee et al., 2008); NOTT-116 (Yan et al., 2010); PCN-66 (Zhao et al., 2009); MOP-1 (Eddaoudi et al., 2001); DO-MOF (Mulfort et al., 2009); UMCM-2 (Koh et al., 2009); $Be_{12}(OH)_{12}(BTB)_4$ (Sumida et al., 2009)). (Copyright 2010, Royal Society of Chemistry)*

In the field of nano-drug carriers, MOFs nanomaterials possess unique properties that cannot be matched: 1. Diversity of species, the choice of metal centres of MOFS materials includes almost all metals, such as main group elements, transition elements, lanthanide, while the variety of organic ligands available is even wider. For example, a variety of functionalized MOFs can be synthesized by using carboxylic acid ligands modified with different groups, and MOFs materials with different pore sizes, cavity sizes and physicochemical properties are obtained by using binary carboxylic acid ligands with longer sizes coordinated with metal ions. It is due to the diversity of organic ligands and metal centres that many new MOFs materials are reported every year (Figure 7) (Stock and Biswas 2012; Xiang et al., 2010). 2. With huge specific surface area and high porosity, their specific surface area can reach as high as 4000-8000 $m^2 \cdot g^{-1}$, their density can even be as small as 0.21 $g \cdot cm^{-3}$, the porosity is about 91%, and the pore structure is more ordered and developed than that of conventional porous materials (Horcajada et al., 2012). This unique porous structure can make the drug loading capacity much higher and has potential application value in drug slow release. 3. Due to the low bonding energy of coordination bonds between metals and organic ligands, most MOFs are inherently degradable in biological systems, thus avoiding toxic side effects due to bioaccumulation. Some MOFs materials are environmentally responsive and can denature or degrade under certain conditions, which provides an opportunity to design stimuli-responsive nano-drug delivery systems. Currently, MOFs materials are still in their infancy in the field of stimuli-responsive controlled drugs release, but their unique advantages allow them to have a wide range of biomedical applications.

Zeolitic imidazolate framework-8 (ZIF-8), one of the MOFs materials, is a metal-organic framework compound with zeolitic sodium squared topology synthesized using divalent zinc salts and 2-methylimidazole and belongs to porous nanomaterials. In which, the organoimidazole is cross-linked to the transition metal to form a tetrahedral structure. Many different ZIF can be developed by simply adjusting the crosslink interactions (Kaneti et al., 2017). ZIF-8 has a pore size of 0.34 nm, a cage diameter of 11.6 nm, a large specific surface area of 1630 $m^2 \cdot g^{-1}$ and a pore volume of 0.63 $m^3 \cdot g^{-1}$, which gives it a great adsorption capacity for water vapor and small molecules of drugs (Park et al., 2006). ZIF-8 also has very good thermal and chemical stability, not easy to change its structure due to changes in the environment (Banerjee et al., 2008). In addition, ZIF-8 is easy to obtain raw materials and low cost.

Since MOFs nanomaterials are microporous materials, their pore size is often smaller than that of the drug, so the drug loading method is different from mesoporous materials (mainly loaded by post-synthesis diffusion and chemical modification). The drug loading of MOFs is divided into two ways (Figure 8): one is to dope the drug molecules during the synthesis of MOFs (He et al., 2015; Imaz et al., 2010; Rieter et al., 2008; Zheng et al., 2016). The drug molecules are embedded in the framework structural scarf of the material in the form of non-covalent bonds. This approach can be used for multiple and multi-class drug loading. In addition, an increasing number of studies have shown that some

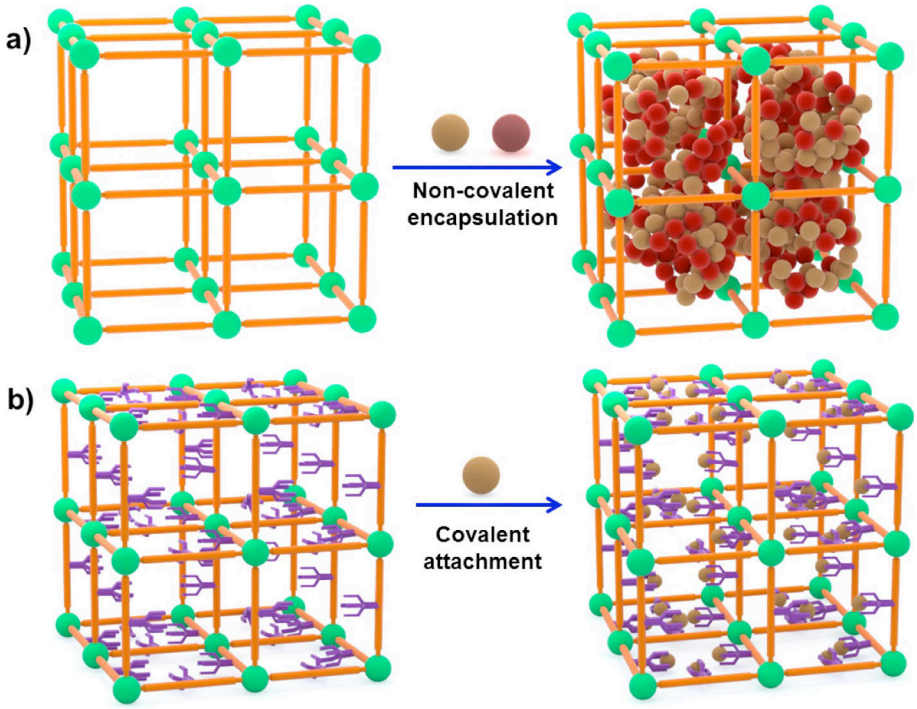

Figure 8. *Scheme of postsynthetic encapsulation by non-covalent encapsulation (a) and covalent attachment (b). (Copyright 2015, American Chemical Society)*

drugs and imaging reagents can themselves act as metal centers or organic ligands that participate in the framework composition. Another wrapping method is the covalent or non-covalent modification of MOFs after synthesis. The loading capacity and encapsulation rate of this loading method depend on factors such as the nature of the drug and the stability of the particles. The ultrahigh porosity and specific surface area of MOFs nanomaterials allow them to act as molecular "sponges" and greatly improve the loading capacity of drugs. For example, Horcajada et al. selected trivalent iron ions as metal centers and used various carboxylic acid organic compounds as ligands to synthesize MIL-53, MIL-88A, MIL-88Bt, MIL-89, MIL-100, MIL-101 series MOFs nanomaterials for loading drug molecules with different polarity, size and functional groups (Bauer et al., 2008; Horcajada et al., 2007; Serre et al., 2004; Surble et al., 2006; Whitfield et al., 2005). The results showed that all these carriers exhibited good drug loading and slow release performance, with MIL-100 having 25, 21, 16 and 29 wt% loading capacity for the drugs Ibuprofen, Chilox, Cidofovir and Adriamycin, respectively, which is several times higher than the general nano-drug carriers (less than 5 wt%) (Horcajada et al., 2010).

2.4. The applications of stimuli-responsive nanomaterials

Nowadays, a variety of stimuli-responsive porous nanoparticles are widely used in cancer therapy research, which can be divided into two major categories according to different types of stimulations (Figure 9), such as endogenous

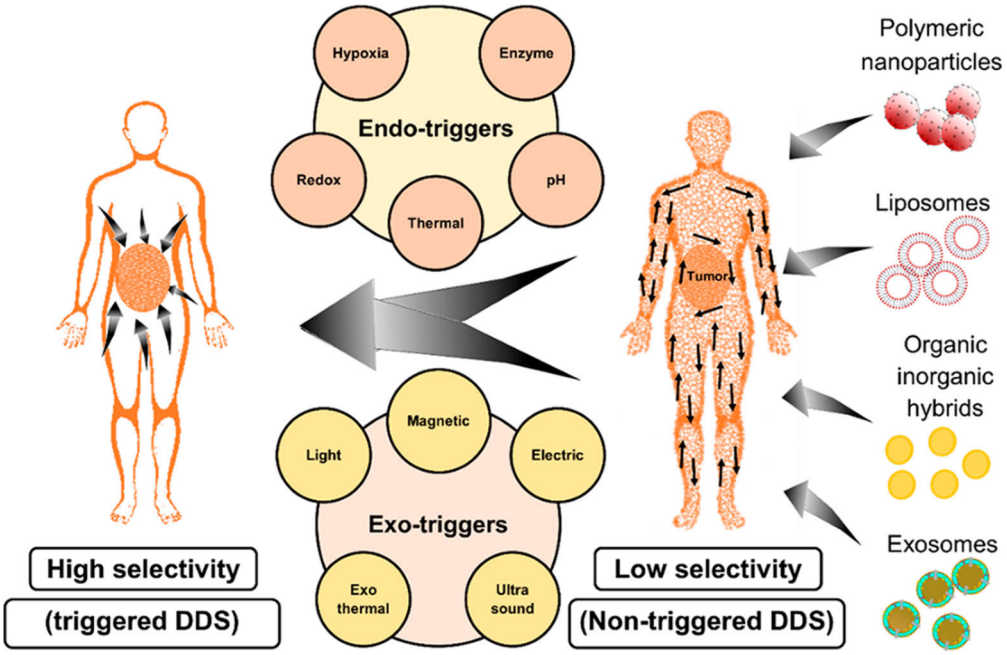

Figure 9. *Different stimulus sources that can be utilised by responsive nanoparticles (Copyright 2018, American Chemical Society)*

stimuli, such as pH, redox substances, enzymes, and external field stimuli, including light, magnetic, electric fields (El-Sawy et al., 2018).

2.4.1. Endogenous stimulus response

(1) pH responsive controlled-release system

pH has been used as a common endogenous stimuli-responsive signal to control drug delivery to specific organs such as gastrointestinal tract or intracellular organelles like lysosomes, as well as for controlled drug release studies (Liu et al., 2014). The pH of certain organs, such as the stomach (pH = 2) and intestine (pH = 7) can be used to initiate drug release in different formulations. Precise pH changes at specific disease sites (e.g.,, inflammation, local ischemia, tumor tissue, and even in certain cellular organelles) can trigger drug release from the designed carriers. Under normal conditions, the pH of extracellular tissues and blood is usually maintained at around 7.4, while in various solid tumors it drops to about 6.5. In addition, acidic organelles within tumor cells, such as lysosomes and endosomes, have a much lower pH (4.5-6) (Lee et al., 2007; Neri and Supuran 2011; Wang et al., 2014). Therefore, pH differences can be regarded as a critical design principle for the development of stimuli-responsive nano-drug delivery systems (Liu et al., 2016). The pH-responsive nanosystems mainly employ the following two strategies. One approach is to prepare carriers using several unstable chemical bonds that are stable under physiological conditions, however, under tumor micro-acidic environments, the chemical bonds break, allowing drug release or facilitating

carrier-tumor cell interactions to improve drug uptake. There are many acid-sensitive linkage bonds, including hydrazone bonds, acetal bonds, acid ester bonds, vinyl esters, acid anhydrides, and methacrylate-based ethers that can be used to construct pH-responsive systems. Another approach is to synthesize carriers with the help of proton-containing groups that are differentially charged at different pH environments, allowing the drug to be released in a slightly acidic environment.

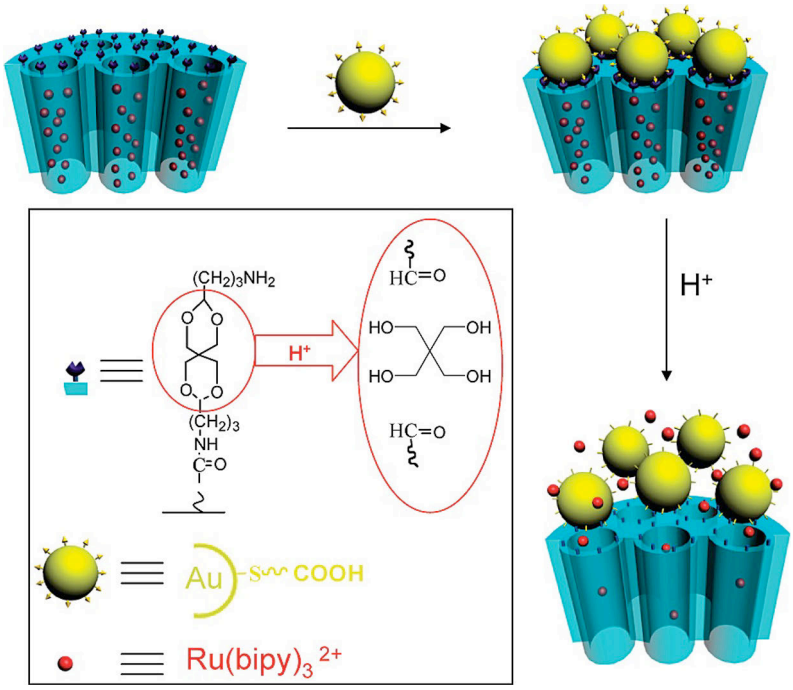

Figure 10. *Scheme of pH-responsive MSNs-based drug controlled release system. (Copyright 2010, American Chemical Society)*

Liu et al. used an acid-sensitive acetal-linked chain to covalently cross-link gold nanoparticles (AuNP) and MSNs to construct a novel pH-controlled release system (Figure 10) (Liu et al., 2010). Under neutral conditions, AuNP remained stably bound to the mesoporous surface of MSNs and blocked the drug molecules inside the mesopores. While under acidic conditions, the acetal bond is hydrolyzed and AuNP is shed from the mesopore surface, thus achieving pH-responsive controlled release of the drug. In addition to using pH-sensitive linkage bonds to block the surface of MSNs with nanoparticles, pH-sensitive inorganic nanoparticles themselves can be used as blocking molecules, such as $CaCO_3$ (Liu et al., 2019; Moreira et al., 2014) and ZnO (Kuang et al., 2019; Muhammad et al., 2011; Muhammad et al., 2013; Zhang et al., 2015), and with the change of pH, the drug can be released from the pore channel as the nanoparticles under certain pH conditions undergo dissolution. Except for controlled release systems using nanoparticles as blocking molecules there are also polymers that undergo hydrophilic/hydrophobic or conformational

changes at different pH conditions, which are also commonly used to construct pH-responsive release systems. Cyclodextrins have special structural and physicochemical properties that allow them to form intron complexes with a variety of molecules, and such complexes can also undergo reversible separation and assembly in response to external stimuli. Based on this, Zink et al. modified methyl orange on mesoporous surface to achieve controlled drug release by changing the hydrophilic force of β-cyclodextrin and methyl orange under different pH conditions (Meng et al., 2010). Under acidic conditions, the amino group modified on the surface of hollow mesoporous silica microspheres underwent protonation and weak interaction with cyclodextrin, resulting in the separation of cyclodextrin from the aniline group to release the drug.

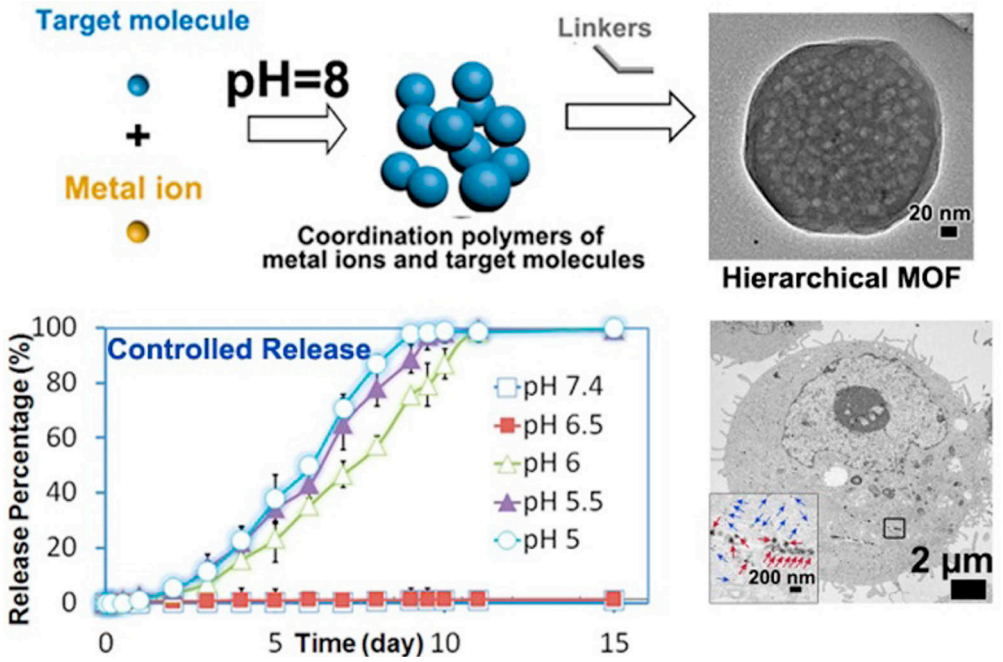

Figure 11. *The pH-induced one-pot synthesis of MOFs and controlled drug release. (Copyright 2016, American Chemical Society)*

At present, studies on nanomedicine carriers based on MOFs nanomaterials have focused on the drug release due to the degradation of their framework structures, highlighting their drug-controlled release behavior. ZIF-8 is a common acid-sensitive MOFs material, and its degradation is caused by the weakened coordination between metal ions and ligands in an acidic environment. Because of its simple and rapid preparation and pH responsiveness, ZIF-8 has attracted a lot of attention for its application in cancer therapy (Jia et al., 2018; Wang et al., 2020; Yan et al., 2020; Zheng et al., 2017). Zheng et al. obtained CCM@ZIF-8 by one-pot loading of curcumin (CCM) inside ZIF-8, which is pH-responsive and has significantly improved anticancer effects compared with free CCM (Zheng et al., 2015). The Doxorubicin (DOX) was loaded into ZIF-8 (Figure

11) by a one-pot method and obtained DOX@ZIF-8 with very good pH responsiveness and almost no drug release under normal tissue pH conditions, while the drug could maintain a stable release for about 10 days in the tumor microenvironment (Zheng et al., 2016). This system has the advantages of large loading capacity (20%), controlled release process, easy synthesis, and has promising for *in vivo* drug delivery. Ren et al. prepared PAA@ZIF-8 nanocarrier material to adsorb DOX (Ren et al., 2014). The strong electrostatic interaction between PAA and DOX gave PAA@ZIF-8 a high drug loading capacity, while ZIF-8 gave the nanocarrier pH responsiveness. The hollow carrier material ZIF-8@FA-CHI-5-FAM (Gao et al., 2016) was produced by Gao et al. to load the anticancer drug 5-fluorouracil (5-Fu). In addition to ZIF-8, PB@MIL-100 (Wang et al., 2016) prepared by Wang et al, ZJU-101 (Yang et al., 2016) prepared by Yang et al, and PCN-221 (Lin et al., 2016) prepared by Lin et al are also pH responsive.

(2) Redox responsive controlled-release system

Redox reactions are the most important type of biochemistry in living organisms. The main oxidizing substances in cells mainly include reactive oxygen species (ROS) (Batandier et al., 2002), such as superoxide anion radicals ($\cdot O^{2-}$), lipid radicals ($\cdot$OOR), hydrogen peroxide (H_2O_2), hydroxyl radicals ($\cdot$OH), and reactive nitrogen species (RNS), such as peroxynitrite anion ($ONOO^-$), nitric oxide (NO). The main reducing substances are divided into enzymes and non-enzymes, with enzymes represented by glutathione peroxidase (GSH-Px), superoxide dismutase (SOD), glutathione S-transferase (GST), and catalase; non-enzymes reducing substances mainly contain protein thiols such as thioredoxin (TRX), small molecule thiols such as glutathione (GSH) (Hwang et al., 1992), cysteine and homocysteine, reduced nicotinamide adenine dinucleotide phosphate (NADPH) (Janiszewski et al., 2000), and vitamin C and E (Wu et al., 2004). GSH is an important reducing agent in living organisms, and the significant difference in its concentration between tumor cells and normal cells provides an opportunity to achieve stimuli-responsive drug release within tumor cells. Therefore, the design of controlled release systems that can respond to redox signals is important for intracellular transport and release of antitumor drugs to kill tumor cells.

Many redox stimuli-responsive controlled release systems have been constructed using the differences in the levels of reducing substances such as GSH, and the design principles mainly include the disulfide bond breakage induced by reducing substances and the degradation of blocking materials (Meng et al., 2019; Palanikumar et al., 2015; Wan et al., 2019; Wu et al., 2016; Yang et al., 2015). Lin et al. used cadmium sulfide (CdS) quantum dots as gated blockers of mesopores, modified on the surface of MSNs by disulfide bonding to achieve the blocking of drugs in mesopores and the release of drugs in the presence of dithiothreitol (DTT) or mercaptoethanol (ME) (Lai et al., 2003). This system is the first to use a gating system to achieve controlled release of drugs under stimulation conditions, which is significant and pioneering. Stimulus response mechanisms through the degradation of blocking agents by reductive

substances were subsequently developed. Wang et al. used a grafting method to graft polyethylene glycol (PEG) to MSNs modified with disulfide bonds on the surface to prepare a drug-controlled release system with PEG polymer as a gateway and investigated the relationship between graft density and drug release (Wang et al., 2015).

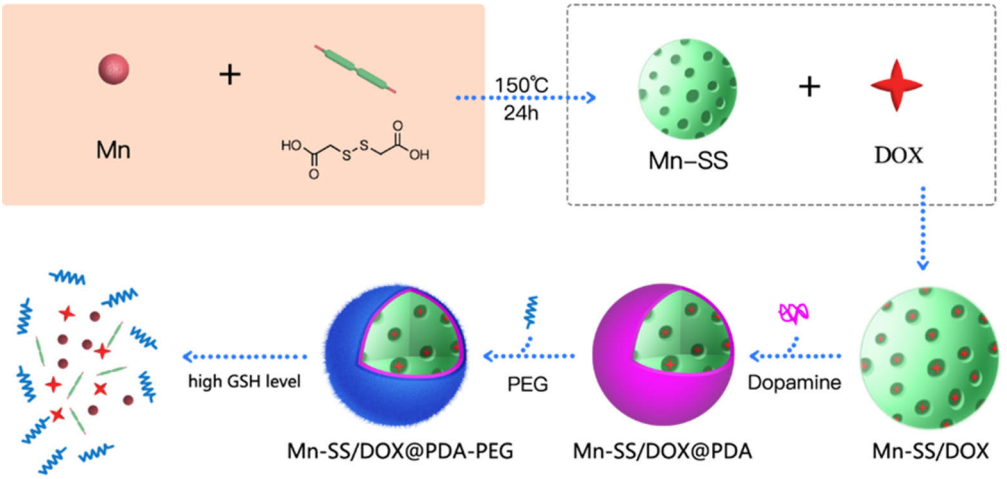

Figure 12. *Scheme for the preparation of drug-loaded nanoscale coordination polymerss, and GSH-triggered nanoparticle decomposition and drug release. (Copyright 2017, American Chemical Society)*

Redox-responsive MOFs can also be constructed by introducing disulfide bonds in the ligand (Jiang et al., 2020; Lei et al., 2018), and a unique GSH sensitive mode (Mn-SS/DOX@PDA-PEG) was prepared by Zhao et al (Figure 12) (Zhao et al., 2017). Modification of DOX-loaded Mn-SS nanoparticles with polydopamine (PDA) and PEG resulted in the cleavage of the disulfide bond of dithiodiglycolic acid in the presence of GSH, leading to efficient redox-responsive MOF degradation and followed by drug release. In practice, the direct construction of MOFs based on GSH-responsive ligands is inherently difficult, and post-synthetic surface modification of MOFs provides the possibility to achieve this type of drug delivery. When exposed to GSH, the linker or coating on the MOF surface will be destroyed instead of their structure. Liu et al. cross-linked polymers containing disulfide bonds in situ on the surface of Zr-MOF nanoparticles to enhance physiological stability and impart GSH-responsive intracellular drug delivery (Liu et al., 2020). The polymer attached to the surface not only protects MOFs from decomposition by either phosphate ions or acids, but also prevents leakage of the loaded cargos. The problem of premature drug release due to poor stability of conventional Zr-MOF in PBS was solved, and the inhibition of leakage by blocking MOFs with a cleavable cross-linker opened new prospects for the development of stimuli-responsive carriers.

(3) Other endogenous stimuli-responsive controlled-release system

Concentration levels of a wide range of small molecules in the body are closely related to the state of cellular life activity and therefore endogenous small

molecule-based stimulus-response release systems are developing rapidly. Diabetes, for example, is a high-risk disease behind cardiovascular disease and cancer, and the development of glucose-responsive controlled drug release systems is therefore important for the personalized treatment of diabetes, as individual blood glucose levels must be tightly controlled to reduce the risk. Zhao et al. encapsulated glucose oxidase (GOx) and insulin into MOFs structures (Ins-GOx/ZIF-8) by self-assembly (Duan et al., 2018). When the glucose concentration increases, it is catalyzed by GOx to produce gluconic acid and oxygen peroxide, and the acidic environment created by the cascade reaction can degrade the nanoparticles and releases insulin to lower blood glucose levels.

Adenosine triphosphate (ATP) is another important endogenous biomolecule involved in a variety of life activities and is therefore also often used to design stimuli-responsive systems (Chen et al., 2017; Lai et al., 2015).

2.4.2. Exogenous stimulus response

In tumor therapy, in addition to endogenous stimuli such as pH, redox molecules, biomacromolecules and physiological stimuli specifically generated by the tumor microenvironment, exogenous stimuli like light, temperature and magnetic field are also widely used as stimulation signals for smart material response. Using external physical stimuli as induction factors, the timing and site of drug release can be conveniently regulated by artificially changing the time and site of applied stimuli, reducing the toxic side effects of the therapeutic process on adjacent areas. In addition, with the help of external stimulation sources, novel treatment methods for tumors can be developed, such as photothermal therapy (PTT), which refers to the use of photothermal conversion reagents to convert light energy into heat energy to produce heat to kill tumor cells and thus treat tumors. It even integrates multifunctional treatment of tumor in one, which greatly enhances the treatment effect of tumor.

(1) Photo responsive controlled-release system

Light is a stimulus signal that is non-invasive, easily controlled, and has some penetrating ability to tissues. Photo responsive release is the controlled release of a drug by light using light as a stimulus signal (He et al., 2012; Li et al., 2017; Weissleder 2001). Photo responsive nano-drug delivery systems often use photosensitive molecules (e.g., azobenzene (Luo et al., 2015; Ma et al., 2015), coumarin (Lin et al., 2010; Yan et al., 2019)) to close the nanopores of porous nanoparticles, and upon irradiation with specific wavelengths of light (e.g., ultraviolet, visible, or near-infrared light), the photosensitive molecules undergo conformational transitions and the nanopores open, thus triggering drug release. In 2003, Mal et al. attached a light-sensitive coumarin to the outlet of mesoporous silica MCM-41 pore to form a photochemically controlled molecular switch (Mal et al., 2003). When the incident light wavelength >350mn, photodimerization reaction occurs between coumarin molecules and a cyclobutene dimer is formed to close the pore channel of mesoporous silica; when high energy incident light of 250nm is used, the dimer is photocleaved, the coumarin monomer reappears, and the mesoporous silica pore channel opens.

The system achieved the first light-response controlled release, which laid a good foundation for the future research of light-controlled release system.

Since UV radiation causes some damage to the normal body and does not penetrate tissues as well as NIR light, NIR light is often used as a stimuli-responsive signal to control drug release. There are same nanomaterials with strong NIR absorption ability, such as gold nanorods and nanoshells, carbon cores and shells (Kuo et al., 2010; Park et al., 2009; Ryplida et al., 2019; Yao et al., 2019). When there is NIR light irradiation, these nanomaterials absorb the energy of NIR light, so that it can be effectively converted into heat energy, and combining such materials with porous nanoparticles, the drug can be released from the carrier through the photothermal effect and at the same time can kill the killing effect to achieve chemo-photothermal synergistic therapy (Botella et al., 2009). Yang et al. obtained DOX/Pd@Au@ZIF-8 nanocomposites (Figure 13) by using MOF to encapsulate both Pd@Au nanoparticles with superior photothermal conversion and DOX (Yang et al., 2017). The ZIF-8 framework can be decomposed under acidic conditions to release encapsulated DOX. In addition, Pd@Au nanoparticles can effectively convert NIR into thermal energy, further promoting the release of DOX while achieving synergistic chemotherapy on cancer cells. With the synergistic chemo-photothermal therapeutic properties of pH and NIR-triggered nanocomposite systems, the door is opened to realize

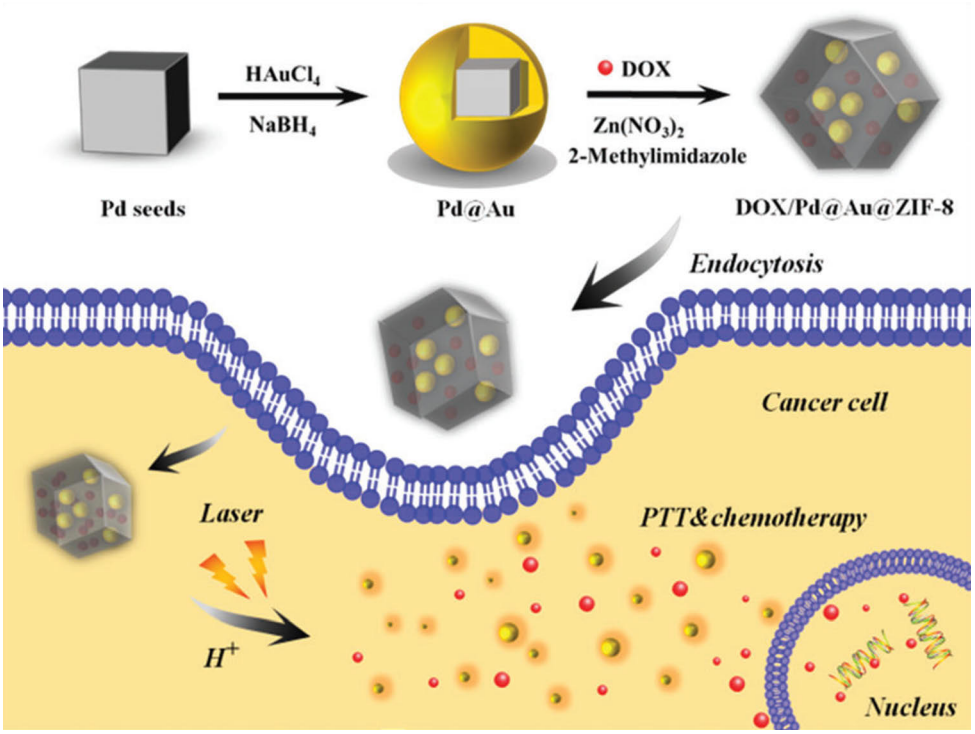

Figure 13. *Scheme of DOX/Pd@Au@ZIF-8 formation and pH and NIR-triggered chemo-photothermal synergistic treatment of cancer cells. (Copyright 2017, Royal Society of Chemistry)*

diverse applications for cancer therapy (Deng et al., 2019; Li et al., 2018; Zhang et al., 2018; Zhu et al., 2016).

(2) Thermal responsive controlled-release system

Thermal stimuli responsive nanocarriers are mainly covalently modified on the surface of porous nanoparticles by temperature-sensitive polymers or complementary DNA chains, and their conformational changes at different temperatures are used to achieve gated switching and drug release. When the body temperature rises, normal tissues increase blood flow and speed up the flow rate to improve heat dissipation and reduce the damage to the body, while tumor tissues have difficulties in heat dissipation due to rapid cell proliferation and neovascular malformation. Under the same warming conditions, tumor tissues are generally 4-8°C higher than normal tissues (Hildebrandt et al., 2002; Issels 2008). According to this feature, local heating of tumor can be used to induce temperature-sensitive carriers to target tumor. When the ambient temperature is below the lower critical solubility temperature (LCST) of temperature-sensitive polymers, the polymeric material is in a water-soluble dissolved state, and the increase in temperature leads to a decrease in the water-solubility of the temperature-sensitive polymer and then dissociation. This phase change behavior is the main principle of thermally responsive drug delivery systems.

Currently, the commonly used temperature-sensitive material is poly(N-isopropylacrylamide) (PNIPAM). At its critical temperature (about 32°C),

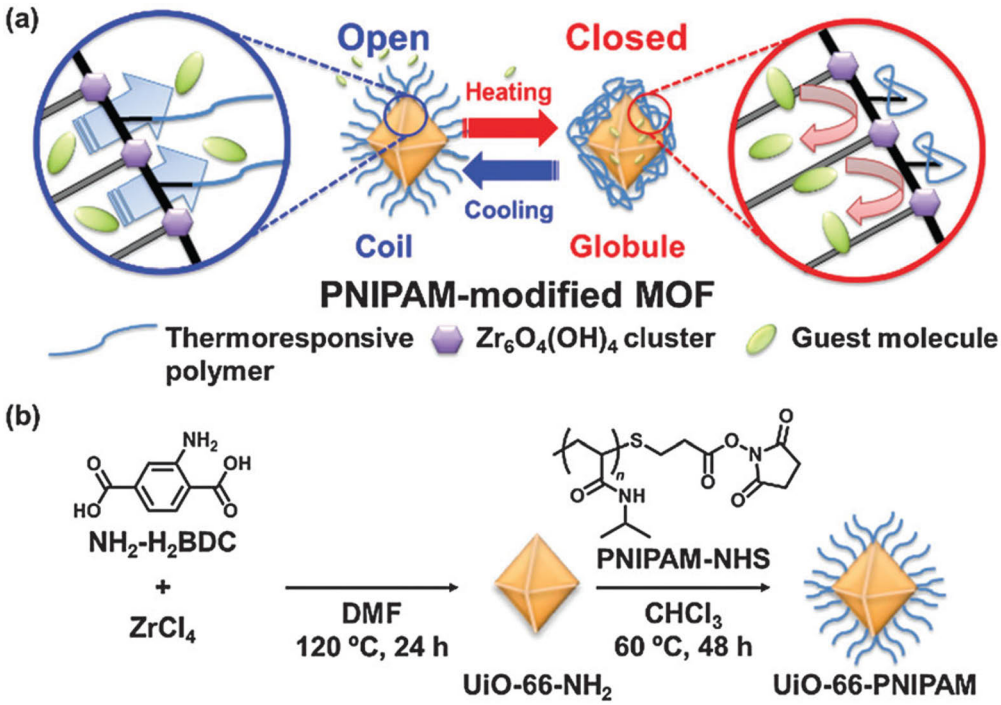

Figure 14. *Scheme of thermal-responsive MOF tethering PNIPAM-based controlled drug release and preparation approach. (Copyright 2015, Royal Society of Chemistry)*

PNIPAM is hydrophilic, and the structural chains are stretched, while above 32°C, the hydrogen bond between PNIPAM and water molecules is broken and it exhibits hydrophobicity, causing it to shrink (Halperin et al., 2015). You et al. used this property to modify the temperature-sensitive polymer PNIPAM on the surface of MSNs (You et al., 2008). When the temperature was higher than 38°C, PNIPAM was spherical and blocked the silica mesopores, which could prevent the early release of drugs. And when the temperature was below 32°C, PNIPAM was curled and the fluorescent molecules in the mesopores were released. In addition, in MOF-based thermoresponsive drug carriers, a thermoresponsive blocking substance can be modified on the surface of the MOF, whose conformation changes or dissociates upon stimulation by a heat source (light or magnetic field), losing the ability to block the release of the loaded drug (Jiang et al., 2017; Silva et al., 2019; Wu et al., 2018; Wu et al., 2018). The first MOF tethering a thermoresponsive polymer was fabricated by Nagata et al. through a surface-selective post-synthetic modification technique (Nagata et al., 2015). The conformational change of the thermoresponsive polymer grafted onto the MOFs (Figure 14) by a simple temperature change easily switches the "open" (low temperature) and "closed" (high temperature) states of the polymer-modified MOF, thus enabling the release of the guest molecules (e.g.,, resorufin, caffeine, and procainamide) entrapped in the smart MOF to be controlled.

(3) Other exogenous stimuli-responsive controlled-release system

Magnetic field response has better tissue penetration compared to light response, which not only allows for precise driving of the drug-loaded magnetic nanoparticles to the targeted site to improve treatment efficacy, but also acts as a non-invasive external stimulus to trigger controlled release of the drug (Kumar and Mohammad 2011). The magnetically responsive nano-drug delivery system is based on the combination of superparamagnetic iron oxide nanoparticles with porous nanomaterials. There are two main forms of binding: a typical core-shell structure formed by the iron oxide nanoparticles as the core and the porous materials as the shell; and a conjugation of the iron oxide nanoparticles to the surface of the porous materials. Due to the superparamagnetic property of iron oxide, the iron oxide-porous nanoparticles generate heat when exposed to an oscillating magnetic field, and the increased temperature in the porous materials can be used to open the capped nano-valve thereby enabling the release of drugs. Thomas et al. incorporated zinc-doped iron tetroxide (Fe_3O_4) nanoparticles into the structure of MSNs (Thomas et al., 2010). When an AC magnetic field is administered, the internal heating of the Fe_3O_4 particles following magneto-thermal action will lead to the decomposition of the molecule (PNIPAM) acting as a valve and induce the release of the drug from the pores. Similarly, Chen et al. developed a novel Fe_3O_4@C@MIL-100(Fe) (FCM) nanoparticles for the simultaneous delivery of dihydroartemisinin (DHA) and Fe(III) ions for cancer therapy, demonstrating an increased intracellular accumulation of the DHA in tumors through the presence of Fe_3O_4 nanoparticles guided by an external magnetic field (Wang et al., 2016).

Ultrasound, which is widely used in clinical applications (imaging, flow analysis, physiotherapy and tumor ablation), can also be used to stimuli-responsive drug delivery which enables spatiotemporal controlled drug release at the targeted site to reduce damage to healthy tissues, and also allows manipulation of tissue penetration depth by adjusting frequency, duty cycle and exposure time (Frenkel 2008; Gao et al., 2005). Ultrasound-induced thermal and/or mechanical effects have been used to trigger the release of drugs from various nanocarriers. Studies have shown that non-invasive ultrasound can destabilize nanocarriers, achieve drug release and increase vascular permeability to enhance the cellular uptake of therapeutic molecules (Kheirolomoom et al., 2010).

2.4.3. Multiple stimulus responses

In addition to a single stimulus response, the development of multiple stimulus response signals for the controlled release behavior of the same carrier can further improve the controlled release of drugs in a specific time and space and increase the chemotherapeutic effect of anticancer drugs. Simultaneous design of nanocarriers with multiple stimulus responsiveness can help to integrate multiple therapeutic modalities for tumors and significantly enhance the therapeutic effect of tumors. Generally multi-responsive nanocarriers can be triggered by a combination of two or more stimuli (Kim et al., 2015; Loh et al., 2012; Luo et al., 2019; Wang et al., 2012; Yang et al., 2014), such as pH and redox (GSH or ROS) response, pH and temperature response, dual pH response, light and temperature response, which are more controllable responsive modes. The responses of these combinations of triggers can occur simultaneously at the target site or sequentially as the nanocarriers enter the cell. Multi-stimulus responsive systems are designed by adding some functional nanoparticles or modifying various functional molecules in addition to molecular switches on the surface of porous nanocarriers, which can give full play to the characteristics of different environmentally responsive substances and are important for achieving specific delivery of drugs. The design of responsive drug delivery systems will provide a novel strategy for antitumor research. However, multiple stimuli-responsive drug carriers are more difficult to modify the carrier structure, more complex to synthesize and more difficult to control the qualities than single-responsive carriers. It is hoped that such problems will be effectively solved in the future with the continuous development and interpenetration of polymeric materials and molecular oncology. In addition, there is still a long way to go for porous nanomaterial-based drug delivery systems to enter the clinical market, and more evidence on safety and efficacy is yet to be discovered.

3. Hypothesis and objectives of the work

As a new type of nanocarrier, porous nanomaterials have high specific surface area, modifiable internal and external surfaces, uniform and adjustable pore size and unique pore structure, and other physicochemical properties, which are widely used in the field of controlled release of drug stimulus response, and their stimulus response mechanisms are diverse. However, various stimuli-responsive release systems based on porous nanomaterials developed so far have defects such as high biotoxicity of blocking molecules, insufficient drug loading capacity, and bioenrichment of carrier materials. Therefore, based on the scientific issues of further improving the loading capacity of carriers, reducing the biotoxicity of carrier materials and blocking molecules, exploring different synthesis methods and developing multifunctional stimuli-responsive nano-drug carriers, based on an extensive review of the latest literature reports related to porous nanomaterials and combined with the research base and conditions in our laboratory, this thesis proposes to carry out research in the following aspects.

Firstly, we were to utilize the biocompatible MSNs nanoparticles as small molecule drug delivery carriers, e.g.,, for targeted treatment of antibody-mediated rejection after kidney transplantation, by developing NIR-induced photothermal responsive nanoparticles to deliver immunosuppressive drugs to the allograft organ after transplantation and to reduce local inflammation and immune infiltration. The MSNs was then used for the encapsulation and delivery of nucleic acid-like biomolecules for proof-of-concept gene editing technologies. (Paper I and II)

Furthermore, through post-synthetic modifications, biomimetic mineralization and microfluidic-assisted synthesis, we were to explore the encapsulation, protection and delivery of small molecule drugs and biomacromolecules by MOF-based porous nanomaterials, investigate the relationship between nanostructures and molecule functions, and stimuli-responsive cargoes release, ultimately enabling effective delivery of anti-cancer drugs, CRISPR-Cas9 plasmids and proteins, and the potential for anti-cancer efficacy and gene therapy based on such nanotechnology. (Paper III, IV and V)

4. Materials and methods

In this section, the materials and methods used in the thesis work are described. The main materials involved in the synthesis of MOFs and MSNs are discussed in the materials section. The main characterization methods are discussed in the methods section. More details can be found in the attached Papers I-IV.

4.1. Materials

All chemicals were purchased from Sigma-Aldrich, ACROS Organics, TCI, Alfa Aesar, Lumiprobe Corporation, Abcam, Novex or VWR and used without further purification.

4.2. Fractionation and preparation approaches

4.2.1. Preparation of materials and technics

Plasmid amplification and extraction (IV)

100 μL of plasmid contained E. coli cell solution was spread on the LB agar plates and incubated overnight at 37°C. A single colony of E. coli cells on the agar plate was transferred to the 50 mL LB medium and incubated for 8 hours at 37°C with continuous low speed shaking. Next, Miniprep kit was used to collect purified plasmids according to their protocol provided with the kit. Plasmid concentration measurements were performed on a NanoDrop 2000c (Thermo Fisher Scientific, USA) at 260 nm. The A260/A280 ratio was measured to assess the purity. Finally, the two plasmids were dissolved in DNase free water and stored in -20°C for further use.

Fabrication of microfluidic chip (V)

The 3D microfluidic co-flow focusing chip was produced by assembling two borosilicate glass capillaries (World Precision Instruments Ltd, UK) on a glass slide. The two glass capillaries, with outer diameter of 1000 and 1100 μm, were named as inner and outer capillaries. Briefly, the end of the inner capillary was tapered with a magnetic glass microelectrode horizontal needle puller (P-31, Narishige Co., Ltd, Japan) and polished with sandpaper (Indasa Rhynowet, Portugal) until the cross-section was flat. The inner tapered capillary was then put in the outer capillary and coaxially aligned. After fixing them on the glass slide, one hypodermic needle was placed on the outer capillary and sealed with transparent epoxy resin.

4.2.2. Synthesis of nano-drug carriers

Synthesis of CuS nanoparticles (I)

40 μL of CTAC was added to 10 mL of $CuCl_2$ (13.5 mg, 0.1 mmol) solution and stirred for 15 min, followed by the addition of 0.1 mL of sodium sulfide (1 M) solution and stirred for another 15 min at room temperature. The mixture was then heated to 90 °C and stirred for 15 min, then moved to dry ice and cooled for 10 min, resulting in the formation of CTAC-stabilized CuS (CuS-CTAC) nanoparticles.

Preparation of PB (V)

3 g of PVP and 226.7 mg of $K_3[Fe(CN)_6]$ were dissolved in 40 mL of water and stirred until clear. Then 35 μL of concentrated hydrochloric acid was added to the above solution and stirred for 30 min, followed by heating at 80 ℃ for 20 hours. The product PB was collected by centrifugation and washed three times with water and ethanol.

Synthesis of DCA-UiO-66-NH_2 (III)

1.0 g of $ZrCl_4$ (4.2 mmol) and 761.0 mg of $H_2BDC\text{-}NH_2$ (4.2 mmol) were dissolved in 150 mL of DMF, mixed and transferred to a 250 mL vial. 3.0 mL of dichloroacetic acid (DCA, 36.0 mmol) was added to the mixture and heated at 120 ℃ for 24 hours. After cooling to room temperature, the nanoparticles were collected by centrifugation and washed 3 times with DMF and ethanol.

Preparation of MSNs (II)

24 mL of CTAC (25 wt%) and 0.18 g of TEA were added to 36 mL of water and stirred at 60 °C for 1 hour. Then 20 mL of TEOS (10 v/v%) in cyclohexene was carefully added to the above solution under stirring. The reaction was kept at 60 °C with gentle magnetic stirring overnight to obtain the products. After that, the MSNs were collected by centrifugation and washed several times with ethanol to remove the residual reactants. To remove the template, the collected products were extracted with a 0.6 wt% NH_4NO_3 ethanol solution at 60 °C for 6 hours each.

Synthesis of CuS@MSN (I)

2 g CTAC (25 wt % solution), 20 mg TEA and 2.5 mL of preprepared CuS-CTAC were dissolved in 20 mL of water and stirred for 1 hour at room temperature. Then, 200 μL of TEOS was added to the above solution and stirred in a water bath at 85-90 °C for another 1 hour. The cooled mixture was collected by centrifugation and washed with water to remove residual reactants, then dispersed in 1 wt % NaCl methanol solution and stirred for 24 hours, repeated 3 times to remove the template.

Biomineralisation of ZIF-8 with plasmids (IV)

Different amounts of P1 were dispersed into 2 μL of zinc nitrate solution (67.5 $mg{\cdot}mL^{-1}$) and stirred for 5 min, and then added to 8 μL of 2-methyl imidazole solution (2-MIM, 463.75 $mg{\cdot}mL^{-1}$). The mixture was aged for 1 hour, and the formed P1-ZIF-8 (P1Z) biocomplex was collected by centrifugation and then washed three times to remove loosely adsorbed plasmids.

In a similar synthetic procedure, P1 was dispersed into 8 μL of 2-MIM solution and stirred for 5 min, followed by the addition of 2 μL of zinc acetate solution. The mixture was aged for 1 hour, and the formed ZIF-8-P1 (ZP1) biocomplex was collected by centrifugation and washed three times to remove the attached plasmids.

The synthesis of P1P2-ZIF-8 (P1P2Z) nanostructures were performed similarly. P1 and P2 were mixed (in 1:1 ratio) with 2 μL of zinc nitrate solution and stirred for 5 min at room temperature before added into 8 μL of 2-MIM solution slowly. 1 hour later, the final product was obtained after centrifugation, washed, and dispersed into water.

Microfluidic-assisted synthesis of PB-EuMOFs (V)

PB-EuMOFs core-shell nanoparticles were prepared at room temperature using a microfluidic 3D co-flow device. First, PB and Eu^{3+} were mixed and stirred for 5 min to form a stable solution under electrostatic interaction as the inner phase. The aqueous GMP solution was used as the outer fluid. The inner and outer fluids were pumped separately into a microfluidic device, where the inner fluid was focused by the outer continuous fluid, and the flow rates of the different liquids were controlled by pumps (PHD 2000, Harvard Apparatus, USA). The formed EuMOFs particles were coated on the PB, and the obtained products were collected by centrifugation and washed 3 times with water to remove any residues. To optimize the physicochemical properties of the prepared core-shell nanoparticles, the process variables and formulation parameters were evaluated, such as the total flow rate of inner and outer fluids, the flow ratio between the inner and outer fluids, and the concentration of PB, Eu^{3+} and GMP.

4.2.3. Modification & functionalization of nanoparticles

Modification of CuS@MSN (I)

The amino modified CuS@MSN was obtained by adding 1 mL of APTEOS to 20 mL of CuS@MSN (2 mg·mL^{-1}) ethanol solution and reacting for 48 h at room temperature. CuS@MSN-NH_2 was collected by centrifugation and washed several times with ethanol to remove the free APTEOS.

Surface functionalization of MSNs (II)

50 mg MSNs and 50 μL APTEOS were refluxed overnight in ethanol at 60 °C to obtain aminated MSNs particles (MSNs-NH_2), and the resulting product was collected by centrifugation and washed twice with ethanol.

NLS conjugation with MSNs (II)

2 mg (2 μmol) of NLS was dissolved in 10 mL of PBS (pH = 6), and then 19.17 mg of EDC (0.1 mmol) and 17.26 mg mmol NHS (0.15 mmol) were added and stirred for 30 min to activate the carboxyl group. 20 mg of MSNs-NH_2 particles were then added to the NLS mixture and stirred for 2 h to obtain NLS-modified MSNs particles (MSNs-NLS).

Postsynthetic modification of DCA-UiO-66-NH_2 (III)

The amino groups of MOFs reacted with 3,3′-dithiodipropionic anhydrides (DTDPA) to form carboxylic acid-functionalized DCA-UiO-DTDP. 192.25 mg of DTDPA (4.0 mmol) was added to the synthesised DCA-UiO-66-NH_2 (4.0 mmol of -NH_2) DMF solution and placed at room temperature for 24 hours. DCA-UiO-DTDP was collected by centrifugation and washed three times with fresh DMF and ethanol.

Folic acid-targeted modification of DCA-UiO-DTDP (III)

5 mg of DCA-UiO-DTDP was dispersed in MeOH, and then EDC and NHS were added to activate the carboxyl groups on DCA-UiO-DTDP in the ration of 1:1.2:2. After 6 hours, 5 mg of aminated FA was added to the solution overnight at room temperature. DCA-UiO-DTDP-FA were collected by centrifugation and washed twice with MeOH.

Preparation of CuS@MSN@PMcN (I)

5mg of poly(N-isopropylacrylamide-co-methacrylic acid) (PNcM) was added to CuS@MSN-NH_2 aqueous solution and stirred overnight to coat the polymer on the nanoparticles by electrostatic interaction. The obtained CuS@MSN@PMcN was separated by centrifugation and washed with water to remove the free polymer.

Conjugation of the complement component 4d (C4d) antibody with CuS@MSN@PMcN (I)

1.0 mg of CuS@MSN@PMcN was dispersed in 1 mL of PBS, followed by adding 1.0 mg EDC and 1.0 mg of NHS, 1.0 mg, and mixed for 6 h at room temperature. Then 20.0 μg of C4d antibody was added to the mixture and stirred at 4 ℃ for 24h. The suspension was then centrifuged and washed twice with PBS and stored in the same buffer solution at 4 ℃ in the dark until use.

Polymer coating with MSNs-NLS (II)

PDDA (1.25 mg·mL^{-1}) and plasmid-loaded MSNs-NLS (P1P2@NPs, 250 μg·mL^{-1}) were mixed in water as inner phase, and ethanol as the outer phase. The two liquids were injected into the microfluidic device separately, and the flow rates were controlled by pumps. The hydrophilic polymer was precipitated on the nanocarrier surface in ethanol to form a uniform layer. The coated nanoparticles (P1P2@NPs@PDDA) were obtained after centrifugation.

4.3. Characterization methods

4.3.1. Composition and structure analysis

High-performance liquid chromatography

The standard curves, drug loading efficiencies and release profiles were both determined by an Agilent 1100 HPLC (Agilent Technologies, USA) system equipped with a Waters Symmetry Shield RP18 Column (4.6×250 mm, 5 mm, Waters Corporation, USA) and a UV detector. The samples were run at 30 °C and eluted with a mobile phase of PBS (50 mM, pH=6.0) and acetonitrile at 1.0 mL·min^{-1}.

Fourier-transform infrared spectroscopy

FTIR spectra were recorded on a FTIR spectrophotometer (PerkinElmer Spectrum Two FT-IR Spectrometer, Waltham, USA). Each sample was recorded with 64 scans from 4000 to 400 cm^{-1} with a resolution of 0.5 cm^{-1}. The fingerprint region was baseline corrected between 1900 and 750 cm^{-1}.

X-ray diffraction (XRD) patterns

The XRD patterns were recorded with a Bruker Discover D8 (Bruker-AXS, Karlsruhe, Germany), Ni-filtered Cu Kα radiation, operating at 45 kV and a filament current of 40 mA. The scattering angle (2θ) of the XRD patterns ranges from 0 to 80°.

Nuclear magnetic resonance (NMR) analysis

^1H spectra of the MOFs were recorded at room temperature with deuterated sulfuric acid (D_2SO_4) and dimethyl sulfoxide (DMSO-d_6) as solvents, using a 500 MHz Bruker AMX 500 instrument equipped with a 5-mm broadband probe with a gradient field in the Z-direction.

UV-Vis spectrophotometers

The plasmid purity and drugs concentration analysis were determined a full-spectrum (190-840 nm), NanoDrop 2000/2000c UV-Vis spectrophotometers (Thermo Scientific).

Transmission electron microscopy

The TEM images were obtained using a JEM-1400 Plus TEM microscope (JEOL Ltd., Japan) with a measurement voltage of 80 kV. The samples were sonicated in solution and coated on a carbon supported copper grid.

Dynamic light scattering (DLS) and zeta-potential

The size distribution and zeta-potential of the obtained nanoparticles were determined by a Zetasizer Nano ZS instrument (Malvern Instruments Ltd., UK). The samples were uniformly dispersed by sonication and measured 3 times.

4.3.2. *In vitro* cell studies

Cell proliferation assay for cytotoxicity

Breast cancer cell line (MDA-MB-231), non-tumorigenic epithelial cell line (MCF-10A), human osteosarcoma epithelial cells (U2OS), human cervical cancer cells (Hela), human cervical cancer cells introduced with green fluorescence protein genes (Hela/GFP), C57BL/6 mouse primary kidney glomerular endothelial cells (mGEnCs) were used to determine the toxicity of nanoparticles. The water-soluble tetrazolium salt (WST-1) assay was performed according to the manufacturer's instructions. Briefly, different cells (5×10^3 cells·well^{-1}) were seeded onto 96-well plates overnight, and then treated with different concentration of drugs or nanoparticles for 12/48/72 hours. 10 μl WST-1 reagent was added to each well and the absorbance at 450 nm was measured after 4 hours incubation using a multi-mode plate reader (Varioskan Flash, Thermo Fisher Scientific, USA).

Confocal laser scanning microscopy (CLSM)

The cellular endocytosis in different cell lines was observed by CLSM. Different cells (2×10^5 cells·well^{-1}) were seeded in confocal dishes overnight and then incubated by added 2 mL of nanoparticles suspensions. At different time points, the cells were washed with PBS to remove the free nanoparticles. 4% paraformaldehyde (2 mL·well^{-1}) was added and incubated for 10 min to fix the cells, followed by rinsing with PBS. The nuclei were stained with DAPI solution (20 mg·mL^{-1} in PBS, 1 mL·well^{-1}) for 5 minutes, and washed again with PBS, and the samples were examined with a Zeiss LSM880 with air scan instrument.

Flow cytometric analysis of cellular uptake

The cellular endocytosis was also studied by flow cytometer. Following the same procedure as for CLSM, the nanoparticles were added to the cells and incubated. At different time points, cells were detached, collected by centrifugation, washed, and resuspended in 500 μL of PBS for fluorescence analysis with BD LSRFORTESSA.

Optical microscopy

The fluorescence microscopy images of plasmid loaded nanostructures treated U2OS cells or CRISPR-Cas9 RNP treated Hela-GFP cells after different period

were observed using a AMG Evos optical microscope to check the gene transfection and expression *in vitro*.

4.3.3. *In vivo* evaluation assay

Animal materials

The experimental protocol involving animals was approved by the Research Ethics Committee of the First Affiliated Hospital, College of Medicine, Zhejiang University (No. 2019-1231) and performed in accordance with the National Institutes of Health Guide for the Care and Use of Laboratory Animals (NIH Publication No. 80-23). 8-week-old male Balb/c and C57BL/6 mice (weight: 23 ± 2 g) were obtained from the Laboratory Animal Center of Zhejiang University. Animals had free access to water and standard rodent chow, and were maintained in a controlled environment (25℃) under a 12 h light/dark cycle.

Evaluation of *in vivo* toxicity

C57BL/6 mice were received intravenous injection of PBS, methylprednisolone (MP group), MP-NP, or MP-NP-C4dAb every 3 days for 4 weeks. The dosages of methylprednisolone in the MP, MP-NP, or MP-NP-C4dAb groups were equivalent to 1mg/kg. Body weight was monitored weekly. At the end of the 4 weeks, mice were metabolic cage studies for nephrotoxicity assessment, and sacrificed to harvesting serum and multi-organs.

***In vivo* imaging system (IVIS) for targeting**

Spectrum imaging was performed using IVIS Lumina LT Series III (Perkin Elmer, MA, USA) with a Cy5.5 filter set (excitation 675 nm, emission 720 nm, exposure time 1 s) to obtain Cy5.5 conjugated NP signals. All images were acquired and analyzed using Living Image version 4.5 software (PerkinElmer) and displayed in the same fluorescent intensity scale. Fluorescence emission was normalized to photons per second per centimeter square per steradian.

Histological analysis

The fixed tissues were paraffin embedded and cut into 3 μm thick sections. The sections of kidney, heart, liver, spleen, lung, and brain were stained with hematoxylin and eosin (H&E), periodic acid schiff (PAS), and/or Masson's trichrome. Liver sections were additionally stained with Oil Red O to show neutral lipid. Photomicrographs were taken with Leica DM4000 microscopy (Leica, Frankfurt, Germany) and analyzed using NIH Image J software.

5. Results and discussion

5.1. Overview of the thesis work

The overall purpose of this work is to investigate the feasibility of drug/biomolecule delivery under stimulus responsiveness by using biocompatible porous materials such as mesoporous silica and metal organic framework nanoparticles (Figure 15). The *in vivo* applications of MSNs material-based drug delivery systems were first examined, followed by using MSNs for the transportation of proof-of-concept gene editing materials. The MOFs matrix material was then modified in situ for anticancer drug delivery, in addition to investigating the MOFs material encapsulate biomolecules for better controlled gene therapy research with the help of biomineralization and microfluidic technology.

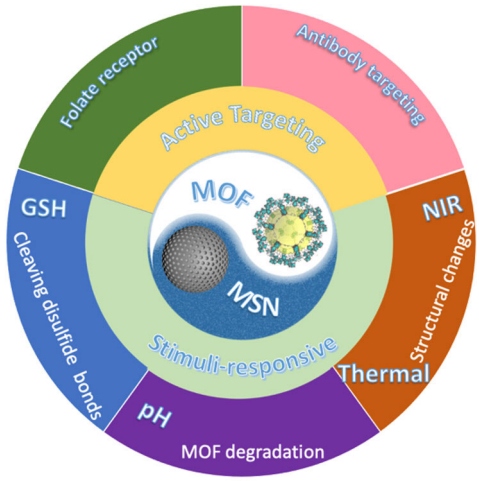

Figure 15. *Overview of the thesis work.*

The specific workflow of the thesis is as follows:
(I) *In vivo* kidney allograft endothelial specific scavengers for on-site inflammation reduction under antibody-mediated rejection.
(II) Effective delivery of the CRISPR-Cas9 system enabled by functionalized mesoporous silica nanoparticles for GFP-Tagged paxillin knock-in.
(III) *In situ* post-synthetic modification of MOFs to explore their synergistic enhancement of anticancer ability as tumor-targeted redox-responsive dual drug carriers.
(IV) Improving the knock-in efficiency of MOFs-encapsulated CRISPR-Cas9 system through controllable embedding structures
(V) Microfluidics-assisted CRISPR-Cas9 RNP encapsulation in NIR-responsive MOFs for programmable gene editing.

5.2. MSNs-based porous nanomaterials for bioapplication (I, II)

In this section, the different synthetic methods have been used to synthesise MSNs with varied structures, followed by step-by-step surface modifications and physicochemical characterisation to obtain the desired nanomaterials for biological applications. The nanomaterials were then evaluated for their drug and biomolecule loading and release capabilities on cargo delivery, and therapeutic efficacy *in vitro* as well as *in vivo*.

Specifically, the core-shell structures of CuS@MSN for the delivery of small molecule immunosuppressive drug (methylprednisolone) and MSNs for the delivery of biomolecules (CRISPR-Cas9 plasmids) have been synthesized based on different synthetic approaches, and further functionalised with different polymers (e.g.,, thermosensitive polymers PNcM and pH-sensitive PDDA), their loading and stimuli-responsive release profiles were also carried out. The biocompatibility of the nanomaterials, such as cytotoxicity and cellular uptake, was subsequently assessed. The targeting capability and therapeutic efficacy of drug-loaded MSNs were also investigated *in vitro* and *in vivo*. The transfection expression and gene knock-in of biomolecule-loaded MSNs were also studied *in vitro* (Ohlfest et al., 2005). The formulation under study and their respective purposes have been summarized in Table 1.

Table 1. *Overview of the studied formulations for the biomedical applications of MSNs-based nanomaterials:*

	Synthesis methods	**Surface modification**	**Targeting**	**Cargo**	**Stimuli responsive**	**Main purpose**
CuS@MSN	Hard template	APTEOS PNcM C4dAb	C4d	MP	NIR	Anti-ABMR
MSNs	Two-phase	NLS PDDA	Cell nucleus	CRISPR-Cas9 Plasmid	pH	Gene editing

5.2.1. Design and characterization of the MSNs-based nanoparticles

MSNs have hosted guest drugs and biomolecules of various sizes, shapes, and functions through different synthetic methods and surface functionalisation. The smart MSNs-based nanocarriers have achieved drug delivery and gene editing effects by utilising a variety of "stimulus responses" (NIR and pH) and "gatekeepers" (PNcM and PDDA) construction strategies that enable them to modulate the release of cargo at targeted locations and for specific time periods.

5.2.1.1. Synthesis and functionalization of MSNs-based nanocarriers

The MSNs carriers used to deliver the CRISPR-Cas9 plasmids were firstly synthesised by a continuous growth one-pot two-phase layering method using surfactant CTAC as a template, TEA as a catalyst, TEOS as a silica source and cyclohexene as an emulsifier (Shen et al., 2014). To achieve stimuli-responsive release in drug delivery, copper sulfide (CuS) with near-infrared (NIR) photothermal conversion (Tian et al., 2011; Tian et al., 2011; Zhou et al., 2010)

was encapsulated in MSNs as a hard template. Since the surfactant CTAC is not only a capping agent to stabilize CuS nanoparticles but also a gelation agent for silica, CTAC-activated CuS (CuS-CTAC) embedded MSNs nanoparticles (denoted as CuS@MSN) were prepared by modulating the reaction conditions. The red fluorescent dye (Sulfo-Cyanine 5.5 NHS ester, Cy5.5) lablled MSNs and CuS@MSN (Cy5.5-MSNs and Cy5.5-CuS@MSN) were synthesized in the same way for intracellular visualization of the particles.

Later amino groups modification has carried out on the surfactant removed MSNs and CuS@MSN, which was reacted with APTEOS to form MSNS-NH_2 and CuS@MSN-NH_2. PNcM is a thermosensitive polymer with a relatively low critical solution temperature (LCST) in the aqueous phase and is used to impart thermo-responsive properties to CuS@MSN-NH_2 while avoiding leakage of the loaded drug from the pores. After loading the MP in the organic phase, since MP is insoluble in water, MP@CuS@MSN-NH_2 was transferred to the PNcM aqueous solution and the PNcM was deposited to encapsulate the drug-loaded CuS@MSN-NH_2 by electrostatic interaction (MP@CuS@MSN@PNcM, abbreviated as MP-NP). The nuclear loaction signal peptide (NLS) was conjugated to the surface of MSNs-NH_2 (MSNs-NLS) via a typical amidation to facilitate DNA transfection (Zhao et al., 2019). The polyelectrolyte PDDA, which acts as a pH-responsive gatekeeper molecule, subsequently encapsulated the plasmid-loaded MSNs-NLS by microfluidic nanoprecipitation. The P1P2@MSNs-NLS (P1P2@NPs) and PDDA were co-mixed, where PDDA was electrostatically adsorbed onto the nanoparticles and then pumped into the microfluidic inner capillary to precipitate P1P2@NPs@PDDA in the miscible two phases.

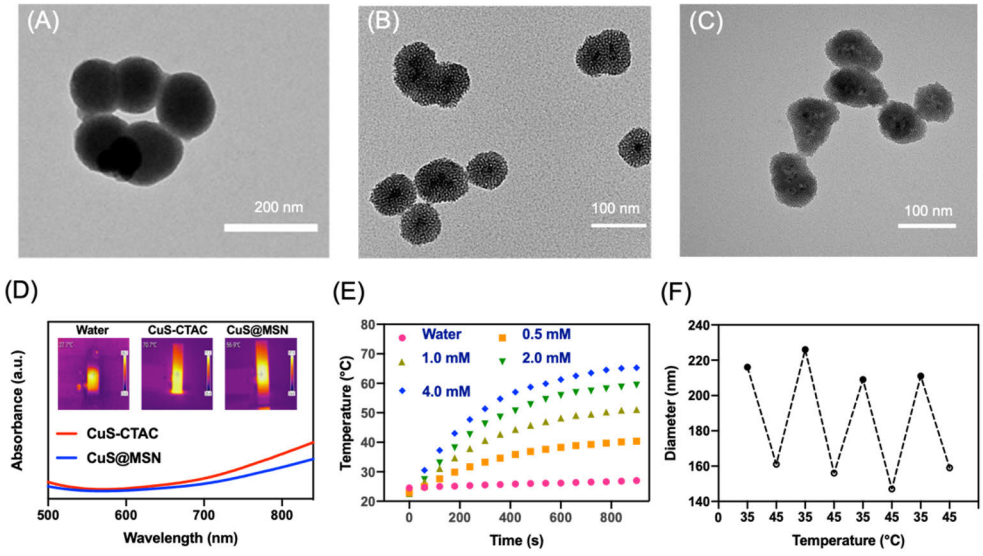

Figure 16. Characterization of the MSNs nanoparticles. *TEM images of prepared P1@NP@PDDA (A), CuS@MSN (B) and CuS@MSN@PNcM (C). (D) UV-vis absorption and photothermal images of CuS-CTAC and CuS@MSN. (E) Temperature variation of CuS@MSN solution versus 808 nm laser irradiation time. (F) The mean hydrodynamic diameters of NP versus temperature by DLS.*

5.2.1.2. Physicochemical characterization of the synthesized MSNs

The synthesized MSNs-based stimuli-responsive nanoparticles were confirmed by different techniques to determine their particle size, dispersion, and morphology. The highly ordered and pore visible core-shell structured CuS@MSN and polymers encapsulated P1@NP@PDDA and CuS@MSN@PNcM are shown by TEM (Figure 16A-C). DLS and zeta potential measurements reveal the degree of monodispersity and surface charge of the MSNs and CuS@MSN nanoparticles after surface amination and polymer coating. The green CuS@MSN has a strong absorption peak near 808 nm in the UV-Vis absorption spectrum (Figure 16D). The quantitative temperature variation with increasing laser irradiation time for different concentrations of CuS@MSN aqueous solution is investigated (Figure 16E). The photothermal conversion efficiency (η) of CuS@MSN after coating is higher than that of CuS-CTAC, making it very superior as a promising photothermal conversion agent (Liu et al., 2013). DLS measured (Figure 16F) the temperature-induced changes in the size of the NP nanoparticles and observed that the average hydrodynamic diameter of the nanoparticles oscillated in response to the temperature change. The diameter decreased when heated to 45 °C and returned to its original size when cooled to 35 °C. The temperature-induced size change demonstrates that the material exhibits controlled MP release using CuS@MSN@PNcM under intermittent 808 nm laser irradiation.

5.2.2. Drug loading and stimuli-responsive release

5.2.2.1. Loading of MP and NIR induced release (I)

The synthesized CuS@MSN with photothermal conversion properties can also be used for drug delivery. The small molecule immunosuppressive drug MP was loaded in CuS@MSN and sealed by PNcM (MP-NP). According to the standard curve, the loading capacity of MP was 326.1 $mg \cdot g^{-1}$ after 24 h of incubation. The *in vitro* release profile of MP-NP was investigated in PBS buffer under NIR-induced temperature changes (Figure 17A). In the ambient temperature without laser radiation, the loose polymer brush blocked the drug leakage and the solution concentration remained almost unchanged in the subsequent time,

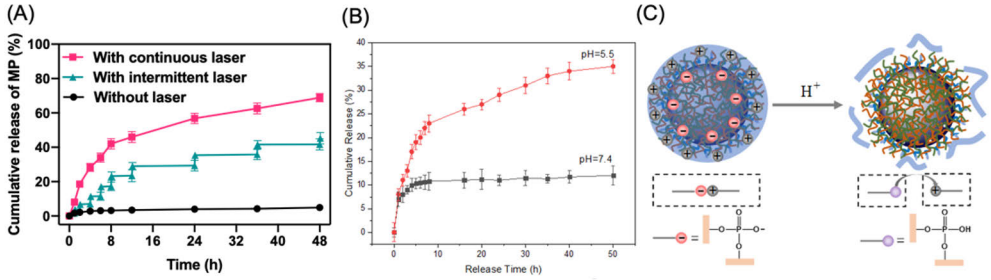

Figure 17. Evaluation of the drug release properties. *(A) Cumulative release of MP from MP-NP under various laser irradiation conditions. (B) Release profile of CRISPR-Cas9 plasmids from P1P2@NP@PDDA at different pH buffer (37 ℃). (C) The mechanism of pH-responsive plasmids release.*

except for the initial small burst effect caused by the MP adhering to the surface. In contrast, the sustained rapid release of MP at 45 °C resulting from continuous NIR irradiation remained consistent with the crumpling of the PNcM brush at high temperatures. Also, the instantaneous temperature increase inside the nanoparticles caused by intermittent irradiation of the NIR laser can accelerate MP release from the NP, which provides a new approach to tailor the drug release flow rate to achieve the desired therapeutic effect.

5.2.2.2. Loading nucleic acid and pH triggered release (II)

When MSNs-NLS was mixed with two plasmids (P1 and P2, mass ratio=1:1) in HEPES buffer (pH=6.5) solution and stirred continuously overnight at 4 °C. MSNs-NLS exhibited a strong positive charge to enhance the packaging on the negative charged nucleic acids, which was denoted as P1P2@NP@PDDA after coating by the polyelectrolyte PDDA. The loading capacity of MSNs-NLS on P1 and P2 was 50 μg·mg^{-1} as quantified by UV-Vis, suggesting that the prepared MSNs-NLS nanoparticles can be an superior carriers for effective integration of CRISPR-Cas9 plasmids. To verify the nucleic acids release under pH response of nanocarriers, they were immersed in PBS buffers of different pH values and detected by UV-Vis spectrophotometry for the change of solution concentration. The plasmid release shows a time dependence at different pH values (Figure 17B). Under physiological condition, the release is very little and essentially constant (~10%), demonstrating that the gate state around the mesopore is still closed due to the electrostatic interaction PDDA and plasmid. In contrast, the charge reversal of the plasmid due to a decrease in pH led to a conversion from phosphate ions (-PO_4^-) to protonated moiety (-PO_4H) (Figure 17C), and as the interaction between the plasmid and PDDA became weaker, the gatekeeper detached from the outside of P1P2@NPs@PDDA (Yang et al., 2005), resulting in a rapid release, reaching a maximum of 33% within 35 hours.

5.2.3. Cellular interactions

In this section, the cytotoxicity and biocompatibility of the biomaterials used, the targeting capability of nanoparticles on lesion cells, the effective endocytosis of

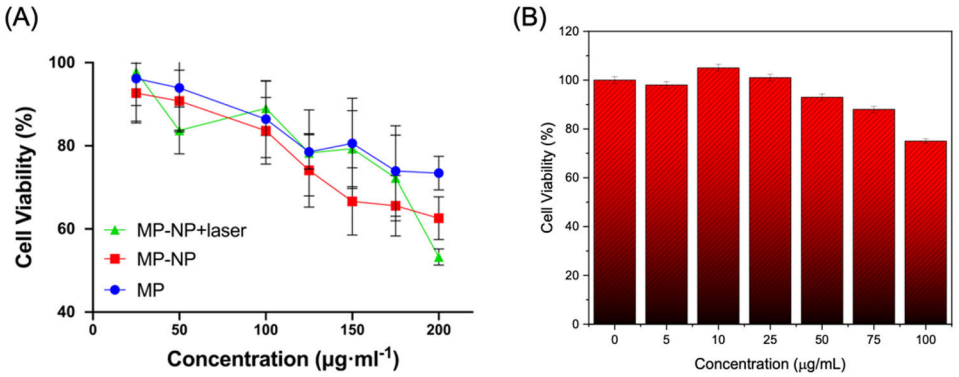

Figure 18. The cytotoxicity effects of nanoparticles. *(A) The viability of mGEnCs after incubated with different concentrations of free MP, MP-NP, and MP-NP. (B) U2OS cells viability after cultured with various concentration of P1P2@NPs@PDDA.*

nanoparticles, the expression and editing of loaded genes, and the therapeutic effects of delivered drugs are all investigated.

5.2.3.1. Cytotoxicity assay (I, II)

The cytotoxicity of MP-loaded NPs (MP-NP and MP-NP+Laser) and P1P2@NPs@PDDA was investigated by WST-1 assay on different cell lines to evaluate the cytocompatibility of the drug/biomolecule delivery system (Figure 18A). Even after incubation with high concentrations of free MP at 200 $\mu g \cdot mL^{-1}$, 70 % of mouse primary kidney glomerular endothelial cells (mGEnCs) were still viable. The MP-NP system exhibited similar toxicity of MP to mGEnCs after 24 hours of incubation without irradiation. With increasing drug concentration, the cytotoxic effect of MP-NP under NIR irradiation was slightly enhanced compared to MP-NP, which may be due to the excess concentration of MP suddenly released from NIR-induced NP. The cell viability of human bone osteosarcoma epithelial cells (U2OS) incubated with P1P2@NPs@PDDA for 48 hours with different concentrations of nanovihecals did not change significantly compared with the control (Figure 18B). The results indicated that the above two delivery systems were safe and biocompatible.

5.2.3.2. Intracellular targeting and therapeutics assay (I)

Specific inflammatory cell recognition is essential to achieve *in vivo* vascular endothelial targeting and drug therapeutic efficacy, and C4d-positive mGEnCs cells after complement activation were used for targeting studies of C4dAb-conjugated NPs (Figure 19A). A strong red signal was observed in C4d+ cells co-incubated with Cy5.5-NP-C4dAb (FITC-C4dAb), but no Cy5.5 signal was observed in cells co-incubated with Cy5.5-NP, indicating that the nanoparticles with C4d antibody bind exclusively to positive cells. Subsequent Transwell assays of lymphocyte invasion to endothelial monolayers were used to assess the *in vitro* therapeutic effect of drugs released in stimulus response (Figure 19B). A

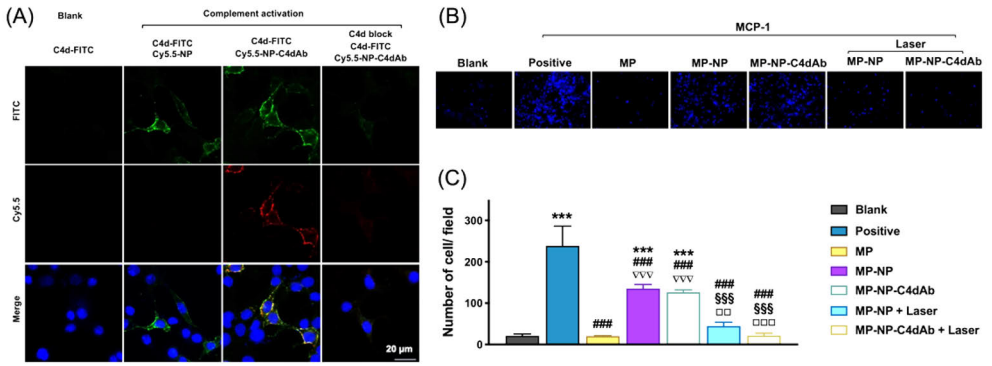

Figure 19. In vitro targeting and treatment efficacy assessment. *(A) CLSM of mGEnCs following immunofluorescence staining and nanoparticle targeting. (B) Transwell migration assay of lymphocytes across mGEnCs monolayer. (C) A statistical graph of migrating lymphocytes on mGEnCs monolayer. ***P < 0.001 vs Blank. ### P < 0.001 vs Positive. ▽▽▽P < 0.001 vs MP. §§§P < 0.001 vs MP-NP. □□P < 0.01, □□□P < 0.001 vs MP-NP-C4dAb.*

dramatic reduction in migrating inflammatory cells was clearly observed after MP administration compared to the positive group, indicating a strong anti-inflammatory effect of MP on lymphocytes. Nanoparticles loaded with equal amounts of MP drug (MP-NP and MP-NP-C4dAb) in both groups showed no immunosuppressive effect due to negligible drug release (Figure 19C). On the contrary, the infiltration of lymphocytes was significantly inhibited in both groups under NIR irradiation, which demonstrated the excellent therapeutic effect of the drug with precise laser-controlled release

5.2.3.3. Cellular uptake, gene expression and editing (II)

For effective genetic editing, the nucleic acid-loaded nanoparticles need to be effectively endocytosed by the target cells. CLSM and flow cytometry evaluated the uptake of two Cy5.5-labeled nanoparticles (P1P2@NPs and P1P2@NPs@PDDA) with U2OS cells incubated for different periods of time. The red fluorescence of P1P2@NPs@PDDA gradually increased with time (Figure 20A), compared to the lower level of fluorescent signal in P1P2@NPs-treated cells. Flow cytometry analysis obtained results consistent with CLSM (Figure 20B). The quantitative assay showed that the cells treated with P1@NPs@PDDA had a higher endocytosis efficiency, which may be due to the positively charged PDDA layer coated on the surface of the nanocarriers.

The capacity of nanovectors to deliver CRISPR-Cas9 plasmids was assessed by monitoring the expression of the loaded plasmids in the targeted cells. P1 fused with GFP sequences (Ran et al., 2013) and P1 loaded nanoparticles (P1@NPs@PDDA) were incubated with U2OS cells, respectively, and tracked for green fluorescence signal after transfection for 2, 4, 6 and 7 days. (Figure 20C) a clear GFP signal could be detected by fluorescence microscopy in a portion of U2OS cells treated with P1@NPs@PDDA for 2 days. In comparison, no fluorescence was observed in the free P1-treated U2OS cells, suggesting the feasibility of using the devised delivery approach for plasmid transfection. Subsequently, the number of GFP-positive cells decreased drastically as the plasmids were diluted with cell division. Only a low expressed signal could be observed at 4 and 6 days of treatment, , while the GFP signal almost disappeared after 7 days.

To verify the gene editing efficiency of nanovectors, the ability of PXN knock-in was investigated *in vitro*. In this assay, U2OS cells were transfected with equimolar ratios of P1 and P2 loaded nanovectors. P1 expresses sgRNA targeting the PXN coding region and Cas9 protein to creat double-stranded breaks (DSBs). The PXN sequence encoding GFP in P2 is inserted into the target site via the HDR pathway to repair the DSBs and the knock-in results can be detected by fluorescence microscopy. After 7 days of P1P2@NPs@PDDA treatment, significant GFP fluorescence could be observed in U2OS cells (Figure 20D). To examine GFP localized to the appropriate structure of paxillin, co-localization of focal adhesion and immunofluorescence of fibronectin staining was explored. The plated fibronectin can bind to paxillin in U2OS cells, displaying a dotted distribution of bright green fluorescence at localized focal adhesion sites. When the cells were incubated with monoclonal paxillin antibody and Alexa

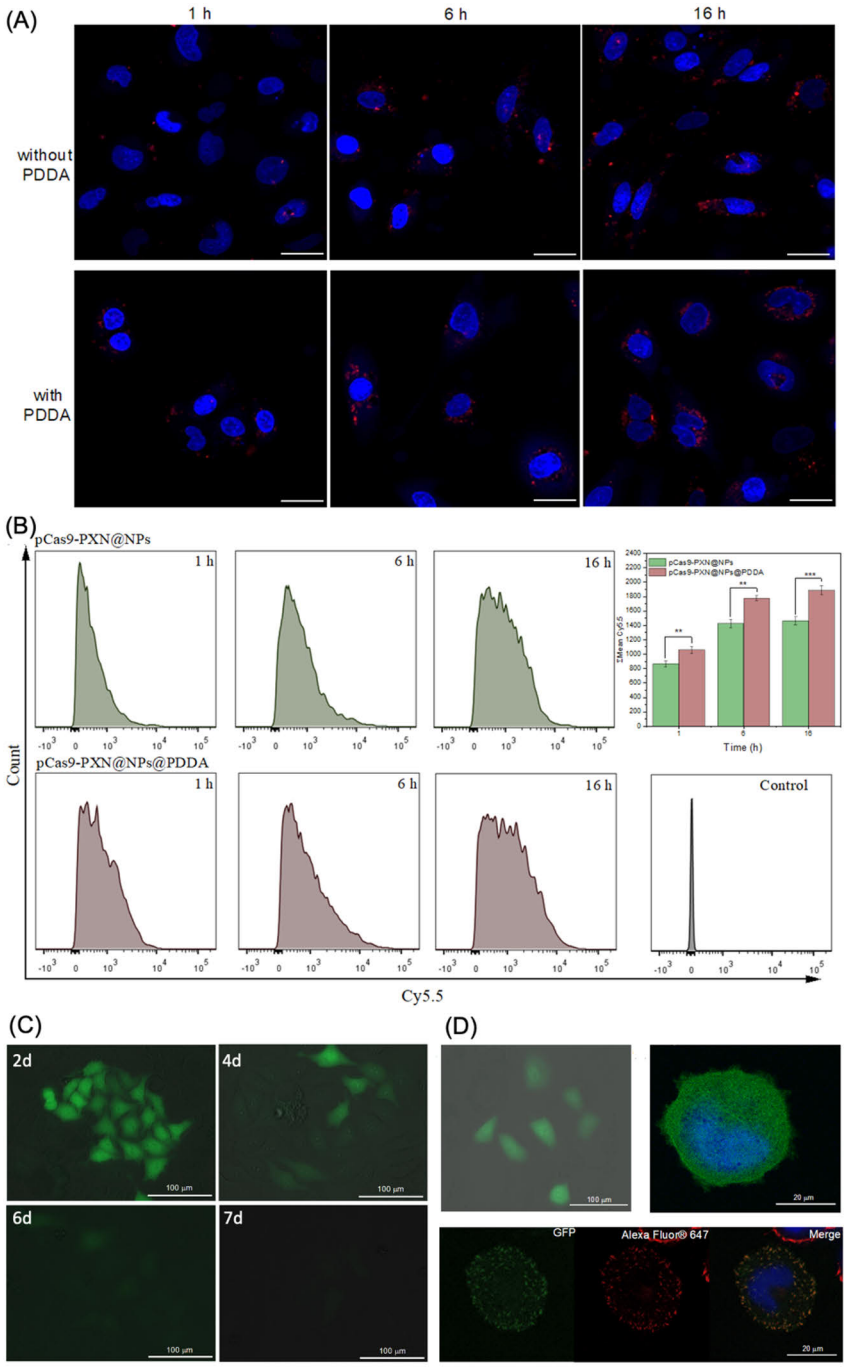

Figure 20. Cellular endocytosis, transfection, expression and gene editing assessment. *(A) CLSM and (B) flow cytometry for cell endocytosis of the plasmids loaded nanocarriers with and without PDDA. (C) Fluorescence microscopy images of U2OS cells treated with P1@NPs@PDDA (50 μg/mL) after 2-7days incubation. (D) Fluorescence microscopy, confocal image and immunofluorescent analysis of U2OS cells treated with P1P2@NPs@PDDA after 7 days incubation.*

Fluor@647-conjugated goat anti-rabbit lgG, a clear co-localization of different fluorescent signals was observed. Altogether, the results confirm that the GFP-coded paxillin sequence has been inserted into the appropriate location in the targeted cells, demonstrating the efficient gene editing capability of the CRISPR-Cas9 system based on functionalized MSNs nanovectors.

5.2.4. *In vivo* bio-distribution and pharmacodynamics studies

Following thorough *in vitro* studies, the nanoparticles used were further validated in *in vivo* studies for more clinically relevant applications. The targeting ability of the nanoparticles, the therapeutic ability of the released drugs in stimulus response and the toxicity of the nanoparticles over a long-term circulation were investigated.

5.2.4.1. *In vivo* vascular endothelium targeting (I)

In vivo endothelial targeting imaging was performed in mice receiving allogeneic kidney transplants after Cy5.5-NP-C4dAb injection to show the C4d targeting and biodistribution (Figure 21A). Accumulation of Cy5.5-NP-C4dAb could be clearly detected in the transplanted kidney, but not in the native kidney. Immunofluorescence results showed a clear C4d+ (C4d-FITC) signal on the vascular endothelial luminal side in allograft kidneys with endothelial injury and

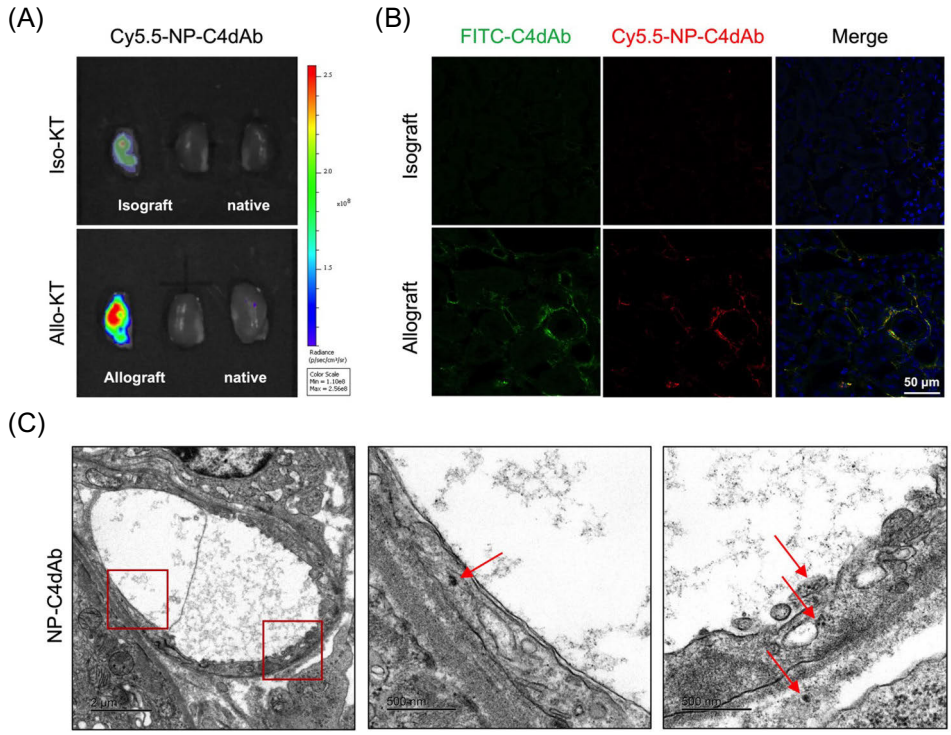

Figure 21. In vivo targeted imaging and biodistribution of nanoparticles. *(A) In vivo imaging of nanoparticles distribution in Isograft, Allograft and native kidney. (B) Confocal images of sectioned Isograft and Allograft following nanoparticle targeting and immunofluorescence staining. (C) TEM images of NP-C4dAb (red arrows) nanoparticles in the renal vascular endothelium.*

complement activation, and a good co-localization of Cy5.5-NP-C4dAb and C4d-FITC signals demonstrates the *in vivo* specific vascular targeting of NP-C4dAb (Figure 21B). In addition, NP-C4dAb nanoparticles were found in TEM of frozen sections of allografts within a vascular lumen region(Figure 21C), suggesting that C4dAb-coated nanoparticles enter the endothelium through a target-mediated process.

5.2.4.2. *In vivo* therapeutics assay (I)

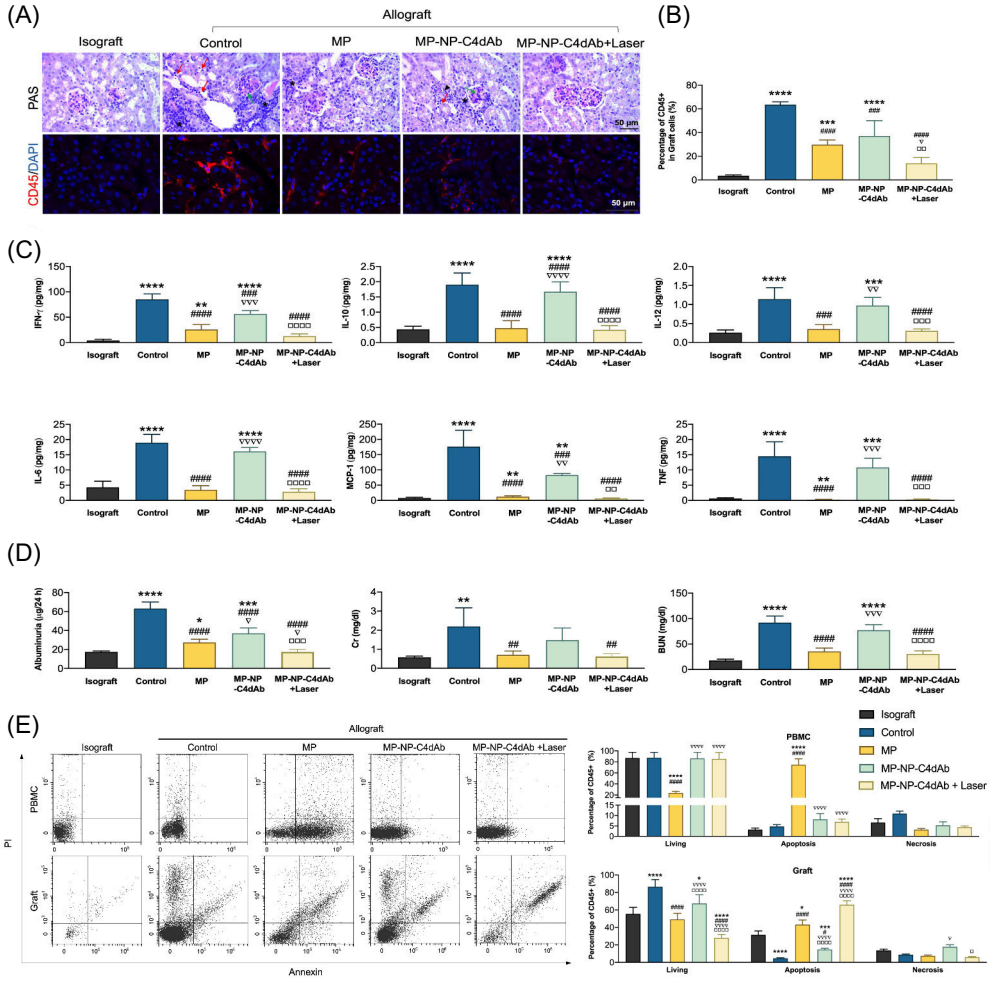

Figure 22. In vivo immunosuppression, allograft function evaluation and leukocytes apoptotic profile. *(A) PAS staining of paraffin tissue and CD45 immunostaining of frozen tissue showing the extent of inflammatory infiltration. (B) Quantitative analysis of CD45+ cells by flow cytometry. (C) Levels of pro-inflammation factors in the graft. (D) Albuminuria in urine, creatinine (Cr) and blood urea nitrogen (BUN) levels in the graft blood. (E) Characterization of leukocyte apoptosis in graft tissue and PBMC using pure MP and MP-NP-C4dAb with/without Laser. *P <0.05, **P <0.01, ***P <0.001, ****P <0.0001 vs Isograft. #P <0.05, ##P <0.01, ###P <0.001, ####P <0.0001 vs Control. ▽P <0.05, ▽▽P <0.01, ▽▽▽P <0.001, ▽▽▽▽P <0.0001 vs MP. □P <0.05, □□P <0.01, □□□P <0.001, □□□□P <0.0001 vs MP-NP-C4dAb.*

The *in vivo* drug release and therapeutic effect of MP-loaded nanoparticles as inflammation inhibitors under NIR irradiation were analyzed by histopathology, immunohistochemistry and flow cytometry (Figure 22A and B). Paraffin sections (PAS stained) and frozen sections (anti-CD45 stained) after allografting showed that lymphocytes burst in glomeruli, capillaries and interstitium, and more than half of the cells were CD45-positive (CD45+) in flow cytometry. The number of infiltrating inflammatory cells was significantly reduced after MP administration. The MP-NP-C4dAb group had a weak anti-inflammatory effect, with focal severe and diffuse interstitial inflammation and glomerulitis in the sections. In contrast, the drug was released in the laser-activated MP-NP-C4dAb group, resulting in a reduction of CD45+ to the same level as in the Isograft, and very little inflammation could be seen in the sections.

In MP and MP-NP-C4dAb+laser treated Allograft, the expression of major pro-inflammatory cytokines (IL-6, IL-10, IL-12p70, TNF, IFN-γ and MCP-1, Figure 22C) (Chu 2013; Cranford et al., 2016; O'Neill and Hidalgo 2021; Steensberg et al., 2003; Tait Wojno et al., 2019; Takada et al., 2010) was lowest in kidney lysates and blood serum, indicating reduced endothelium activation, substantial recruitment and ABMR-related NK infiltration as well as a decrease in overall inflammation. Elevated levels of renal function markers (albuminuria, serum creatinine (Cr) and blood urea nitrogen (BUN), Figure 22D) in transplanted mice suggest that ABMR after Allo-KT caused impairment. After treatment with MP and MP-NP-C4dAb+laser, the indicators were comparable to those of the Iso-KT group and renal function was restored due to reduced inflammation.

The systemic effects of the drug on circulating lymphocytes were subsequently assessed by flow cytometry measurement of leukocyte apoptosis in grafts and PBMC (Figure 22E). Effective inhibition of ABMR was seen in the MP group, but also triggered significant side effect of systemic lymphocytopenia. In contrast, in the MP-NP-C4dAb+laser group, the exposure of MP to circulating lymphocytes was greatly eliminated due to the targeting effect of the C4dAb coating that allowed the nanoparticles to be enriched at the inflammatory site of the graft, while the drug release was later precisely controlled by laser irradiation, and the therapeutic effect was concentrated only at the allograft site suffering from ABMR, with a significant increase in lymphatic apoptosis at this site only. Thus, these data suggest that MP-NP-C4dAb+laser exhibits an excellent therapeutic effect on inflammatory infiltrates in Allo-KT mice, while effectively reducing systemic side effects.

5.2.4.3. *In vivo* long-term toxicity evaluation (I)

To evaluate the *in vivo* long-term toxicity of drug-loaded nanoparticles, (Figure 23A) there was no obvious sign of weakness, spontaneous death and significant weight gain or loss observed in mice injected with PBS, MP, MP-NP and MP-NP-C4dAb within 28 days, indicating that all mice continued to mature without apparent toxic effects. Meanwhile, serum biochemical assays (especially kidney and liver function) after 28 days quantitatively assessed the potential toxicity of nanoparticles to mice. The levels of kidney function indicators including Cr and BUN in the treated groups were similar to those in the control mice(Figure 23B).

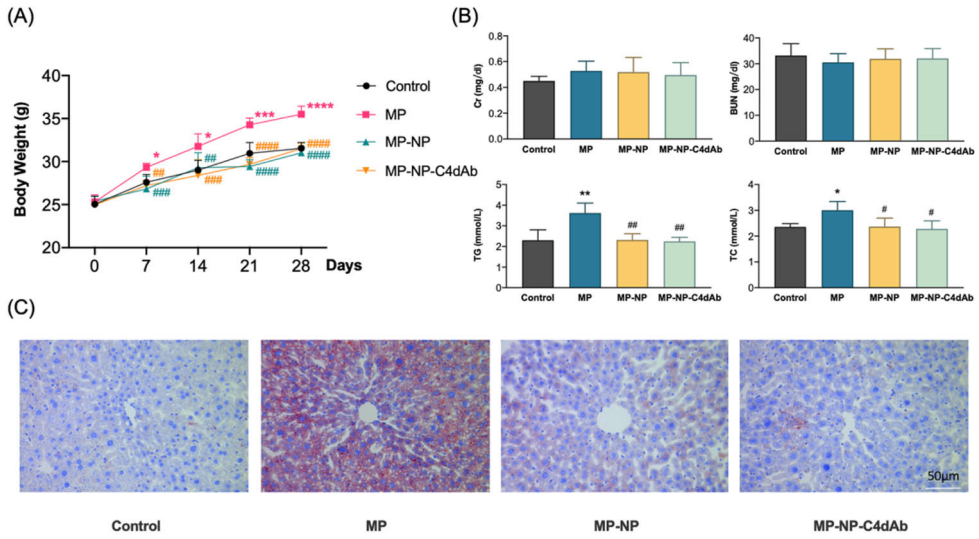

Figure 23. Long-term circulating toxicity test in vivo. *(A) Changes in body weight of C57BL/6 mice treated with PBS (control group), MP, MP-NP and MP-NP-C4dAb (treatment groups) at various time points. (B) Serum biochemical analysis, including creatinine (Cr), blood urea nitrogen (BUN), triglyceride (TG) and total cholesterol (TC) levels in the blood were determined. (C) Liver sections from each group of mice stained with Oil Red O. *P<0.05, **P<0.01 vs Control, #P<0.05, ##P<0.01, ###P<0.001, ####P<0.0001 vs MP.*

Liver function indicators including triglyceride (TG) and total cholesterol (TC) levels were increased in mice due to MP induction, while drug-loaded nanoparticles attenuated the effect of MP on liver function in a dose-dependent manner to a range comparable to control mice, which is consistent with the results of oil red O special staining with an obvious remission of liver steatosis (Figure 23C). These results suggest that NP injection did not induce significant toxicity and that it has a strong clinical potential.

5.3. MOFs-based porous nanomaterials for bioapplication (III, IV & V)

Although the feasibility of MSNs-based biomolecular delivery for medical applications has been demonstrated in the previous section, the established pore and channels of MSNs showed low efficiency for delivering biomacromolecules, so we have shifted our attention to the novel MOFs-based porous nanomaterial.

Firstly, the MOFs materials were used to encapsulate and stimulate the responsive release (redox, pH and photothermal) of small molecules and biomolecules such as nucleic acids and proteins through post-synthetic modifications (PSM) (Tanabe and Cohen 2011; Wang and Cohen 2009), biomimetic mineralisation (Chen et al., 2020; Lian et al., 2017; Liang et al., 2015), and microfluidic-assisted (Liu et al., 2017; Wang et al., 2019) synthesis methods. We then have evaluated the biocompatibility of the nanomaterials at the cellular level, including cytotoxicity, cellular uptake and endo/lysosome escape capacity. The therapeutic effect of the dual drug-loaded MOFs on tumour cells was investigated. The efficiency of transfection expression and gene knock-in of nucleic acid-loaded MOFs in cells were studied. The efficiency of gene editing of CRISPR-Cas9 RNP-loaded MOFs material was also assessed. The synthesis, functionalisation and respective aims of the MOFs-based materials are summarised in Table 2.

Table 2. *Overview of the studied formulations for the biomedical applications of MOFs-based nanomaterials:*

MOFs	**Surface modification**	**Cargo**	**Loading method**	**Stimuli-responsive**	**Main purpose**
UiO-66-NH_2	-Anhydride acid -FA-NH_2	DCA 5-FU	Immersion	Redox	Anti-cancer
ZIF-8		CRISPR-Cas9 Plasmid	Mineralization	pH	Gene knock-in
PB@Eu-MOFs		CRISPR-Cas9 RNP	Microfluidics	NIR	Gene editing

5.3.1. Design and characterization of the MOFs-based nanoparticles

When MOFs are used as drug carriers, their organic components are more focused on subsequent post-synthetic modifications, which are covalently linked by a variety of organic reactions to provide new chemical functions for the loading and grafting of drug molecules. Through rational PSM, MOFs drug carriers can enable intra-tumour cell drug delivery and potentially stimulus responsive drug release. Subsequently, we investigated a wide range of biomolecules, including nucleic acids and proteins, which can potently trigger the formation of MOFs and control the morphology of the resulting porous crystals through a biomimetic mineralisation process under physiological

conditions. In addition, we introduced microfluidics to assist biomineralization and impart the material with the ability to stimulus responsiveness.

5.3.1.1. Synthesis and modification of MSNs-based nanoparticles

Conventional synthesis (III)

Dichloroacetic acid (DCA) is a pyruvate dehydrogenase kinase inhibitor (Heshe et al., 2011) (overexpressed in cancer cells), and to realise its synergistic enhancement of anticancer effects with the subsequently loaded drugs, DCA-doped MOFs (DCA-UiO-66-NH_2) was synthesized by a solvothermal method. Two-step covalent modification of DCA-UiO-66-NH_2 was performed later by using previously synthesized dithionic anhydride (DTDPA) (Liu et al., 2014) and ammoniated folate (NH_2-FA) (Lee et al., 2003) to obtain DCA-UiO-DTDP-FA which has redox stimulus responsive gatekeeper to avoid drug leakage, and active targeting ability to cancer cells.

Biomineralization synthesis (IV)

The cyclic, double stranded P1 plasmid (P1) was used as a model molecule for biomineralization. For the specific procedure, a certain amount of P1 (0.5-3 μg) was dispersed in a metal ion solution and then added to an organic ligand solution to form P1-ZIF-8 (P1Z) nanostructures. Or the plasmid was distributed in an organic linker solution and then metal ions were added to form ZIF-8-P1 (ZP1) nanostructures. Biomineralization, which occurs by natural processes, is mainly the enrichment of biomolecules (amino acids, peptides and more complex biological entities) for inorganic cations (e.g., Ca^{2+} and Zn^{2+}) to form seed biominerals (Hwang et al., 2013; Trzaskowski et al., 2008; Wang et al., 2013). When P1 was added to Zn^{2+} solution, plasmids with rich phosphate groups agglomerate Zn^{2+} and promote the formation of P1Z complexes. But the nucleation rate of ZP1 nanoparticles is much slower due to the coordination competition effect between the plasmid and 2-MIM ligand.

Microfluidics synthesis (V)

Prussian blue (PB) nanocubes were prepared by a modified single precursor method (Wang et al., 2016) and used as hard templates for the biomineralization of MOFs. PB and Eu^{3+} were mixed and injected into the inner channel of a 3D microfluidic co-flow focusing device, and guanosine monophosphate (GMP, 10 mM) was pumped into the outer tube. The two fluids were blended at the orifice of the tap capillary to achieve the assembly of Eu^{3+} and GMP (Duan et al., 2017). Due to the growth of EuMOFs on PB hard templates, core-shell structures (PB@EuMOFs) were prepared in the interphase of both solutions.

5.3.1.2. Physicochemical characterization of the synthesized MOFs

As observed by TEM, the surface of DCA-UiO-66-NH_2 underwent a stepwise reaction with anhydride acid (DCA-UiO-DTDP) and folic acid (DCA-UiO-DTDP-FA) without any significant change in the morphology of the nanoparticles (Figure 24A). The PXRD patterns (Figure 24B) match well with the simulated patterns and the crystallinity does not show any difference, indicating the integrity of their framework after covalent modification. FT-IR (Figure 24C) demonstrates the characterization of the carboxylic acid in the synthesized DCA-UiO-66-NH_2

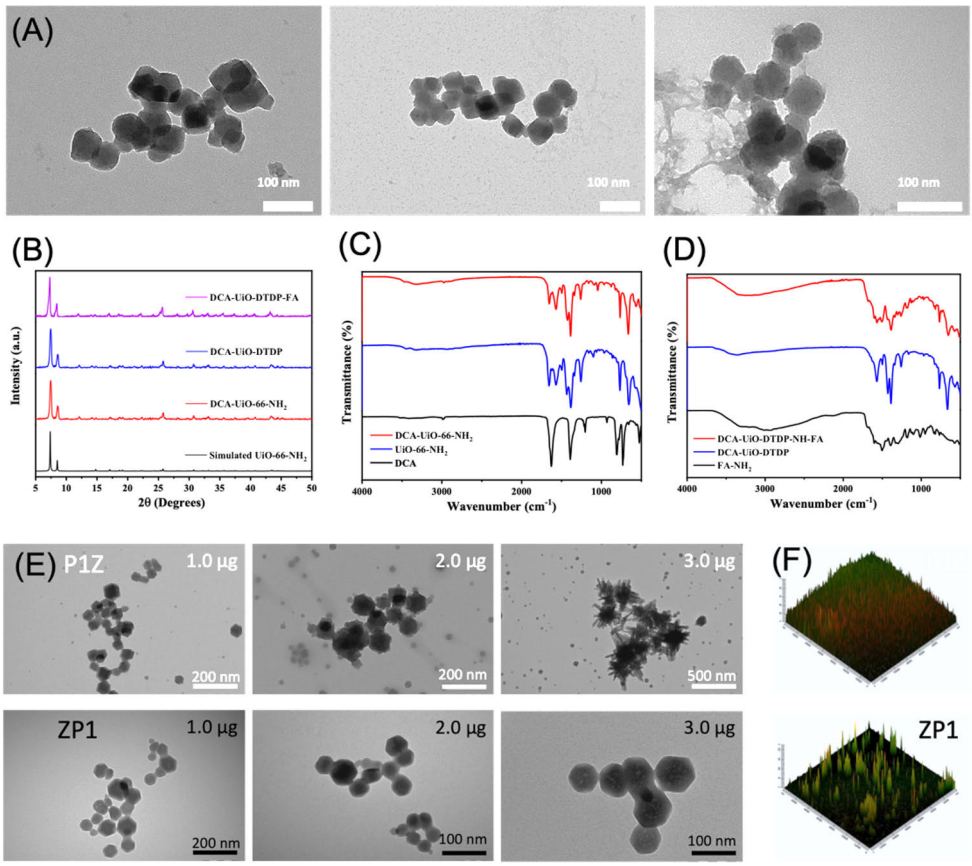

Figure 24. Characterization of the MOFs nanoparticles. *(A) TEM images and (B) XRD patterns of DCA-UiO-66-NH₂, DCA-UiO-DTDP and DCA-UiO-DTDP-FA nanoparticles. (C) FT-IR spectra of DCA-UiO-66-NH₂, UiO-66-NH₂ and DCA. (D) FT-IR spectra of DCA-UiO-66-DTDP-FA, DCA-UiO-66-DTDP and FA-NH₂. (E) TEM images of the morphologies P1Z and ZP1 nanoparticles. (F) 3D-CLSM images of the plasmid distribution (green fluorescence) in P1Z and ZP1.*

with DCA connected to the Zr_6 unit. The absorption peak of FA contributes strongly to the FT-IR spectrum of DCA-UiO-DTDP-FA (Figure 24D), suggesting the success of folate binding.

The evolution of the embedding structure of the composite was studied by TEM (Figure 24E). In the P1Z system, the morphology of the nanoparticles changed from uniformly rhombohedral dodecahedron to irregular polyhedron with spiky surfaces up to decussation, as the amount of plasmid increased. The morphology of ZP1 nanoparticles remains homogeneous rhombohedral dodecahedron with only a slight increase in size. DAPI-labeled P1, ZIF-8 precursor and Cy5.5 were mixed, and the same encapsulation step was performed to determine the distribution of P1 in ZIF-8. CLSM images (Figure 24F) displayed that P1 was homogeneously dispersed in P1Z structure, while heavily aggregated in ZP1 nanoparticles.

5.3.1.3. Stability of biomolecules after encapsulation

The protection of the carrier from the degradation of the contained biomolecules (plasmids and Cas9/sgRNA RNP) is a key issue in gene delivery. The stability of P1 to degradation by the restriction enzyme Eco32I (EcoRV) was investigated by gel electrophoresis in both structures. After EcoRV treatment, P1 was collected from ZP1 and P1Z disintegrates, with 82.3% of intact P1 in P1Z, which was superior to ZP1 (64.5%), showing better protection of the P1Z structure. To prove that the encapsulated plasmids were fully functional, the plasmid released from P1Z and ZP1 can transfect cells and show fluorescence by using the packaged plasmids for transfection (Figure 25A). This implies that the plasmids were not damaged in any way during encapsulation and do not negatively affect functional activity. DSF was used to determine the protection of Cas9 protein by MOFs and unfolding/denaturation results by measuring the ratio of fluorescence at 330 nm and 350 versus temperature (Figure 25B). The thermal stability of proteins is usually described by the thermal unfolding transition midpoint Tm (°C). The native RNP produced a distinct and stable melting point at 45 °C, which disappeared completely after treatment with trypsin and SDS for 5 min at room

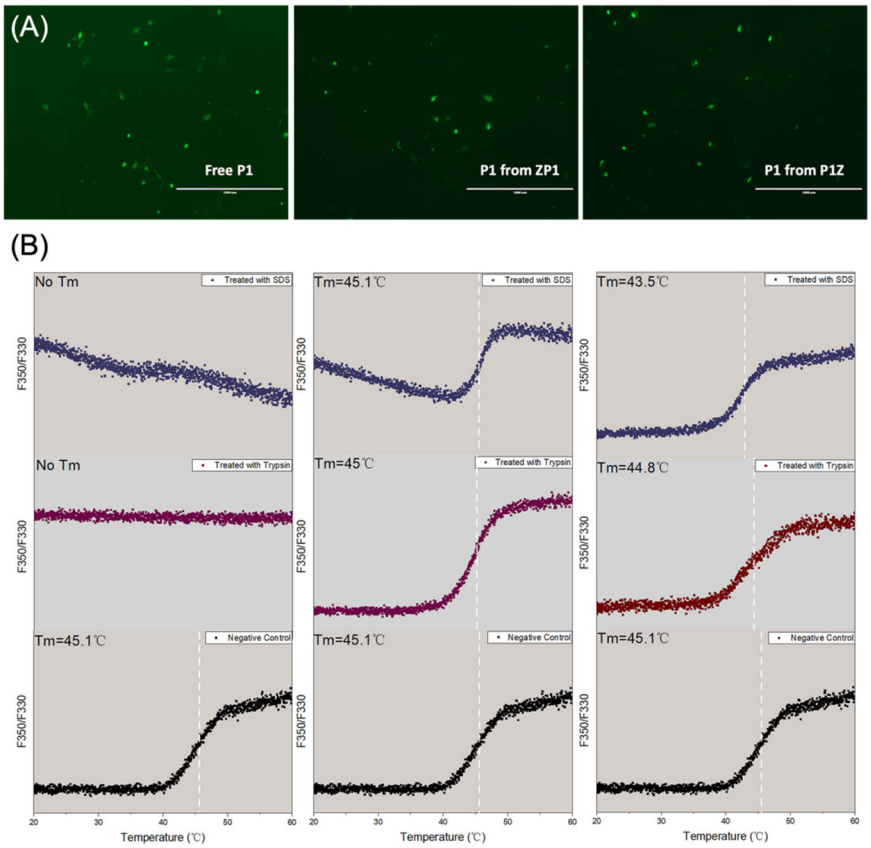

Figure 25. Protection evaluation of biomolecular activity contained in nanocarriers. *(A) Fluorescence microscopy images of cells transfected with free P1, P1 released from ZP1 and P1Z structures, scale bar:1000 μm. (B) Typical nanoDSF thermal unfolding curves of pure Cas9 protein, Cas9 protein released from microfluidic-prepared and bulk-prepared PB@RNP-EuMOFs. Tm points were shown as vertical dotted lines.*

temperature. In comparison, the released RNP of PB@RNP-EuMOFs composites after the same treatment maintained almost the same temperature as the free RNP, indicating that the MOFs scaffolds are shielded against different harsh environments.

5.3.2. Drug loading and stimuli-responsive release

The loading capacity of postsynthetic surface-modified MOFs for anticancer drugs, the encapsulation ability of biomineralized MOFs for nucleic acid-like biomolecules, and the packaging capacity of microfluidic-assisted MOFs mineralisation for proteins were evaluated. The cargoes release of these materials was investigated under different stimuli (redox, pH and NIR) responsiveness.

5.3.2.1. Anticancer drug loading and GSH induced release (III)

The anticancer drug 5-FU can synergize with DCA in the MOFs structure to enhance cytotoxicity and reduce drug resistance in cancer cells, which was used to assess the drug loading and release behavior of DCA-UiO-DTDP-FA. The loading efficiency of DCA-UiO-DTDP-FA on 5-FU was determined to be 31.6 wt % after 24 h according to the standard curve of 5-FU. DCA-UiO-DTDPA nanoparticles have redox-responsive disulfide bonds on surface, which then conjugated with NH_2-FA to avoid the leakage of the loaded drug. The overexpressed GSH in cancer cells can form intracellular redox buffers (Saito et al., 2003) and attack the thiolate moiety, breaking the existing disulfide bonds. Dithiothreitol which mimics the reduction of GSH, was used to study the release behavior of 5-FU in 5-FU-DCA-UiO-DTDP-FA nanoparticles. (Figure 26A) In the presence of 10 mM DTT, approximately 80% of drug was released after 24 h due to the high concentrations of DTT cleaving more disulfide bonds. In contrast, the control group without DTT released a limited amount of drug in 24 hours. The above results have important implications for the postsynthetic modification of anticancer drug delivery systems based on redox-responsive MOFs nanoparticles.

5.3.2.2. Nucleic acid loading and pH triggered release (IV)

Effective loading and release of plasmids by the vector is an important factor to achieve gene therapy. The encapsulation of both P1Z and ZP1 nanoparticles was determined by measuring the concentration of P1 in the solution after encapsulation by UV-Vis absorption spectroscopy. The loading capacity of P1 in two embedding modes was investigated, and the maximum package capacity of P1 was 2.0 μg in P1Z and 1.2 μg in ZP1, respectively. In addition, the pH-responsive release behavior of the two nanoparticles was determined by dispersing them in PBS solutions with different pH values (Figure 26B). The P1Z and ZP1 nanostructures were stable in PBS (pH=7.4) with no significant release of P1 (<10%). In simulated endo/lysosomes (pH=5.5), 52% of P1 was released from the ZP1 nanostructures after 48 hours. Due to the rapid nucleation of P1Z nanoparticles, which are more pH dependent, the burst release is

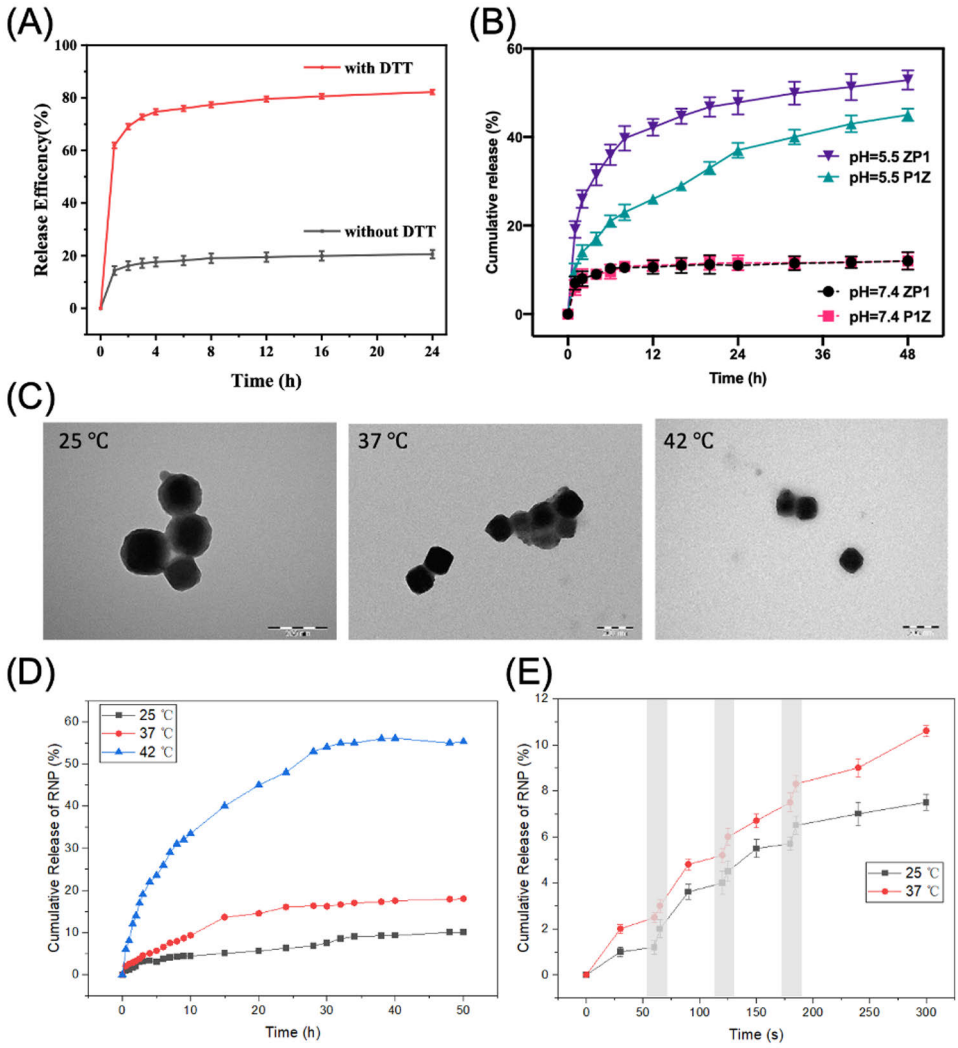

Figure 26. Stimuli-responsive release experiments for loaded drugs and biomolecules. *(A) Release efficiency of 5-FU from 5-FU-DCA-UiO-DTDP-FA. (B) Cumulative release of P1 from P1Z and ZP1 nanostructures at different pH value. (C) Mophology of PB@EuMOFs after different temperature treatment: 25 ℃, 37 ℃ and 42 ℃ detected by TEM. (D) Cumulative release profile of RNP from PB@RNP-EuMOFs under different temperature within 50 h. (E) NIR-triggered cumulative release profile of RNP from PB@RNP-EuMOFs at different temperature and different time points in grey boxes.*

negligible within 12 h and reaches 40% after 48 h. These results indicate that P1Z-based nanovectors have an efficient pH-responsive release, which is a more desirable property for gene delivery and transfection.

5.3.2.3. CRISPR-Cas9 RNP loading and NIR activated release (V)

CRISPR-Cas9 ribonucleoprotein (RNP) was encapsulated by a microfluidic co-flow focusing device during MOFs nucleation of PB@EuMOFs core-shell structure. Eu^{3+} and PB were mixed as fluid 1 due to electrostatic interaction, RNP

was mixed with ligand GMP as fluid 2, and the concentration of each precursor (PB:Eu:GMP:Cas9) was 1:2:2:0.5. After centrifugation and washing, RNP-encapsulated PB@EuMOFs (PB@RNP-EuMOFs) were obtained. By encapsulating RNP with Cy5.5-labeled Cas9 protein, the loading efficiency and capacity of RNP were calculated to be 60% and 1.3 mg/g, respectively, based on the UV-Vis absorption of Cy5.5 before and after encapsulation.

Subsequently, the degradation of MOFs shells was investigated by modulating the photothermal conversion of PB to achieve effective RNP release. The TEM images of PB@RNP-EuMOFs treated at different temperatures (25 °C, 37 °C and 42 °C, Figure 26C) showed that there was no structural degradation at 25 °C, while the morphology of the EuMOFs shells underwent a relatively obvious collapse from 37 °C to 42 °C. The cumulative RNP release curves at different temperatures showed corresponding thermo-responsive release properties (Figure 26D), with the increase in temperature from 25 to 42 °C, the RNP release rate increased from 16% to 55% after 50 h. Then, the release behavior of RNP under NIR-induced photothermal responsive was explored by irradiating solutions at different temperatures with 808 nm (Figure 26E). The RNP release curves of two solutions under laser stimulation showed that explosive release occurred when the PB@RNP-EuMOFs solution irradiated for 2 min at 25 °C and 1 min at 37 °C up to a maximum temperature of 42 °C. The final release capacity increased sharply from 4% to 8% in 25 °C and 5% to 11% in 37 °C within 5 h, indicating that the photothermal conversion effect of PB@EuMOFs can accurately trigger the release of RNP.

5.3.3. Cellular interactions

In this section, the biocompatibility of MOFs nanomaterials carrying different cargoes, endocytosis after targeting modifications of nanoparticles, cellular uptake and lysosomal escape of biomolecule-loaded nanoparticles, anticancer therapeutic efficacy after drug release, intracellular transfection and knock-In of plasmids, and gene editing of CRISPR-Cas9 RNP have been investigated.

5.3.3.1. Cytotoxicity assay (III, IV & V)

The biocompatibility and cytotoxicity of nanomaterials for delivery of anticancer drugs and biomolecules were evaluated using the WST-1 assay. The effects of nanocarriers (DCA-UiO-DTDP and DCA-UiO-DTDP-FA, P1Z and P1P2Z and PB@EuMOFs) on cell proliferation (MDA-MB-231 and MCF-10A cells, U2OS cells, Hela and Hela/GFP cells) were measured. Various concentrations of DCA-UiO-DTDP and DCA-UiO-DTDP-FA incubated with MDA-MB-231 cancer cells showed no toxicity for up to 500 $\mu g \cdot mL^{-1}$ (Figure 27A), and cell viability was maintained at 80%, with no effect on the proliferation of normal MCF-10A cells despite the active targeting ability of DCA-UiO-DTDP-FA. At different concentrations of P1Z and P1P2Z, there was no significant change in U2OS cell survival compared to the control based on the amount of P1 (up to 2000 $ng \cdot mL^{-1}$). PB@EuMOFs exhibited low cytotoxicity in both Hela and Hela/GFP cells (Figure 27B), with over 90% cell survival even at high particle concentrations of 200 $\mu g \cdot mL^{-1}$. Meanwhile, PB@EuMOFs showed high cell viability (>60%) in both cell lines after three cycles of laser irradiation. These results suggest that the pre-prepared

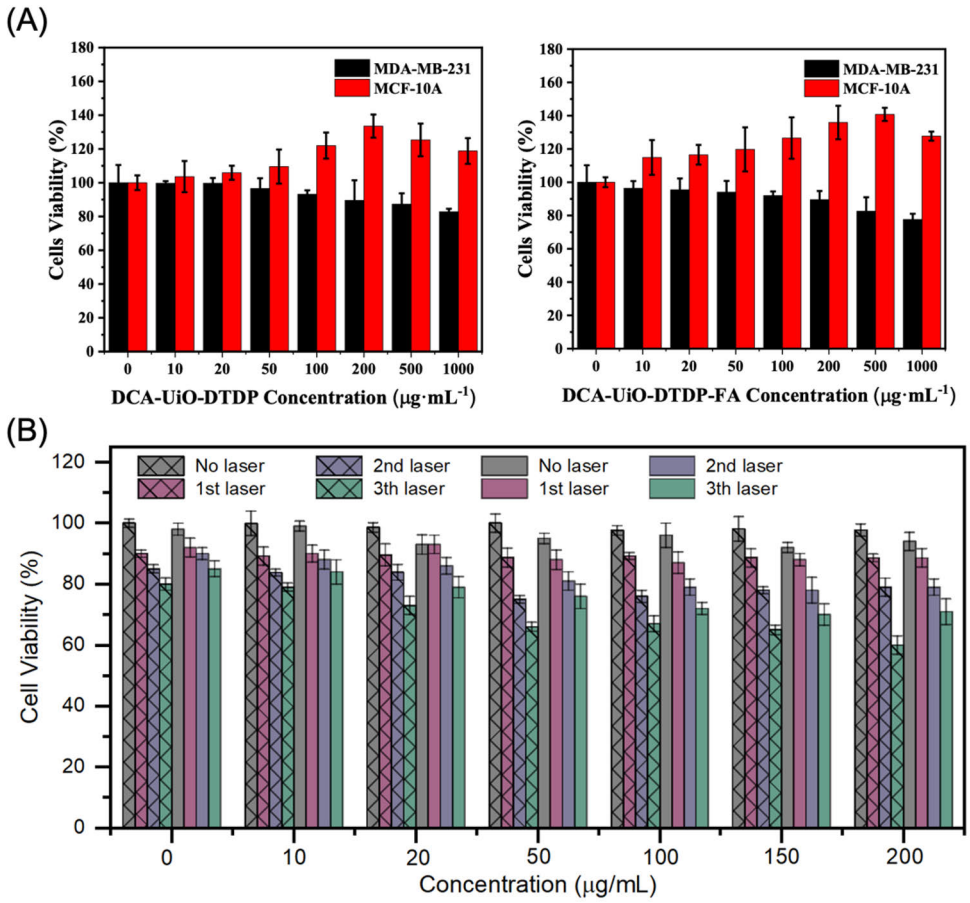

Figure 27. Cytotoxicity evaluation by cell proliferation assay. *(A) MDA-MB-231 cancer cell and MCF-10A cells cultured with different concentrations of DCA-UiO-DTDP and DCA-UiO-DTDP-FA nanoparticles for 72 hours. (B) Cell viability of Hela and Hela/GFP cells treated with different concentration of PB@EuMOFs and laser irradiation (808 nm, 2 W·cm-2) after 48 h incubation.*

PB@EuMOFs are a safe nanocarrier even at high concentrations and under laser irradiation.

5.3.3.2. Cellular uptake (III, IV & V)

The endocytosis of Cy5.5-labeled DCA-UiO-DTDP-FA and DCA-UiO-DTDP by MDA-MB-231 cancer cells exhibited significant differences in CLSM images at 16 hours (Figure 28A), with stronger red fluorescence observed in the cytoplasm and nucleus of the DCA-UiO-DTDP-FA group, indicating that more aminated-FA modified nanoparticles particles were endocytosed by MDA-MB-231 cells. In contrast, MCF-10 normal cells showed no difference in endocytosis of the two types of nanoparticles, indicating that the prepared nanoparticles were effectively internalized through receptor-mediated approach to cancer cell targeting. The endocytosis of the cell lines to be gene-edited (U2OS and Hela/GFP cells) to nanomaterials used for delivery of biomolecules showed time-

dependence from CLSM and flow cytometry results (Figure 28B and C), which confirmed that plasmid-ZIF and PB@EuMOFs can efficiently penetrate cells, which is a necessary condition for genetic materials.

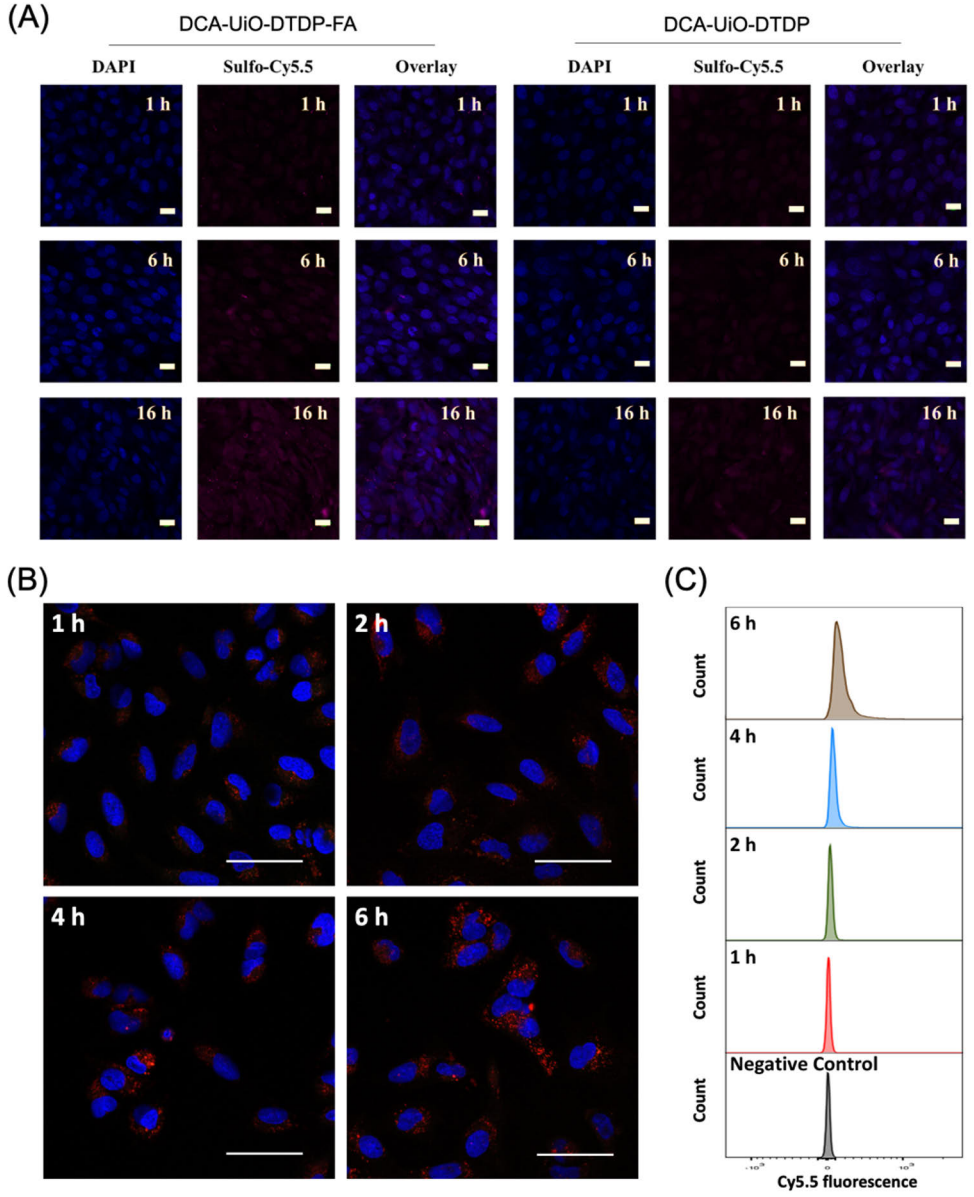

Figure 28. Cellular uptake and intracellular distribution of nanoparticles. *(A) Confocal images of MDA-MB-231 cancer cells incubated with DCA-UiO-DTDP-FA and DCA-UiO-DTDP for different time period, scale bar: 20 μm. (B) CLMS and (C) flow cytometry analysis of P1Z nanocarriers incubated with U2OS cells after 1, 2, 4 and 6 hours, scale bar: 50 μm. The nanoparticles were both labeled with Cy5.5.*

5.3.3.3. Cellular endo/lysosome escape (IV, V)

To determine the endo/lysosomal escape capacity of nanocarriers, the co-localization of red fluorescence of nanocarriers (Cy5.5 labeled) and green fluorescence of endo/lysosomes (LysoTracker@Green) was recorded by CLSM within 6 h (Figure 29A) and the overlap of fluorescence was quantified according to the Pearson correlation coefficient (PCC). The results showed that over time, most of the nanoparticles excellently escaped from the endo/lysosomes within 6 h via the proton sponge effect, avoiding the degradation of biomolecules in cellular transmembrane transport. The effect of laser irradiation on the endo/lysosomal escape process of PB@EuMOFs nanoparticles was also investigated (Figure 29B and C). 808 nm laser irradiation resulted in a more uniform distribution of red fluorescence, suggesting that the photothermal conversion effect of PB@EuMOFs could promote their ability to escape from endo/lysosomes.

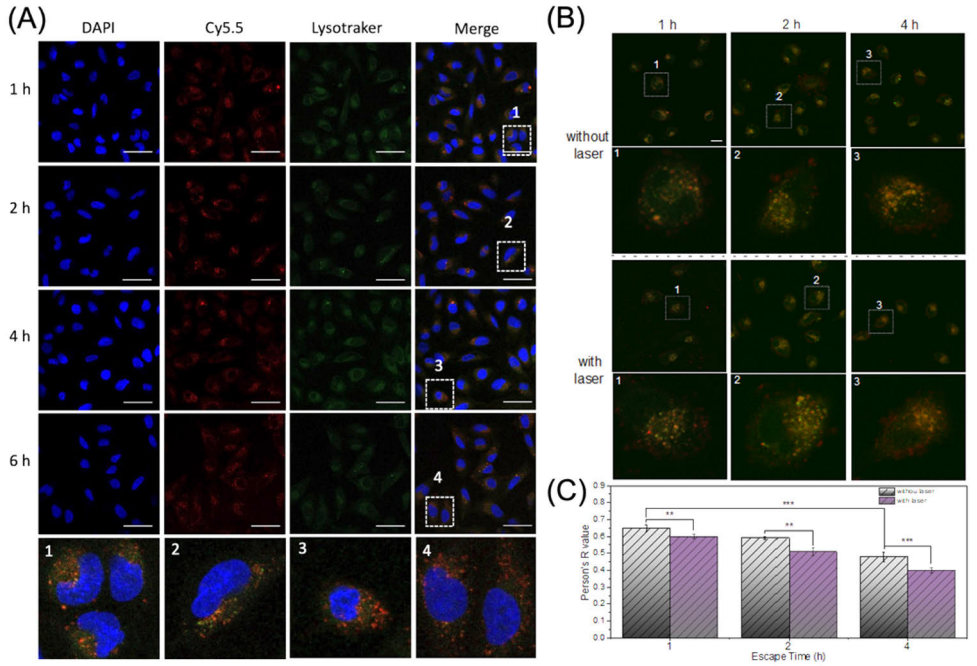

Figure 29. Endo/lysosomal escape efficiency of nanoparticles. *(A) CLSM images of U2OS cells after incubation with P1Z (red) for different time period, scale bar:50 μm. (B) CLSM and (C) Person's R value calculated by ImageJ of PB@EuMOFs treated Hela cells after 1, 2 and 4 h incubation. Statistical analysis was determined using T-test (***P<0.001, **P<0.01, *P<0.05), scale bar: 20 μm. Endosomes were stained with Lysotracker Green (green) and nanoparticles were both labeled with Cy5.5 (red).*

5.3.3.4. Cellular therapeutics (III)

Concerning the synergistic enhancement of cytotoxicity for anticancer effects, although the combination of DCA and 5-FU did enhance free 5-FU toxicity, the 5-FU-DCA-UiO-DTDP-FA sample was more poisonous to MDA-MB-231 cancer cells

(Figure 30). This may be due to the more effective cellular internalization of nanoparticles with FA conjugation. For MCF-10A cells, these nanoparticles showed limited cytotoxicity, which proves that it is more selective for cancer cells than normal cells.

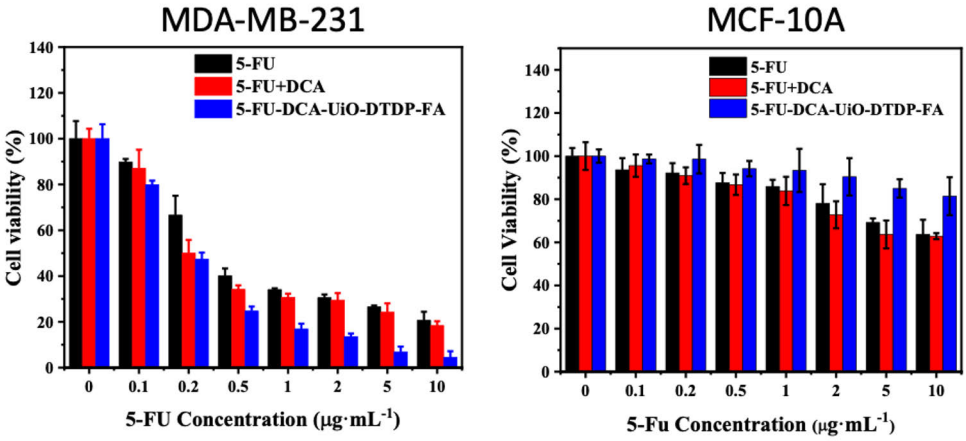

Figure 30. Synergistic enhancement of anti-cancer effects. *The cell viabilities of MDA-MB-231 cancer cells and MCF-10A normal cells cultured with different concentration of 5-FU, 5-FU+DCA, and 5-FU-DCA-UiO-DTDP-FA.*

5.3.3.5. Cellular transfection and gene editing (IV, V)

To evaluate the ability of the MOFs nanovectors for CRISPR-Cas9 biomolecules delivery, the loaded plasmid expression in targeted cancer cells was studied. Fluorescence microscopy recorded the expression of green fluorescence in U2OS cells after incubation with P1Z for 2, 4, 6 and 7 days (Figure 31A). A clear bulk GFP signal was seen in cells after 2 days, indicating that plasmid transfection using the designed delivery platform is feasible and the transfection efficiency is comparable to that of commercial Lipofectamine-2000, but P1Z has the great advantage of low cost and easy preparation.

To verify the gene editing efficiency of this nanovector, PXN knock-in assays were investigated *in vitro*, and whole cell lysates from edited cells were analyzed by Western blotting after U2OS cells were transfected with P1P2Z for 96 and 120 hours (Figure 31B) (Stubb et al., 2019; Stubb et al., 2020). The immunoblotting with an antibody against the endogenous Paxillin protein yielded products with the expected molecular weight of untagged and EGFP-tagged proteins. The expression of the fused EGFP-Paxillin protein increased progressively after knock-in and repair, demonstrating that the EGFP-Paxillin sequence in P2 was well integrated into the DSB of the endogenous Paxillin cleaved by the P1-transfected Cas9/sgRNA RNP and successfully expressed. The immunofluorescence results of focal adhesion and fibronectin staining (Figure 31C)

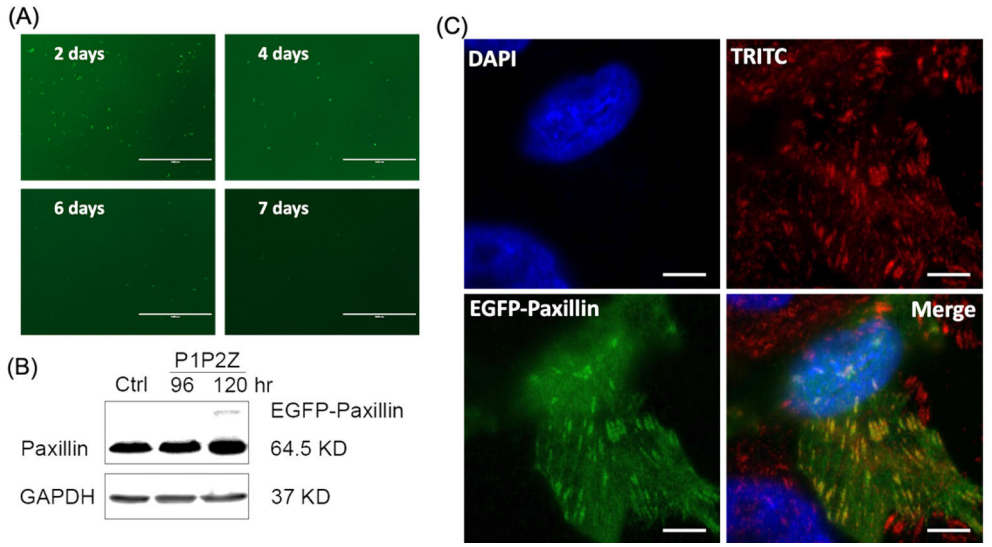

Figure 31. Transfection, expression and knock-in assessment of loaded biomolecules. *(A) Fluorescence microscopy images of cells incubated with P1Z after 2, 4, 6, and 7 days to determine the in vitro transfection, scale bar: 1000 μm. (B) Western blotting analysis of EGFP-Paxillin protein expression. (C) CLSM immunofluorescent analysis of P1P2Z-treated U2OS cells, scale bar: 5 μm.*

demonstrate that the plasmid-ZIF nanostructures are both reliable and specialized for delivery of the CRISPR-Cas9 editing system.

The gene editing ability of the CRISPR-Cas9 RNP nanovectors was assessed by targeting DNA cleavage and NHEJ-induced repair. sgRNA targeting of the coding region of green fluorescent protein (GFP) in Hela/GFP cells resulted in the shift of the reading frame, which prevented the expression of GFP (Hansen-Bruhn et al., 2018). When PB@RNP-EuMOFs were incubated with Hela/GFP cells (Figure 32A), there was no significant change in GFP fluorescence, while the fluorescence intensity decreased by 40% after laser irradiation, indicating a photothermal responsive controlled release of CRISPR-Cas9 RNP. Fluorescence microscopy images also confirmed the quenching of GFP signal upon incubation of PB@RNP-EuMOFs and laser irradiation (Figure 32B). Subsequently, different times of laser irradiation were performed in Hela/GFP cells after treatment with PB@RNP-EuMOFs and the editing efficiency of GFP was compared after 48 h of incubation. The fluorescence intensity of GFP significantly decreased with increasing number of irradiations, and the results verified that the photothermal conversion effect of PB@EuMOFs can trigger controlled gene editing *in vitro*.

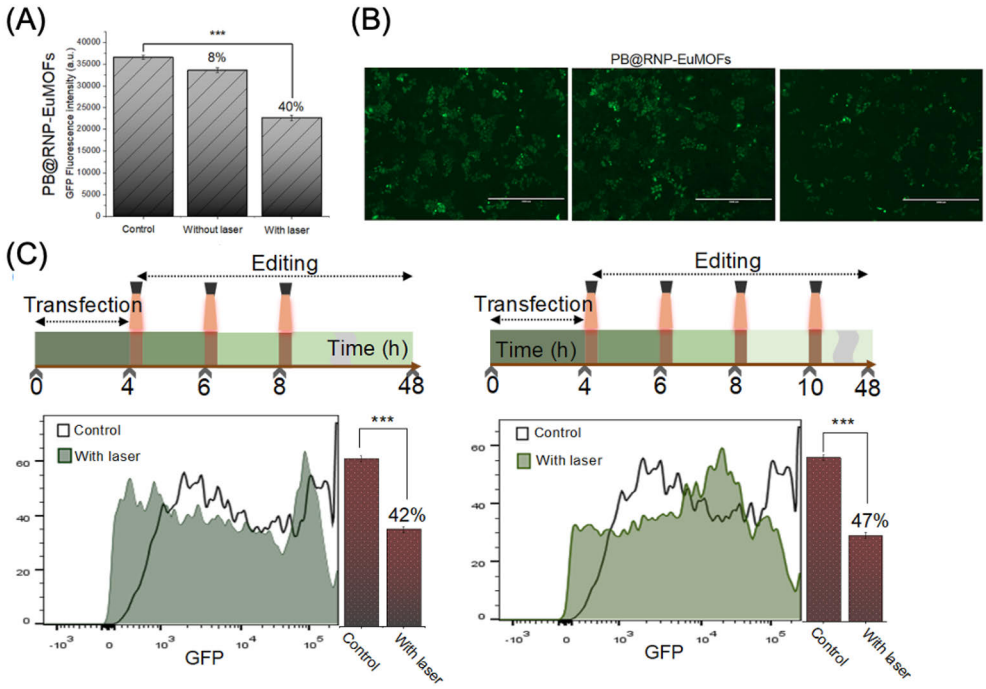

Figure 32. GFP gene editing efficiency assay. *(A) flow cytometry and (B) fluorescence microscopy of PB@RNP-EuMOFs in Hela/GFP cells under the condition with and without laser irritation. (C) PB@RNP-EuMOFs-mediated photo control of GFP editing efficiency detected by flow cytometry. The transfection, irradiation and gene-eiditng processes were illustrated and the laser irradiation time should be controlled temperature does not exceed 42 ℃.*

6. Concluding and future remarks

6.1. Summary of the thesis

In this thesis, a series of functionalized bio-endogenous and non-invasive exogenous stimuli-responsive drug/biomolecular-controlled release systems were designed and constructed based on two inorganic nanomaterials, mesoporous silica and metal-organic frameworks, to address the scientific issues of improving the loading capacity and targeted delivery of porous nanocarriers, the efficiency of gene editing tools, and reducing the biotoxicity of blocking molecules, and their performance was systematically investigated. The specific research results are as follows:

As one of the basic materials in this thesis, MSNs was combined with a photothermal conversion agent and surface engineered for allograft kidney endothelial antigen region targeting and in situ immune system inhibition therapy. The cytotoxicity studies evaluated the cytocompatibility of this drug delivery system and showed that the photothermal process had a negligible effect on cell viability and controlled drug release without exacerbating inflammation and tissue damage. The specificity and significantly increased allogeneic endothelial targeting of NP conjugated to C4d antibodies *in vitro* and *in vivo* was further validated by non-invasive *in vivo* imaging, biodistribution and histological studies. After accumulation of nanoparticles in the injured endothelium, remote NIR light onto the allograft triggered the release of drugs that induce the apoptosis of inflammation recruited lymphocytes, while reducing the pro-inflammatory cytokines in the ABMR attacked graft. It also preserved the innate immunity with a significantly limited dysfunction effect on the circulating lymphocytes and have a significant impact on their bench-to-bedside translation.

Subsequently, the functionalized MSNs were used to deliver biological macromolecules and verified that the loaded CRISPR-Cas9 plasmids enable intracellular knock-in of specific genes through stimuli-responsive release. Porous MSNs can efficiently load CRISPR-Cas9 plasmids, and microfluidic-based polymer (PDDA) coatings can effectively avoid payload leakage in nanocarriers. The pH-induced degradation of PDDA promotes rapid endo/lysosomal escape and plasmids release from the nanovectors, successfully knocking GFP-tagged paxillin into the U2OS cell genome. However, the lack of effective protection of the loaded biomolecules due to the freely accessible pores and adsorptive loading mechanism of MSNs, as well as the increased biotoxicity of the polymers used to block the pores, lead to inefficient physiological functions of biomolecules, and require the development of new nano-delivery vehicles.

As a novel nanocarrier, MOFs were first investigated for endogenous stimuli-responsive anticancer drug delivery. During the synthesis of MOFs, a small molecule drug DCA was inserted into the defective site in situ, which could not only regulate the particle size to promote endocytosis, but also further synergize with another loaded 5-fluorouracil to enhance cytotoxicity, thus constructing a MOFs-based dual drug delivery system. The postsynthetic modification of MOFs with acid anhydride and folic acid in sequence experimentally demonstrated that

the internally and externally modified MOF nanoparticles were effective in targeted delivery to cancer cells, redox-responsive dual drugs-controlled release, and synergistically enhanced anticancer effects. The combination of in situ and post-synthetic modification methods of MOFs is a strategy worth further exploration and has great potential to overcome issues with drug resistance and poor efficacy.

For delivery of biomolecules, plasmids were encapsulated in MOFs by biomimetic mineralization to tailor controllable nanostructures with plasmid modulation, and the significance of MOFs structures for maintaining the physiological functions of the loaded biomolecules was also explored. It was found that biomolecules can be well distributed throughout the mineralized nanostructures, and the CRISPR-Cas9 plasmid-MOFs system exhibits good loading, proper protection against enzymatic degradation, better cellular endocytosis and efficient endo/lysosome escape properties, and pH-responsive controlled release of the plasmid making it outstanding for gene knock-in. Compared to MSN-based delivery, this method not only provides a fast, facile, and low-cost way to load gene editing tools into controlled nanostructures for efficient intracellular transfection, but also reveals the potential of MOF-based non-viral vectors in various gene therapies.

While using MOFs for protein delivery, a microfluidic-assisted biomineralization strategy for MOFs was constructed and applied for efficient CRISPR-Cas9 RNP delivery and NIR-responsive remote control gene editing. The thermo-responsive degraded EuMOFs were coated on the photothermal conversion template PB by adjusting the microfluidic parameters to encapsulate RNP during the crystallization of MOFs. Due to the combination of microfluidics and MOF-based biomineralization, the RNP encapsulated nanocarrier particles were more uniform in size, with higher encapsulation efficiency and better protection of RNP than traditional bulk nanoprecipitation method. Under NIR laser irradiation, the heat induced by PB conversion can trigger the degradation of MOFs, thus promoting endosomal escape and RNP controlled release, which successfully downregulated the expression of target GFP genes *in vitro*. The gene-editing activity can be programmed by modulating the exposure time, which shows higher editing efficiency and provides a useful tool for precise biomedical therapies based on CRISPR-Cas9 gene editing.

In conclusion, this thesis constructs several stimuli-responsive MSNs and MOFs nano-drug delivery carriers to achieve controlled release of antitumor drugs, immunosuppressive agents and bioactive macromolecules by exploiting the features of the tumor microenvironment and the stimulation of external light sources, achieving enhanced therapeutic effects in tumors, suppression of rejection after kidney transplantation, and efficiency of gene editing, paving the way for the application of porous materials in the biomedical field.

6.2. Future remarks

6.2.1. Drug delivery for ABMR inhibition

Besides targeting the blocking of immune attack at site of allograft, the most popular treatment for ABMR is the inhibition of DSA secretion with antibodies or drugs, which lack selectivity and often cause systemic immunodeficiency. T follicular helper (Tfh) cells play a pivotal role in antibody-secreting plasma cells (PC) differentiation from B cell via germinal center selection. Tacrolimus (Tac) is the most widely used immunosuppressive drug after transplantation globally, and the administration need to be under close monitoring to avoid toxicities, rejection, and infection. The precise targeted delivery of Tac into $CD4^+$ helper T cells by porous nanorobotics can reduce multiple side effects of long-term Tac uptake and achieve powerful humoral rejection suppression after kidney transplantation via decreasing naïve $CD4^+$ activation into effect Tfh cells and PC differentiation. This study provides a potential therapeutic strategy with more specific and controlled drug delivery against even refractory humoral rejection and reveals the possibility of clinical translation.

6.2.2. Targeted delivery of biomolecules

Although biomineralization has been extensively studied in inorganic systems, the concept is only starting to be applied to MOFs. This thesis demonstrates that the biomimetic mineralization of MOFs forms a porous nanoshell that encapsulates biomolecules, provides unprecedented protection, and maintains biological activity. In addition, the encapsulated biomolecules can be released by pH changes in the physiological environment. However, this thesis is limited to investigating the relationship between MOFs structures and biomolecular functions. The subsequent *in vivo* validation experiments will need to enhance the targeting capability of the developed nanocarriers. Therefore, further work is required to demonstrate the feasibility of other MOFs such as HKUST-1 and ZIF-90, highlighting the versatility of this biomimetic mineralization approach, while engineering the surface of the nanomaterials for the targeted delivery of loaded biomolecules.

6.2.3. mRNA-MOFs mineralization nanosystem

The successful commercialization of Moderna and Pfizer/BioNTech Covid-19 vaccines has led to new insights into the use of lipid nanoparticles for mRNA delivery as a nanotechnology-based delivery platform. However, this mRNA-lipid nanoparticles are susceptible to degradation in the physiological environment before reaching the target tissue due to stability issues, and lead to premature nucleic acid leakage, while having to be stored at low temperatures. In contrast, inorganic nanocarriers formed by MOFs biomineralization can provide very effective protection for sensitive encapsulated molecules, allowing for long periods of room temperature storage without deactivation, reducing storage and transportation costs while allowing for targeted and controlled release. More mineralized mRNA-MOFs nanosystems will be explored in the future, such as for activating the tumor suppressor PTEN by delivered mRNA to enhance antitumor immunity in preclinical models.

7. Acknowledgements

This doctoral thesis was carried out during the time of 01.2018-12.2021 in the Pharmaceutical Sciences Laboratory (PSL) at the Faculty of Science and Engineering of Åbo Akademi University and Turku Bioscience Centre, University of Turku and Åbo Akademi University. The main funding support was from the Doctoral Network in Materials Research (DNMR) at Åbo Akademi University which are gratefully acknowledged.

First of all, I would like to express my sincere gratitude to my supervisor, Prof. Hongbo Zhang. Your hard work has been involved in every aspect of my PhD study, from the selection of the topics, the design of the experiments, the progress of the research work, the solution of the problems, to the writing of the final thesis. Your cutting-edge academic ideas and attainments have inspired my interest in research. Your rigorous and realistic attitude and indomitable spirit have made me admire and respect from the bottom of my heart. You are a guiding light on my research journey, a role model for me to follow and a big brother in my life. I hope our research group will grow bigger and stronger under your leadership.

I would like to thank my co-supervisor Prof. Jessica M. Rosenholm for choosing me to be a PhD student in PSL group and making my four years in beautiful Finland enjoyable. Thanks for your continuous guidance and selfless help and encouragement. From the structure and content of the thesis to the final review, I could not have done it without your help and patience!

Thanks to my many collaborators, especially Pengpeng Yan and Prof. Jia Shen at Zhejiang University, despite all the inconveniences caused by the epidemic, it did not affect our fruitful outcomes in any way. I look forward to seeing you and working with you in the future!

I would like to thank all of current and former colleagues in the PSL group for providing such a pleasant working environment for me. I am especially grateful to Yuezhou Zhang, Ming Ma, Junnian Zhou, Yong Guo and Ye Liang for their help and guidance in my research. Thanks to D.K., Wali, Oliver, Jiaqi, Xiaodong, Ezgi, Rawand, Wenhui, Yonghui, Meixin for their company, assistance, scientific discussions and laughs. I would like to express my deep gratitude to my friends in Finland, especially Li Chen, Emma Ci, Jinghui Yang, Kang Chen and Weihua Zhang, who provided me with the support and friendship I needed, and all the good time we had together.

I would also like to say a heartfelt gratitude to my beloved parents for their endless love, support, and encouragement. And especially to my wife, Xiaoyu Xu, thank you for your company in Finland and the rest of my life. I love you all!

Turku, 2022

Chang Liu

8. Reference

US Food and Drug Administration GRAS Substances (SCOGS) Database - Select Committee on GRAS Substances (SCOGS) Opinion: Silicates.

Allen, T. M., Cullis P. R., 2013. Liposomal drug delivery systems: from concept to clinical applications. Adv. Drug Del. Rev. 65, 36-48. https://doi.org/10.1016/j.addr.2012.09.037

Ashley, C. E., Carnes E. C., Phillips G. K., Padilla D., Durfee P. N., Brown P. A., Hanna T. N., Liu J., Phillips B., Carter M. B., Carroll N. J., Jiang X., Dunphy D. R., Willman C. L., Petsev D. N., Evans D. G., Parikh A. N., Chackerian B., Wharton W., Peabody D. S., Brinker C. J., 2011. The targeted delivery of multicomponent cargos to cancer cells by nanoporous particle-supported lipid bilayers. Nat. Mater. 10, 389-397. https://doi.org/10.1038/nmat2992

Aznar, E., Oroval M., Pascual L., Murguia J. R., Martinez-Manez R., Sancenon F., 2016. Gated Materials for On-Command Release of Guest Molecules. Chem. Rev. 116, 561-718. https://doi.org/10.1021/acs.chemrev.5b00456

Bae, K. H., Chung H. J., Park T. G., 2011. Nanomaterials for cancer therapy and imaging. Mol. Cells. 31, 295-302. https://doi.org/10.1007/s10059-011-0051-5

Banerjee, R., Phan A., Wang B., Knobler C., Furukawa H., O'Keeffe M., Yaghi O. M., 2008. High-throughput synthesis of zeolitic imidazolate frameworks and application to CO2 capture. Science. 319, 939-943. https://doi.org/10.1126/science.1152516

Batandier, C., Fontaine E., Keriel C., Leverve X. M., 2002. Determination of mitochondrial reactive oxygen species: methodological aspects. J. Cell. Mol. Med. 6, 175-187. https://doi.org/10.1111/j.1582-4934.2002.tb00185.x

Bauer, S., Serre C., Devic T., Horcajada P., Marrot J., Ferey G., Stock N., 2008. High-throughput assisted rationalization of the formation of metal organic frameworks in the Iron(III) aminoterephthalate solvothermal system. Inorg. Chem. 47, 7568-7576. https://doi.org/10.1021/ic800538r

Beck, J. S., Vartuli J. C., Roth W. J., Leonowicz M. E., Kresge C. T., Schmitt K. D., Chu C. T. W., Olson D. H., Sheppard E. W., McCullen S. B., Higgins J. B., Schlenker J. L., 1992. A NEW FAMILY OF MESOPOROUS MOLECULAR-SIEVES PREPARED WITH LIQUID-CRYSTAL TEMPLATES. J. Am. Chem. Soc. 114, 10834-10843. https://doi.org/10.1021/ja00053a020

Blanco, E., Shen H., Ferrari M., 2015. Principles of nanoparticle design for overcoming biological barriers to drug delivery. Nat. Biotechnol. 33, 941-951. https://doi.org/10.1038/nbt.3330

Bobo, D., Robinson K. J., Islam J., Thurecht K. J., Corrie S. R., 2016. Nanoparticle-Based Medicines: A Review of FDA-Approved Materials and Clinical Trials to Date. Pharm. Res. 33, 2373-2387. https://doi.org/10.1007/s11095-016-1958-5

Botella, P., Corma A., Navarro M. T., Quesada M., 2009. Design of optically active nanoclusters of gold particles with mesostructured silica coating. J. Mater. Chem. 19, 3168-3175. https://doi.org/10.1039/b820293a

Bourzac, K., 2012. Nanotechnology: Carrying drugs. Nature. 491, S58-60. https://doi.org/10.1038/491s58a

Bozzuto, G., Molinari A., 2015. Liposomes as nanomedical devices. Int. J. Nanomed. 10, 975-999. https://doi.org/10.2147/IJN.S68861

Brannon-Peppas, L., Blanchette J. O., 2004. Nanoparticle and targeted systems for cancer therapy. Adv. Drug Del. Rev. 56, 1649-1659. https://doi.org/10.1016/j.addr.2004.02.014

Cai, W., Wang J. Q., Chu C. C., Chen W., Wu C. S., Liu G., 2019. Metal Organic Framework-Based Stimuli-Responsive Systems for Drug Delivery. Adv. Sci. 6, https://doi.org/10.1002/advs.201801526

Chae, H. K., Siberio-Perez D. Y., Kim J., Go Y., Eddaoudi M., Matzger A. J., O'Keeffe M.,

Yaghi O. M., 2004. A route to high surface area, porosity and inclusion of large molecules in crystals. Nature. 427, 523-527. https://doi.org/10.1038/nature02311

Chen, G., Huang S., Kou X., Zhu F., Ouyang G., 2020. Embedding Functional Biomacromolecules within Peptide-Directed Metal-Organic Framework (MOF) Nanoarchitectures Enables Activity Enhancement. Angew. Chem. Int. Ed. 59, 13947-13954. https://doi.org/10.1002/anie.202005529

Chen, G., Roy I., Yang C., Prasad P. N., 2016. Nanochemistry and Nanomedicine for Nanoparticle-based Diagnostics and Therapy. Chem. Rev. 116, 2826-2885. https://doi.org/10.1021/acs.chemrev.5b00148

Chen, M., He X., Wang K., He D., Yang S., Qiu P., Chen S., 2014. A pH-responsive polymer/mesoporous silica nano-container linked through an acid cleavable linker for intracellular controlled release and tumor therapy in vivo. J. Mater. Chem. B. 2, 428-436. https://doi.org/10.1039/c3tb21268h

Chen, T., Zhao T., Wei D., Wei Y., Li Y., Zhang H., 2013. Core-shell nanocarriers with ZnO quantum dots-conjugated Au nanoparticle for tumor-targeted drug delivery. Carbohydr. Polym. 92, 1124-1132. https://doi.org/10.1016/j.carbpol.2012.10.022

Chen, W. H., Yu X., Liao W. C., Sohn Y. S., Cecconello A., Kozell A., Nechushtai R., Willner I., 2017. ATP-Responsive Aptamer-Based Metal-Organic Framework Nanoparticles (NMOFs) for the Controlled Release of Loads and Drugs. Adv. Funct. Mater. 27, https://doi.org/10.1002/adfm.201702102

Chen, Y., Yin Q., Ji X., Zhang S., Chen H., Zheng Y., Sun Y., Qu H., Wang Z., Li Y., Wang X., Zhang K., Zhang L., Shi J., 2012. Manganese oxide-based multifunctionalized mesoporous silica nanoparticles for pH-responsive MRI, ultrasonography and circumvention of MDR in cancer cells. Biomaterials. 33, 7126-7137. https://doi.org/10.1016/j.biomaterials.2012.06.059

Chu, W. M., 2013. Tumor necrosis factor. Cancer Lett. 328, 222-225. https://doi.org/10.1016/j.canlet.2012.10.014

Connor, E. E., Mwamuka J., Gole A., Murphy C. J., Wyatt M. D., 2005. Gold nanoparticles are taken up by human cells but do not cause acute cytotoxicity. Small. 1, 325-327. https://doi.org/10.1002/smll.200400093

Cranford, T. L., Enos R. T., Velazquez K. T., McClellan J. L., Davis J. M., Singh U. P., Nagarkatti M., Nagarkatti P. S., Robinson C. M., Murphy E. A., 2016. Role of MCP-1 on inflammatory processes and metabolic dysfunction following high-fat feedings in the FVB/N strain. Int. J. Obes. (Lond.). 40, 844-851. https://doi.org/10.1038/ijo.2015.244

Crucho, C. I. C., 2015. Stimuli-Responsive Polymeric Nanoparticles for Nanomedicine. Chemmedchem. 10, 24-38. https://doi.org/10.1002/cmdc.201402290

Deng, X. R., Liang S., Cai X. C., Huang S. S., Cheng Z. Y., Shi Y. S., Pang M. L., Ma P. A., Lin J., 2019. Yolk-Shell Structured Au Nanostar@Metal-Organic Framework for Synergistic Chemo-photothermal Therapy in the Second Near-Infrared Window. Nano Letters. 19, 6772-6780. https://doi.org/10.1021/acs.nanolett.9b01716

Dokoumetzidis, A., Macheras P., 2006. A century of dissolution research: from Noyes and Whitney to the biopharmaceutics classification system. Int. J. Pharm. 321, 1-11. https://doi.org/10.1016/j.ijpharm.2006.07.011

Dong, H., Yang G. X., Zhang X., Meng X. B., Sheng J. L., Sun X. J., Feng Y. J., Zhang F. M., 2018. Folic Acid Functionalized Zirconium-Based Metal-Organic Frameworks as Drug Carriers for Active Tumor-Targeted Drug Delivery. Chem. Eur. J. 24, 17148-17154. https://doi.org/10.1002/chem.201804153

Dong, K., Zhang Y., Zhang L., Wang Z., Ren J., Qu X., 2019. Facile preparation of metal-organic frameworks-based hydrophobic anticancer drug delivery nanoplatform for targeted and enhanced cancer

treatment. Talanta. 194, 703-708. https://doi.org/10.1016/j.talanta.2018.10.101

Duan, F., Feng X., Yang X., Sun W., Jin Y., Liu H., Ge K., Li Z., Zhang J., 2017. A simple and powerful co-delivery system based on pH-responsive metal-organic frameworks for enhanced cancer immunotherapy. Biomaterials. 122, 23-33. https://doi.org/10.1016/j.biomaterials.2017.01.017

Duan, Y., Ye F., Huang Y., Qin Y., He C., Zhao S., 2018. One-pot synthesis of a metal-organic framework-based drug carrier for intelligent glucose-responsive insulin delivery. Chem. Commun. (Camb.). 54, 5377-5380. https://doi.org/10.1039/c8cc02708k

Eddaoudi, M., Kim J., Wachter J. B., Chae H. K., O'Keeffe M., Yaghi O. M., 2001. Porous metal-organic polyhedra: 25 A cuboctahedron constructed from 12 Cu2(CO2)4 paddle-wheel building blocks. J. Am. Chem. Soc. 123, 4368-4369. https://doi.org/10.1021/ja0104352

El-Sawy, H. S., Al-Abd A. M., Ahmed T. A., El-Say K. M., Torchilin V. P., 2018. Stimuli-Responsive Nano-Architecture Drug-Delivery Systems to Solid Tumor Micromilieu: Past, Present, and Future Perspectives. ACS Nano. 12, 10636-10664. https://doi.org/10.1021/acsnano.8b06104

Fang, I. J., Slowing, II, Wu K. C., Lin V. S., Trewyn B. G., 2012. Ligand conformation dictates membrane and endosomal trafficking of arginine-glycine-aspartate (RGD)-functionalized mesoporous silica nanoparticles. Chemistry (Easton). 18, 7787-7792. https://doi.org/10.1002/chem.201200023

Feng, A. L., Wang Y. N., Ding J. Z., Xu R., Li X. D., 2021. Progress of Stimuli-Responsive Nanoscale Metal Organic Frameworks as Controlled Drug Delivery Systems. Curr. Drug Del. 18, 297-311. https://doi.org/10.2174/1567201817666200917120201

Ferey, G., Mellot-Draznieks C., Serre C., Millange F., Dutour J., Surble S., Margiolaki I., 2005. A chromium terephthalate-based solid with unusually large pore volumes and surface area. Science. 309, 2040-2042. https://doi.org/10.1126/science.1116275

Ferris, D. P., Lu J., Gothard C., Yanes R., Thomas C. R., Olsen J. C., Stoddart J. F., Tamanoi F., Zink J. I., 2011. Synthesis of biomolecule-modified mesoporous silica nanoparticles for targeted hydrophobic drug delivery to cancer cells. Small. 7, 1816-1826. https://doi.org/10.1002/smll.201002300

Frenkel, V., 2008. Ultrasound mediated delivery of drugs and genes to solid tumors. Adv. Drug Del. Rev. 60, 1193-1208. https://doi.org/10.1016/j.addr.2008.03.007

Frenkel, V., Etherington A., Greene M., Quijano J., Xie J., Hunter F., Dromi S., Li K. C., 2006. Delivery of liposomal doxorubicin (Doxil) in a breast cancer tumor model: investigation of potential enhancement by pulsed-high intensity focused ultrasound exposure. Acad. Radiol. 13, 469-479. https://doi.org/10.1016/j.acra.2005.08.024

Gao, X., Cui R., Song L., Liu Z., 2019. Hollow structural metal-organic frameworks exhibit high drug loading capacity, targeted delivery and magnetic resonance/optical multimodal imaging. Dalton Trans. 48, 17291-17297. https://doi.org/10.1039/c9dt03287h

Gao, X., Hai X., Baigude H., Guan W., Liu Z., 2016. Fabrication of functional hollow microspheres constructed from MOF shells: Promising drug delivery systems with high loading capacity and targeted transport. Sci. Rep. 6, 37705. https://doi.org/10.1038/srep37705

Gao, Z. G., Fain H. D., Rapoport N., 2005. Controlled and targeted tumor chemotherapy by micellar-encapsulated drug and ultrasound. J. Control. Release. 102, 203-222. https://doi.org/10.1016/j.jconrel.2004.09.021

Golombek, S. K., May J. N., Theek B., Appold L., Drude N., Kiessling F., Lammers T., 2018. Tumor targeting via EPR: Strategies to enhance patient responses. Adv. Drug Del. Rev. 130, 17-38.

https://doi.org/10.1016/j.addr.2018.07.007
Gomes, H. I. O., Martins C. S. M., Prior J. A. V., 2021. Silver Nanoparticles as Carriers of Anticancer Drugs for Efficient Target Treatment of Cancer Cells. Nanomaterials (Basel). 11, https://doi.org/10.3390/nano11040964
Graf, N., Lippard S. J., 2012. Redox activation of metal-based prodrugs as a strategy for drug delivery. Adv. Drug Del. Rev. 64, 993-1004. https://doi.org/10.1016/j.addr.2012.01.007
Gregoriadis, G., Ryman B. E., 1971. Liposomes as carriers of enzymes or drugs: a new approach to the treatment of storage diseases. Biochem. J. 124, 58P. https://doi.org/10.1042/bj1240058p
Guillet-Nicolas, R., Laprise-Pelletier M., Nair M. M., Chevallier P., Lagueux J., Gossuin Y., Laurent S., Kleitz F., Fortin M. A., 2013. Manganese-impregnated mesoporous silica nanoparticles for signal enhancement in MRI cell labelling studies. Nanoscale. 5, 11499-11511. https://doi.org/10.1039/c3nr02969g
Guimaraes, R. S., Rodrigues C. F., Moreira A. F., Correia I. J., 2020. Overview of stimuli-responsive mesoporous organosilica nanocarriers for drug delivery. Pharmacol. Res. 155, https://doi.org/10.1016/j.phrs.2020.104742
Halperin, A., Kroger M., Winnik F. M., 2015. Poly(N-isopropylacrylamide) Phase Diagrams: Fifty Years of Research. Angew. Chem. Int. Ed. 54, 15342-15367. https://doi.org/10.1002/anie.201506663
Hansen-Bruhn, M., de Avila B. E., Beltran-Gastelum M., Zhao J., Ramirez-Herrera D. E., Angsantikul P., Vesterager Gothelf K., Zhang L., Wang J., 2018. Active Intracellular Delivery of a Cas9/sgRNA Complex Using Ultrasound-Propelled Nanomotors. Angew. Chem. Int. Ed. 57, 2657-2661. https://doi.org/10.1002/anie.201713082
Hao, R., Xing R., Xu Z., Hou Y., Gao S., Sun S., 2010. Synthesis, functionalization, and biomedical applications of multifunctional magnetic nanoparticles. Adv. Mater. 22, 2729-2742. https://doi.org/10.1002/adma.201000260
Harris, J. M., Chess R. B., 2003. Effect of pegylation on pharmaceuticals. Nat. Rev. Drug Discov. 2, 214-221. https://doi.org/10.1038/nrd1033
Hasan, A. S., Socha M., Lamprecht A., Ghazouani F. E., Sapin A., Hoffman M., Maincent P., Ubrich N., 2007. Effect of the microencapsulation of nanoparticles on the reduction of burst release. Int. J. Pharm. 344, 53-61. https://doi.org/10.1016/j.ijpharm.2007.05.066
He, C., Liu D., Lin W., 2015. Nanomedicine Applications of Hybrid Nanomaterials Built from Metal-Ligand Coordination Bonds: Nanoscale Metal-Organic Frameworks and Nanoscale Coordination Polymers. Chem. Rev. 115, 11079-11108. https://doi.org/10.1021/acs.chemrev.5b00125
He, D. G., He X. X., Wang K. M., Cao J., Zhao Y. X., 2012. A Light-Responsive Reversible Molecule-Gated System Using Thymine-Modified Mesoporous Silica Nanoparticles. Langmuir. 28, 4003-4008. https://doi.org/10.1021/la2047504
He, Q., Shi J., 2014. MSN anti-cancer nanomedicines: chemotherapy enhancement, overcoming of drug resistance, and metastasis inhibition. Adv. Mater. 26, 391-411. https://doi.org/10.1002/adma.201303123
Heshe, D., Hoogestraat S., Brauckmann C., Karst U., Boos J., Lanvers-Kaminsky C., 2011. Dichloroacetate metabolically targeted therapy defeats cytotoxicity of standard anticancer drugs. Cancer Chemother. Pharmacol. 67, 647-655. https://doi.org/10.1007/s00280-010-1361-6
Hildebrandt, B., Wust P., Ahlers O., Dieing A., Sreenivasa G., Kerner T., Felix R., Riess H., 2002. The cellular and molecular basis of hyperthermia. Crit. Rev. Oncol. Hematol. 43, 33-56. https://doi.org/10.1016/s1040-8428(01)00179-2
Horcajada, P., Chalati T., Serre C., Gillet B., Sebrie C., Baati T., Eubank J. F., Heurtaux D., Clayette P., Kreuz C., Chang J. S.,

Hwang Y. K., Marsaud V., Bories P. N., Cynober L., Gil S., Ferey G., Couvreur P., Gref R., 2010. Porous metal-organic-framework nanoscale carriers as a potential platform for drug delivery and imaging. Nat. Mater. 9, 172-178. https://doi.org/10.1038/nmat2608

Horcajada, P., Gref R., Baati T., Allan P. K., Maurin G., Couvreur P., Ferey G., Morris R. E., Serre C., 2012. Metal-organic frameworks in biomedicine. Chem. Rev. 112, 1232-1268. https://doi.org/10.1021/cr200256v

Horcajada, P., Surble S., Serre C., Hong D. Y., Seo Y. K., Chang J. S., Greneche J. M., Margiolaki I., Ferey G., 2007. Synthesis and catalytic properties of MIL-100(Fe), an iron(III) carboxylate with large pores. Chem. Commun. (Camb.). 2820-2822. https://doi.org/10.1039/b704325b

Hou, X. C., Zaks T., Langer R., Dong Y. Z., 2021. Lipid nanoparticles for mRNA delivery. Nat. Rev. Mater. https://doi.org/10.1038/s41578-021-00358-0

Huang, C. K., Lo C. L., Chen H. H., Hsiue G. H., 2007. Multifunctional Micelles for Cancer Cell Targeting, Distribution Imaging, and Anticancer Drug Delivery. Adv. Funct. Mater. 17, 2291-2297. https://doi.org/10.1002/adfm.200600818

Huang, X., Zhuang J., Teng X., Li L., Chen D., Yan X., Tang F., 2010. The promotion of human malignant melanoma growth by mesoporous silica nanoparticles through decreased reactive oxygen species. Biomaterials. 31, 6142-6153. https://doi.org/10.1016/j.biomaterials.2010.04.055

Hwang, C., Sinskey A. J., Lodish H. F., 1992. Oxidized redox state of glutathione in the endoplasmic reticulum. Science. 257, 1496-1502. https://doi.org/10.1126/science.1523409

Hwang, E. T., Tatavarty R., Chung J., Gu M. B., 2013. New functional amorphous calcium phosphate nanocomposites by enzyme-assisted biomineralization. ACS Appl. Mater. Inter. 5, 532-537. https://doi.org/10.1021/am302580p

Imaz, I., Rubio-Martinez M., Garcia-Fernandez L., Garcia F., Ruiz-Molina D., Hernando J., Puntes V., Maspoch D., 2010. Coordination polymer particles as potential drug delivery systems. Chem. Commun. 46, 4737-4739. https://doi.org/10.1039/c003084h

Issels, R. D., 2008. Hyperthermia adds to chemotherapy. Eur. J. Cancer. 44, 2546-2554. https://doi.org/10.1016/j.ejca.2008.07.038

Jain, R. K., Stylianopoulos T., 2010. Delivering nanomedicine to solid tumors. Nat. Rev. Clin. Oncol. 7, 653-664. https://doi.org/10.1038/nrclinonc.2010.139

Janiszewski, M., Pedro M. A., Scheffer R. C., van Asseldonk J. H., Souza L. C., da Luz P. L., Augusto O., Laurindo F. R., 2000. Inhibition of vascular NADH/NADPH oxidase activity by thiol reagents: lack of correlation with cellular glutathione redox status. Free Radic. Biol. Med. 29, 889-899. https://doi.org/10.1016/s0891-5849(00)00393-2

Jia, X., Yang Z., Wang Y., Chen Y., Yuan H., Chen H., Xu X., Gao X., Liang Z., Sun Y., Li J. R., Zheng H., Cao R., 2018. Hollow Mesoporous Silica@Metal-Organic Framework and Applications for pH-Responsive Drug Delivery. ChemMedChem. 13, 400-405. https://doi.org/10.1002/cmdc.201800019

Jiang, K., Zhang L., Hu Q., Zhang Q., Lin W. X., Cui Y. J., Yang Y., Qian G. D., 2017. Thermal Stimuli-Triggered Drug Release from a Biocompatible Porous Metal-Organic Framework. Chem. Eur. J. 23, 10215-10221. https://doi.org/10.1002/chem.201701904

Jiang, Z., Wang T., Yuan S., Wang M., Qi W., Su R., He Z., 2020. A tumor-sensitive biological metal-organic complex for drug delivery and cancer therapy. J. Mater. Chem. B. 8, 7189-7196. https://doi.org/10.1039/d0tb00599a

Kandiah, M., Nilsen M. H., Usseglio S., Jakobsen S., Olsbye U., Tilset M., Larabi C., Quadrelli E. A., Bonino F., Lillerud K. P., 2010. Synthesis and Stability of Tagged UiO-66 Zr-MOFs. Chem. Mater. 22, 6632-6640. https://doi.org/10.1021/cm102601v

Kaneti, Y. V., Dutta S., Hossain M. S. A., Shiddiky M. J. A., Tung K. L., Shieh F. K., Tsung C. K., Wu K. C., Yamauchi Y., 2017. Strategies for Improving the Functionality of Zeolitic Imidazolate Frameworks: Tailoring Nanoarchitectures for Functional Applications. Adv. Mater. 29, https://doi.org/10.1002/adma.201700213

Ke, F., Yuan Y. P., Qiu L. G., Shen Y. H., Xie A. J., Zhu J. F., Tian X. Y., Zhang L. D., 2011. Facile fabrication of magnetic metal-organic framework nanocomposites for potential targeted drug delivery. J. Mater. Chem. 21, 3843-3848. https://doi.org/10.1039/c0jm01770a

Kheirolomoom, A., Mahakian L. M., Lai C. Y., Lindfors H. A., Seo J. W., Paoli E. E., Watson K. D., Haynam E. M., Ingham E. S., Xing L., Cheng R. H., Borowsky A. D., Cardiff R. D., Ferrara K. W., 2010. Copper-doxorubicin as a nanoparticle cargo retains efficacy with minimal toxicity. Mol. Pharm. 7, 1948-1958. https://doi.org/10.1021/mp100245u

Kim, J., Lee J. E., Lee S. H., Yu J. H., Lee J. H., Park T. G., Hyeon T., 2008. Designed Fabrication of a Multifunctional Polymer Nanomedical Platform for Simultaneous Cancer- Targeted Imaging and Magnetically Guided Drug Delivery. Adv. Mater. 20, 478-483. https://doi.org/10.1002/adma.200701726

Kim, S., Philippot S., Fontanay S., Duval R. E., Lamouroux E., Canilho N., Pasc A., 2015. pH- and glutathione-responsive release of curcumin from mesoporous silica nanoparticles coated using tannic acid-Fe(III) complex. RSC Adv. 5, 90550-90558. https://doi.org/10.1039/c5ra16004a

Klajnert, B., Bryszewska M., 2001. Dendrimers: properties and applications. Acta Biochim. Pol. 48, 199-208. https://www.ncbi.nlm.nih.gov/pubmed/11440170)

Koh, K., Wong-Foy A. G., Matzger A. J., 2009. A porous coordination copolymer with over 5000 m2/g BET surface area. J. Am. Chem. Soc. 131, 4184-4185. https://doi.org/10.1021/ja809985t

Kooijmans, S. A. A., Fliervoet L. A. L., van der Meel R., Fens M., Heijnen H. F. G., van Bergen En Henegouwen P. M. P., Vader P., Schiffelers R. M., 2016. PEGylated and targeted extracellular vesicles display enhanced cell specificity and circulation time. J. Control. Release. 224, 77-85. https://doi.org/10.1016/j.jconrel.2016.01.009

Kuang, Y., Chen H., Chen Z. Y., Wan L. H., Liu J., Xu Z. Q., Chen X. Q., Jiang B. B., Li C., 2019. Poly(amino acid)/ZnO/mesoporous silica nanoparticle based complex drug delivery system with a charge-reversal property for cancer therapy. Colloids Surf. B. 181, 461-469. https://doi.org/10.1016/j.colsurfb.2019.05.078

Kumar, C. S., Mohammad F., 2011. Magnetic nanomaterials for hyperthermia-based therapy and controlled drug delivery. Adv. Drug Del. Rev. 63, 789-808. https://doi.org/10.1016/j.addr.2011.03.008

Kuo, W. S., Chang C. N., Chang Y. T., Yang M. H., Chien Y. H., Chen S. J., Yeh C. S., 2010. Gold nanorods in photodynamic therapy, as hyperthermia agents, and in near-infrared optical imaging. Angew. Chem. Int. Ed. 49, 2711-2715. https://doi.org/10.1002/anie.200906927

Lai, C. Y., Trewyn B. G., Jeftinija D. M., Jeftinija K., Xu S., Jeftinija S., Lin V. S., 2003. A mesoporous silica nanosphere-based carrier system with chemically removable CdS nanoparticle caps for stimuli-responsive controlled release of neurotransmitters and drug molecules. J. Am. Chem. Soc. 125, 4451-4459. https://doi.org/10.1021/ja028650l

Lai, J., Shah B. P., Zhang Y., Yang L., Lee K. B., 2015. Real-Time Monitoring of ATP-Responsive Drug Release Using Mesoporous-Silica-Coated Multicolor Upconversion Nanoparticles. ACS Nano. 9, 5234-5245. https://doi.org/10.1021/acsnano.5b00641

Latroche, M., Surble S., Serre C., Mellot-Draznieks C., Llewellyn P. L., Lee J. H., Chang J. S., Jhung S. H., Ferey G., 2006. Hydrogen storage in the giant-pore metal-organic frameworks MIL-100 and MIL-101. Angew. Chem. Int. Ed. 45, 8227-8231.

https://doi.org/10.1002/anie.200600105

Lee, C. H., Cheng S. H., Wang Y. J., Chen Y. C., Chen N. T., Souris J., Chen C. T., Mou C. Y., Yang C. S., Lo L. W., 2009. Near-Infrared Mesoporous Silica Nanoparticles for Optical Imaging: Characterization and In Vivo Biodistribution. Adv. Funct. Mater. 19, 215-222. https://doi.org/10.1002/adfm.200800753

Lee, E. S., Na K., Bae Y. H., 2003. Polymeric micelle for tumor pH and folate-mediated targeting. J. Control. Release. 91, 103-113. https://doi.org/10.1016/s0168-3659(03)00239-6

Lee, E. S., Oh K. T., Kim D., Youn Y. S., Bae Y. H., 2007. Tumor pH-responsive flower-like micelles of poly(L-lactic acid)-b-poly(ethylene glycol)-b-poly(L-histidine). J. Control. Release. 123, 19-26. https://doi.org/10.1016/j.jconrel.2007.08.006

Lee, J. E., Lee N., Kim T., Kim J., Hyeon T., 2011. Multifunctional mesoporous silica nanocomposite nanoparticles for theranostic applications. Acc. Chem. Res. 44, 893-902. https://doi.org/10.1021/ar2000259

Lei, B., Wang M., Jiang Z., Qi W., Su R., He Z., 2018. Constructing Redox-Responsive Metal-Organic Framework Nanocarriers for Anticancer Drug Delivery. ACS Appl. Mater. Inter. 10, 16698-16706. https://doi.org/10.1021/acsami.7b19693

Li, B., Wang X., Chen L., Zhou Y., Dang W., Chang J., Wu C., 2018. Ultrathin Cu-TCPP MOF nanosheets: a new theragnostic nanoplatform with magnetic resonance/near-infrared thermal imaging for synergistic phototherapy of cancers. Theranostics. 8, 4086-4096. https://doi.org/10.7150/thno.25433

Li, C., Guo T., Zhou D., Hu Y., Zhou H., Wang S., Chen J., Zhang Z., 2011. A novel glutathione modified chitosan conjugate for efficient gene delivery. J. Control. Release. 154, 177-188. https://doi.org/10.1016/j.jconrel.2011.06.007

Li, F., Yang H., Bie N., Xu Q., Yong T., Wang Q., Gan L., Yang X., 2017. Zwitterionic Temperature/Redox-Sensitive Nanogels for Near-Infrared Light-Triggered Synergistic Thermo-Chemotherapy. ACS Appl. Mater. Inter. 9, 23564-23573. https://doi.org/10.1021/acsami.7b08047

Li, H., Eddaoudi M., O'Keeffe M., Yaghi O. M., 1999. Design and synthesis of an exceptionally stable and highly porous metal-organic framework. Nature. 402, 276-279. https://doi.org/10.1038/46248

Li, J., Ni X., Leong K. W., 2003. Injectable drug-delivery systems based on supramolecular hydrogels formed by poly(ethylene oxide)s and alpha-cyclodextrin. J. Biomed. Mater. Res. A. 65, 196-202. https://doi.org/10.1002/jbm.a.10444

Li, L., Yang W. W., Xu D. G., 2019. Stimuli-responsive nanoscale drug delivery systems for cancer therapy. J. Drug Target. 27, 423-433. https://doi.org/10.1080/1061186x.2018.1519029

Li, Q., Zhang W., Miljanic O. S., Sue C. H., Zhao Y. L., Liu L., Knobler C. B., Stoddart J. F., Yaghi O. M., 2009. Docking in metal-organic frameworks. Science. 325, 855-859. https://doi.org/10.1126/science.1175441

Li, S., Li W. G., Khashab N. M., 2012. Stimuli responsive nanomaterials for controlled release applications. Nanotechnol. Rev. 1, 493-513. https://doi.org/10.1515/ntrev-2012-0033

Li, Y. T., Jin J., Wang D. W., Lv J. W., Hou K., Liu Y. L., Chen C. Y., Tang Z. Y., 2018. Coordination-responsive drug release inside gold nanorod@metal-organic framework core-shell nanostructures for near-infrared-induced synergistic chemo-photothermal therapy. Nano Res. 11, 3294-3305. https://doi.org/10.1007/s12274-017-1874-y

Lian, X., Fang Y., Joseph E., Wang Q., Li J., Banerjee S., Lollar C., Wang X., Zhou H. C., 2017. Enzyme-MOF (metal-organic framework) composites. Chem. Soc. Rev. 46, 3386-3401. https://doi.org/10.1039/c7cs00058h

Liang, K., Ricco R., Doherty C. M., Styles M. J., Bell S., Kirby N., Mudie S., Haylock D., Hill A. J., Doonan C. J., Falcaro P., 2015.

Biomimetic mineralization of metal-organic frameworks as protective coatings for biomacromolecules. Nat. Commun. 6, 7240. https://doi.org/10.1038/ncomms8240

Lim, E. K., Kim T., Paik S., Haam S., Huh Y. M., Lee K., 2015. Nanomaterials for theranostics: recent advances and future challenges. Chem. Rev. 115, 327-394. https://doi.org/10.1021/cr300213b

Lin, Q. N., Huang Q., Li C. Y., Bao C. Y., Liu Z. Z., Li F. Y., Zhu L. Y., 2010. Anticancer Drug Release from a Mesoporous Silica Based Nanophotocage Regulated by Either a One- or Two-Photon Process. J. Am. Chem. Soc. 132, 10645-10647. https://doi.org/10.1021/ja103415t

Lin, W. X., Hu Q., Jiang K., Yang Y. Y., Yang Y., Cui Y. J., Qian G. D., 2016. A porphyrin-based metal-organic framework as a pH-responsive drug carrier. J. Solid State Chem. 237, 307-312. https://doi.org/10.1016/j.jssc.2016.02.040

Lin, Y. S., Hurley K. R., Haynes C. L., 2012. Critical Considerations in the Biomedical Use of Mesoporous Silica Nanoparticles. J. Phys. Chem. Lett. 3, 364-374. https://doi.org/10.1021/jz2013837

Liu, C., Xu X., Zhou J., Yan J., Wang D., Zhang H., 2020. Redox-responsive tumor targeted dual-drug loaded biocompatible metal–organic frameworks nanoparticles for enhancing anticancer effects. BMC Materials. 2, https://doi.org/10.1186/s42833-020-00013-y

Liu, C., Yuan J., Luo X., Chen M., Chen Z., Zhao Y., Li X., 2014. Folate-decorated and reduction-sensitive micelles assembled from amphiphilic polymer-camptothecin conjugates for intracellular drug delivery. Mol. Pharm. 11, 4258-4269. https://doi.org/10.1021/mp500468d

Liu, C. M., Chen G. B., Chen H. H., Zhang J. B., Li H. Z., Sheng M. X., Weng W. B., Guo S. M., 2019. Cancer cell membrane-cloaked mesoporous silica nanoparticles with a pH-sensitive gatekeeper for cancer treatment. Colloids Surf. B. 175, 477-486. https://doi.org/10.1016/j.colsurfb.2018.12.038

Liu, D., Yang F., Xiong F., Gu N., 2016. The Smart Drug Delivery System and Its Clinical Potential. Theranostics. 6, 1306-1323. https://doi.org/10.7150/thno.14858

Liu, D., Zhang H., Fontana F., Hirvonen J. T., Santos H. A., 2017. Microfluidic-assisted fabrication of carriers for controlled drug delivery. Lab Chip. 17, 1856-1883. https://doi.org/10.1039/c7lc00242d

Liu, H. H., Yao J. W., Guo H. H., Cai X. W., Jiang Y., Lin M., Jiang X. J., Leung N., Xu C. S., 2020. Tumor Microenvironment-Responsive Nanomaterials as Targeted Delivery Carriers for Photodynamic Anticancer Therapy. Front. Chem. 8, https://doi.org/10.3389/fchem.2020.00758

Liu, J., Huang Y., Kumar A., Tan A., Jin S., Mozhi A., Liang X. J., 2014. pH-sensitive nano-systems for drug delivery in cancer therapy. Biotechnol. Adv. 32, 693-710. https://doi.org/10.1016/j.biotechadv.2013.11.009

Liu, R., Zhang Y., Zhao X., Agarwal A., Mueller L. J., Feng P., 2010. pH-responsive nanogated ensemble based on gold-capped mesoporous silica through an acid-labile acetal linker. J. Am. Chem. Soc. 132, 1500-1501. https://doi.org/10.1021/ja907838s

Liu, Y., Ai K., Liu J., Deng M., He Y., Lu L., 2013. Dopamine-melanin colloidal nanospheres: an efficient near-infrared photothermal therapeutic agent for in vivo cancer therapy. Adv. Mater. 25, 1353-1359. https://doi.org/10.1002/adma.201204683

Liu, Y., Hou W., Xia L., Cui C., Wan S., Jiang Y., Yang Y., Wu Q., Qiu L., Tan W., 2018. ZrMOF nanoparticles as quenchers to conjugate DNA aptamers for target-induced bioimaging and photodynamic therapy. Chem. Sci. 9, 7505-7509. https://doi.org/10.1039/c8sc02210k

Loh, X. J., del Barrio J., Toh P. P., Lee T. C., Jiao D., Rauwald U., Appel E. A., Scherman O. A., 2012. Triply triggered doxorubicin release from supramolecular nanocontainers. Biomacromolecules. 13, 84-91. https://doi.org/10.1021/bm201588m

Longmire, M. R., Ogawa M., Choyke P. L., Kobayashi H., 2011. Biologically optimized nanosized molecules and particles: more than just size. Bioconjug. Chem. 22, 993-1000. https://doi.org/10.1021/bc200111p

Lu, Y., Sun W. J., Gu Z., 2014. Stimuli-responsive nanomaterials for therapeutic protein delivery. J. Control. Release. 194, 1-19. https://doi.org/10.1016/j.jconrel.2014.08.015

Lukowiak, M. C., Thota B. N., Haag R., 2015. Dendritic core-shell systems as soft drug delivery nanocarriers. Biotechnol. Adv. 33, 1327-1341. https://doi.org/10.1016/j.biotechadv.2015.03.014

Luo, G. F., Chen W. H., Jia H. Z., Sun Y. X., Cheng H., Zhuo R. X., Zhang X. Z., 2015. An indicator-guided photo-controlled drug delivery system based on mesoporous silica/gold nanocomposites. Nano Res. 8, 1893-1905. https://doi.org/10.1007/s12274-014-0698-2

Luo, Z., Jiang L., Yang S., Li Z., Soh W. M. W., Zheng L., Loh X. J., Wu Y. L., 2019. Light-Induced Redox-Responsive Smart Drug Delivery System by Using Selenium-Containing Polymer@MOF Shell/Core Nanocomposite. Adv. Healthc. Mater. 8, e1900406. https://doi.org/10.1002/adhm.201900406

Ma, N., Wang W. J., Chen S., Wang X. S., Wang X. Q., Wang S. B., Zhu J. Y., Cheng S. X., Zhang X. Z., 2015. Cucurbit 8 uril-mediated supramolecular photoswitching for self-preservation of mesoporous silica nanoparticle delivery system. Chem. Commun. 51, 12970-12973. https://doi.org/10.1039/c5cc04631a

Maeda, H., Sawa T., Konno T., 2001. Mechanism of tumor-targeted delivery of macromolecular drugs, including the EPR effect in solid tumor and clinical overview of the prototype polymeric drug SMANCS. J. Control. Release. 74, 47-61. https://doi.org/10.1016/s0168-3659(01)00309-1

Maeda, H., Wu J., Sawa T., Matsumura Y., Hori K., 2000. Tumor vascular permeability and the EPR effect in macromolecular therapeutics: a review. J. Control. Release. 65, 271-284. https://doi.org/10.1016/s0168-3659(99)00248-5

Mal, N. K., Fujiwara M., Tanaka Y., 2003. Photocontrolled reversible release of guest molecules from coumarin-modified mesoporous silica. Nature. 421, 350-353. https://doi.org/10.1038/nature01362

Meek, S. T., Greathouse J. A., Allendorf M. D., 2011. Metal-organic frameworks: a rapidly growing class of versatile nanoporous materials. Adv. Mater. 23, 249-267. https://doi.org/10.1002/adma.201002854

Meng, H., Xue M., Xia T., Zhao Y. L., Tamanoi F., Stoddart J. F., Zink J. I., Nel A. E., 2010. Autonomous in vitro anticancer drug release from mesoporous silica nanoparticles by pH-sensitive nanovalves. J. Am. Chem. Soc. 132, 12690-12697. https://doi.org/10.1021/ja104501a

Meng, X., Deng J., Liu F., Guo T., Liu M. Y., Dai P. P., Fan A. P., Wang Z., Zhao Y. J., 2019. Triggered All-Active Metal Organic Framework: Ferroptosis Machinery Contributes to the Apoptotic Photodynamic Antitumor Therapy. Nano Letters. 19, 7866-7876. https://doi.org/10.1021/acs.nanolett.9b02904

Moreira, A. F., Gaspar V. M., Costa E. C., de Melo-Diogo D., Machado P., Paquete C. M., Correia I. J., 2014. Preparation of end-capped pH-sensitive mesoporous silica nanocarriers for on-demand drug delivery. Eur. J. Pharm. Biopharm. 88, 1012-1025. https://doi.org/10.1016/j.ejpb.2014.09.002

Morgan, M. T., Nakanishi Y., Kroll D. J., Griset A. P., Carnahan M. A., Wathier M., Oberlies N. H., Manikumar G., Wani M. C., Grinstaff M. W., 2006. Dendrimer-encapsulated camptothecins: increased solubility, cellular uptake, and cellular retention affords enhanced anticancer activity in vitro. Cancer Res. 66, 11913-11921. https://doi.org/10.1158/0008-5472.CAN-06-2066

Muhammad, F., Guo M., Qi W., Sun F., Wang A., Guo Y., Zhu G., 2011. pH-Triggered controlled drug release from mesoporous silica nanoparticles via intracelluar dissolution of ZnO nanolids. J. Am. Chem. Soc. 133, 8778-8781. https://doi.org/10.1021/ja200328s

Muhammad, F., Wang A., Guo M., Zhao J., Qi W., Yingjie G., Gu J., Zhu G., 2013. pH dictates the release of hydrophobic drug cocktail from mesoporous nanoarchitecture. ACS Appl. Mater. Inter. 5, 11828-11835. https://doi.org/10.1021/am4035027

Mulfort, K. L., Farha O. K., Stern C. L., Sarjeant A. A., Hupp J. T., 2009. Post-synthesis alkoxide formation within metal-organic framework materials: a strategy for incorporating highly coordinatively unsaturated metal ions. J. Am. Chem. Soc. 131, 3866-3868. https://doi.org/10.1021/ja809954r

Nagata, S., Kokado K., Sada K., 2015. Metal-organic framework tethering PNIPAM for ON-OFF controlled release in solution. Chem. Commun. (Camb.). 51, 8614-8617. https://doi.org/10.1039/c5cc02339d

Nasongkla, N., Bey E., Ren J., Ai H., Khemtong C., Guthi J. S., Chin S. F., Sherry A. D., Boothman D. A., Gao J., 2006. Multifunctional polymeric micelles as cancer-targeted, MRI-ultrasensitive drug delivery systems. Nano Lett. 6, 2427-2430. https://doi.org/10.1021/nl061412u

Neri, D., Supuran C. T., 2011. Interfering with pH regulation in tumours as a therapeutic strategy. Nat. Rev. Drug Discov. 10, 767-777. https://doi.org/10.1038/nrd3554

Nicolas, J., Mura S., Brambilla D., Mackiewicz N., Couvreur P., 2013. Design, functionalization strategies and biomedical applications of targeted biodegradable/biocompatible polymer-based nanocarriers for drug delivery. Chem. Soc. Rev. 42, 1147-1235. https://doi.org/10.1039/c2cs35265f

O'Neill, M. A., Hidalgo L. G., 2021. NK cells in antibody-mediated rejection - Key effector cells in microvascular graft damage. Int. J. Immunogenet. 48, 110-119. https://doi.org/10.1111/iji.12532

Oerlemans, C., Bult W., Bos M., Storm G., Nijsen J. F., Hennink W. E., 2010. Polymeric micelles in anticancer therapy: targeting, imaging and triggered release. Pharm. Res. 27, 2569-2589. https://doi.org/10.1007/s11095-010-0233-4

Ohlfest, J. R., Freese A. B., Largaespada D. A., 2005. Nonviral vectors for cancer gene therapy: prospects for integrating vectors and combination therapies. Curr. Gene Ther. 5, 629-641. https://doi.org/10.2174/156652305774964749

Palanikumar, L., Choi E. S., Cheon J. Y., Joo S. H., Ryu J. H., 2015. Noncovalent Polymer-Gatekeeper in Mesoporous Silica Nanoparticles as a Targeted Drug Delivery Platform. Adv. Funct. Mater. 25, 957-965. https://doi.org/10.1002/adfm.201402755

Park, H., Yang J., Lee J., Haam S., Choi I. H., Yoo K. H., 2009. Multifunctional nanoparticles for combined doxorubicin and photothermal treatments. ACS Nano. 3, 2919-2926. https://doi.org/10.1021/nn900215k

Park, K., 2013. Facing the truth about nanotechnology in drug delivery. ACS Nano. 7, 7442-7447. https://doi.org/10.1021/nn404501g

Park, K. S., Ni Z., Cote A. P., Choi J. Y., Huang R. D., Uribe-Romo F. J., Chae H. K., O'Keeffe M., Yaghi O. M., 2006. Exceptional chemical and thermal stability of zeolitic imidazolate frameworks. Proc. Natl. Acad. Sci. U. S. A. 103, 10186-10191. https://doi.org/10.1073/pnas.0602439103

Peer, D., Karp J. M., Hong S., Farokhzad O. C., Margalit R., Langer R., 2007. Nanocarriers as an emerging platform for cancer therapy. Nat. Nanotechnol. 2, 751-760. https://doi.org/10.1038/nnano.2007.387

Peng, C., Yu M., Hsieh J. T., Kapur P., Zheng J., 2019. Correlating Anticancer Drug Delivery Efficiency with Vascular Permeability of Renal Clearable Versus Non-renal Clearable Nanocarriers. Angew. Chem. Int. Ed. 58, 12076-12080.

https://doi.org/10.1002/anie.201905738
Peng, X. H., Wang Y., Huang D., Wang Y., Shin H. J., Chen Z., Spewak M. B., Mao H., Wang X., Wang Y., Chen Z. G., Nie S., Shin D. M., 2011. Targeted delivery of cisplatin to lung cancer using ScFvEGFR-heparin-cisplatin nanoparticles. ACS Nano. 5, 9480-9493. https://doi.org/10.1021/nn202410f
Pham, S. H., Choi Y., Choi J., 2020. Stimuli-Responsive Nanomaterials for Application in Antitumor Therapy and Drug Delivery. Pharmaceutics. 12, https://doi.org/10.3390/pharmaceutics12070630
Prestipino, C., Regli L., Vitillo J. G., Bonino F., Damin A., Lamberti C., Zecchina A., Solari P. L., Kongshaug K. O., Bordiga S., 2006. Local structure of framework Cu(II) in HKUST-1 metallorganic framework: Spectroscopic characterization upon activation and interaction with adsorbates. Chem. Mater. 18, 1337-1346. https://doi.org/10.1021/cm052191g
Ran, F. A., Hsu P. D., Wright J., Agarwala V., Scott D. A., Zhang F., 2013. Genome engineering using the CRISPR-Cas9 system. Nat. Protoc. 8, 2281-2308. https://doi.org/10.1038/nprot.2013.143
Ren, H., Zhang L., An J., Wang T., Li L., Si X., He L., Wu X., Wang C., Su Z., 2014. Polyacrylic acid@zeolitic imidazolate framework-8 nanoparticles with ultrahigh drug loading capability for pH-sensitive drug release. Chem. Commun. (Camb.). 50, 1000-1002. https://doi.org/10.1039/c3cc47666a
Rieter, W. J., Pott K. M., Taylor K. M., Lin W., 2008. Nanoscale coordination polymers for platinum-based anticancer drug delivery. J. Am. Chem. Soc. 130, 11584-11585. https://doi.org/10.1021/ja803383k
Rosenholm, J. M., Peuhu E., Bate-Eya L. T., Eriksson J. E., Sahlgren C., Linden M., 2010. Cancer-cell-specific induction of apoptosis using mesoporous silica nanoparticles as drug-delivery vectors. Small. 6, 1234-1241. https://doi.org/10.1002/smll.200902355
Rosenholm, J. M., Peuhu E., Eriksson J. E., Sahlgren C., Linden M., 2009. Targeted intracellular delivery of hydrophobic agents using mesoporous hybrid silica nanoparticles as carrier systems. Nano Lett. 9, 3308-3311. https://doi.org/10.1021/nl901589y
Rotello, V. M., 2008. Advanced drug delivery reviews theme issue. Preface. Adv. Drug Del. Rev. 60, 1225. https://doi.org/10.1016/j.addr.2008.04.003
Ryplida, B., Lee G., In I., Park S. Y., 2019. Zwitterionic carbon dot-encapsulating pH-responsive mesoporous silica nanoparticles for NIR light-triggered photothermal therapy through pH-controllable release. Biomater. Sci. 7, 2600-2610. https://doi.org/10.1039/c9bm00160c
Saito, G., Swanson J. A., Lee K. D., 2003. Drug delivery strategy utilizing conjugation via reversible disulfide linkages: role and site of cellular reducing activities. Adv. Drug Del. Rev. 55, 199-215. https://doi.org/10.1016/s0169-409x(02)00179-5
Sanvicens, N., Marco M. P., 2008. Multifunctional nanoparticles--properties and prospects for their use in human medicine. Trends Biotechnol. 26, 425-433. https://doi.org/10.1016/j.tibtech.2008.04.005
Serre, C., Millange F., Surble S., Ferey G., 2004. A route to the synthesis of trivalent transition-metal porous carboxylates with trimeric secondary building units. Angew. Chem. Int. Ed. 43, 6285-6289. https://doi.org/10.1002/anie.200454250
Serre, C., Millange F., Thouvenot C., Nogues M., Marsolier G., Louer D., Ferey G., 2002. Very large breathing effect in the first nanoporous chromium(III)-based solids: MIL-53 or Cr(III)(OH) x [O(2)C-C(6)H(4)-CO(2)] x [HO(2)C-C(6)H(4)-CO(2)H](x) x H(2)O(y). J. Am. Chem. Soc. 124, 13519-13526. https://doi.org/10.1021/ja0276974
Shen, D., Yang J., Li X., Zhou L., Zhang R., Li W., Chen L., Wang R., Zhang F., Zhao D., 2014. Biphase stratification approach to three-dimensional dendritic biodegradable mesoporous silica nanospheres. Nano Letter. 14, 923-932. https://doi.org/10.1021/nl404316v

Shi, J., Kantoff P. W., Wooster R., Farokhzad O. C., 2017. Cancer nanomedicine: progress, challenges and opportunities. Nat. Rev. Cancer. 17, 20-37. https://doi.org/10.1038/nrc.2016.108

Shim, M. S., Kwon Y. J., 2012. Stimuli-responsive polymers and nanomaterials for gene delivery and imaging applications. Adv. Drug Del. Rev. 64, 1046-1058. https://doi.org/10.1016/j.addr.2012.01.018

Siepmann, J., Peppas N. A., 2001. Modeling of drug release from delivery systems based on hydroxypropyl methylcellulose (HPMC). Adv. Drug Del. Rev. 48, 139-157. https://doi.org/10.1016/s0169-409x(01)00112-0

Silva, J. Y. R., Proenza Y. G., da Luz L. L., Araujo S. D., Gomes M. A., Alves S., Soares T. A., Longo R. L., 2019. A thermo-responsive adsorbent-heater-thermometer nanomaterial for controlled drug release: (ZIF-8,EuxTby)@AuNP core-shell. Mater. Sci. Eng. C Mater. Biol. Appl. 102, 578-588. https://doi.org/10.1016/j.msec.2019.04.078

Song, Y. H., Li Y. H., Xu Q., Liu Z., 2017. Mesoporous silica nanoparticles for stimuli-responsive controlled drug delivery: advances, challenges, and outlook. Int. J. Nanomed. 12, 87-110. https://doi.org/10.2147/ijn.s117495

Steensberg, A., Fischer C. P., Keller C., Moller K., Pedersen B. K., 2003. IL-6 enhances plasma IL-1ra, IL-10, and cortisol in humans. Am. J. Physiol. Endocrinol. Metab. 285, E433-437. https://doi.org/10.1152/ajpendo.00074.2003

Stöber, W., Fink A., Bohn E., 1968. Controlled growth of monodisperse silica spheres in the micron size range. J. Colloid Interface Sci. 26, 62-69. https://doi.org/10.1016/0021-9797(68)90272-5

Stock, N., Biswas S., 2012. Synthesis of metal-organic frameworks (MOFs): routes to various MOF topologies, morphologies, and composites. Chem. Rev. 112, 933-969. https://doi.org/10.1021/cr200304e

Stubb, A., Guzman C., Narva E., Aaron J., Chew T. L., Saari M., Miihkinen M., Jacquemet G., Ivaska J., 2019. Superresolution architecture of cornerstone focal adhesions in human pluripotent stem cells. Nat. Commun. 10, 4756. https://doi.org/10.1038/s41467-019-12611-w

Stubb, A., Laine R. F., Miihkinen M., Hamidi H., Guzman C., Henriques R., Jacquemet G., Ivaska J., 2020. Fluctuation-Based Super-Resolution Traction Force Microscopy. Nano Lett. 20, 2230-2245. https://doi.org/10.1021/acs.nanolett.9b04083

Sumida, K., Hill M. R., Horike S., Dailly A., Long J. R., 2009. Synthesis and hydrogen storage properties of Be(12)(OH)(12)(1,3,5-benzenetribenzoate)(4). J. Am. Chem. Soc. 131, 15120-15121. https://doi.org/10.1021/ja9072707

Sumiya, S., Oumi Y., Uozumi T., Sano T., 2001. Characterization of AlSBA-15 prepared by post-synthesis alumination with trimethylaluminium. J. Mater. Chem. 11, 1111-1115. https://doi.org/10.1039/b008168j

Sun, T., Zhang Y. S., Pang B., Hyun D. C., Yang M., Xia Y., 2014. Engineered nanoparticles for drug delivery in cancer therapy. Angew. Chem. Int. Ed. 53, 12320-12364. https://doi.org/10.1002/anie.201403036

Sun, Y. Z., Davis E., 2021. Nanoplatforms for Targeted Stimuli-Responsive Drug Delivery: A Review of Platform Materials and Stimuli-Responsive Release and Targeting Mechanisms. Nanomaterials. 11, https://doi.org/10.3390/nano11030746

Sun, Z., Song C., Wang C., Hu Y., Wu J., 2020. Hydrogel-Based Controlled Drug Delivery for Cancer Treatment: A Review. Mol. Pharm. 17, 373-391. https://doi.org/10.1021/acs.molpharmaceut.9b01020

Surble, S., Serre C., Mellot-Draznieks C., Millange F., Ferey G., 2006. A new isoreticular class of metal-organic-frameworks with the MIL-88 topology. Chem. Commun. (Camb.). 284-286. https://doi.org/10.1039/b512169h

Tait Wojno, E. D., Hunter C. A., Stumhofer J. S., 2019. The Immunobiology of the

Interleukin-12 Family: Room for Discovery. Immunity. 50, 851-870. https://doi.org/10.1016/j.immuni.2019.03.011
Takada, Y., Hisamatsu T., Kamada N., Kitazume M. T., Honda H., Oshima Y., Saito R., Takayama T., Kobayashi T., Chinen H., Mikami Y., Kanai T., Okamoto S., Hibi T., 2010. Monocyte chemoattractant protein-1 contributes to gut homeostasis and intestinal inflammation by composition of IL-10-producing regulatory macrophage subset. J. Immunol. 184, 2671-2676. https://doi.org/10.4049/jimmunol.0804012
Tanabe, K. K., Cohen S. M., 2011. Postsynthetic modification of metal-organic frameworks--a progress report. Chem. Soc. Rev. 40, 498-519. https://doi.org/10.1039/c0cs00031k
Thomas, C. R., Ferris D. P., Lee J. H., Choi E., Cho M. H., Kim E. S., Stoddart J. F., Shin J. S., Cheon J., Zink J. I., 2010. Noninvasive remote-controlled release of drug molecules in vitro using magnetic actuation of mechanized nanoparticles. J. Am. Chem. Soc. 132, 10623-10625. https://doi.org/10.1021/ja1022267
Tian, Q., Jiang F., Zou R., Liu Q., Chen Z., Zhu M., Yang S., Wang J., Wang J., Hu J., 2011. Hydrophilic Cu9S5 nanocrystals: a photothermal agent with a 25.7% heat conversion efficiency for photothermal ablation of cancer cells in vivo. ACS Nano. 5, 9761-9771. https://doi.org/10.1021/nn203293t
Tian, Q., Tang M., Sun Y., Zou R., Chen Z., Zhu M., Yang S., Wang J., Wang J., Hu J., 2011. Hydrophilic flower-like CuS superstructures as an efficient 980 nm laser-driven photothermal agent for ablation of cancer cells. Adv. Mater. 23, 3542-3547. https://doi.org/10.1002/adma.201101295
Torchilin, V., 2011. Tumor delivery of macromolecular drugs based on the EPR effect. Adv. Drug Del. Rev. 63, 131-135. https://doi.org/10.1016/j.addr.2010.03.011
Torchilin, V. P., 2014. Multifunctional, stimuli-sensitive nanoparticulate systems for drug delivery. Nat. Rev. Drug Discov. 13, 813-827. https://doi.org/10.1038/nrd4333
Trewyn, B. G., Slowing, II, Giri S., Chen H. T., Lin V. S., 2007. Synthesis and functionalization of a mesoporous silica nanoparticle based on the sol-gel process and applications in controlled release. Acc. Chem. Res. 40, 846-853. https://doi.org/10.1021/ar600032u
Trzaskowski, B., Adamowicz L., Deymier P. A., 2008. A theoretical study of zinc(II) interactions with amino acid models and peptide fragments. J. Biol. Inorg. Chem. 13, 133-137. https://doi.org/10.1007/s00775-007-0306-y
Tsai, C.-P., Chen C.-Y., Hung Y., Chang F.-H., Mou C.-Y., 2009. Monoclonal antibody-functionalized mesoporous silica nanoparticles (MSN) for selective targeting breast cancer cells. J. Mater. Chem. 19, https://doi.org/10.1039/b905158a
Vallet-Regi, M., Balas F., Arcos D., 2007. Mesoporous materials for drug delivery. Angew. Chem. Int. Ed. 46, 7548-7558. https://doi.org/10.1002/anie.200604488
Vallet-Regi, M., Ramila A., del Real R. P., Perez-Pariente J., 2001. A new property of MCM-41: Drug delivery system. Chem. Mater. 13, 308-311. https://doi.org/10.1021/cm0011559
Villa, C. H., Anselmo A. C., Mitragotri S., Muzykantov V., 2016. Red blood cells: Supercarriers for drugs, biologicals, and nanoparticles and inspiration for advanced delivery systems. Adv. Drug Del. Rev. 106, 88-103. https://doi.org/10.1016/j.addr.2016.02.007
Wan, S. S., Cheng Q., Zeng X., Zhang X. Z., 2019. A Mn(III)-Sealed Metal-Organic Framework Nanosystem for Redox-Unlocked Tumor Theranostics. Acs Nano. 13, 6561-6571. https://doi.org/10.1021/acsnano.9b00300
Wan, Y., Zhao D., 2007. On the controllable soft-templating approach to mesoporous silicates. Chem. Rev. 107, 2821-2860. https://doi.org/10.1021/cr068020s
Wang, B., Cote A. P., Furukawa H., O'Keeffe M., Yaghi O. M., 2008. Colossal cages in zeolitic imidazolate frameworks as

selective carbon dioxide reservoirs. Nature. 453, 207-211. https://doi.org/10.1038/nature06900

Wang, C., Li Z., Cao D., Zhao Y. L., Gaines J. W., Bozdemir O. A., Ambrogio M. W., Frasconi M., Botros Y. Y., Zink J. I., Stoddart J. F., 2012. Stimulated release of size-selected cargos in succession from mesoporous silica nanoparticles. Angew. Chem. Int. Ed. 51, 5460-5465. https://doi.org/10.1002/anie.201107960

Wang, D., Zhou J., Chen R., Shi R., Xia G., Zhou S., Liu Z., Zhang N., Wang H., Guo Z., Chen Q., 2016. Magnetically guided delivery of DHA and Fe ions for enhanced cancer therapy based on pH-responsive degradation of DHA-loaded Fe3O4@C@MIL-100(Fe) nanoparticles. Biomaterials. 107, 88-101. https://doi.org/10.1016/j.biomaterials.2016.08.039

Wang, D., Zhou J., Chen R., Shi R., Zhao G., Xia G., Li R., Liu Z., Tian J., Wang H., Guo Z., Wang H., Chen Q., 2016. Controllable synthesis of dual-MOFs nanostructures for pH-responsive artemisinin delivery, magnetic resonance and optical dual-model imaging-guided chemo/photothermal combinational cancer therapy. Biomaterials. 100, 27-40. https://doi.org/10.1016/j.biomaterials.2016.05.027

Wang, G., Cao R. Y., Chen R., Mo L., Han J. F., Wang X., Xu X., Jiang T., Deng Y. Q., Lyu K., Zhu S. Y., Qin E. D., Tang R., Qin C. F., 2013. Rational design of thermostable vaccines by engineered peptide-induced virus self-biomineralization under physiological conditions. Proc. Natl. Acad. Sci. U. S. A. 110, 7619-7624. https://doi.org/10.1073/pnas.1300233110

Wang, R., Billone P. S., Mullett W. M., 2013. Nanomedicine in Action: An Overview of Cancer Nanomedicine on the Market and in Clinical Trials. J. Nanomater. 2013, 1-12. https://doi.org/10.1155/2013/629681

Wang, X. G., Dong Z. Y., Cheng H., Wan S. S., Chen W. H., Zou M. Z., Huo J. W., Deng H. X., Zhang X. Z., 2015. A multifunctional metal-organic framework based tumor targeting drug delivery system for cancer therapy. Nanoscale. 7, 16061-16070. https://doi.org/10.1039/c5nr04045k

Wang, Y., Han N., Zhao Q., Bai L., Li J., Jiang T., Wang S., 2015. Redox-responsive mesoporous silica as carriers for controlled drug delivery: a comparative study based on silica and PEG gatekeepers. Eur. J. Pharm. Sci. 72, 12-20. https://doi.org/10.1016/j.ejps.2015.02.008

Wang, Y., Li L., Liang H., Xing Y., Yan L., Dai P., Gu X., Zhao G., Zhao X., 2019. Superstructure of a Metal-Organic Framework Derived from Microdroplet Flow Reaction: An Intermediate State of Crystallization by Particle Attachment. ACS Nano. 13, 2901-2912. https://doi.org/10.1021/acsnano.8b06706

Wang, Y., Shahi P. K., Xie R., Zhang H., Abdeen A. A., Yodsanit N., Ma Z., Saha K., Pattnaik B. R., Gong S., 2020. A pH-responsive silica-metal-organic framework hybrid nanoparticle for the delivery of hydrophilic drugs, nucleic acids, and CRISPR-Cas9 genome-editing machineries. J. Control. Release. 324, 194-203. https://doi.org/10.1016/j.jconrel.2020.04.052

Wang, Y., Shim M. S., Levinson N. S., Sung H. W., Xia Y., 2014. Stimuli-Responsive Materials for Controlled Release of Theranostic Agents. Adv. Funct. Mater. 24, 4206-4220. https://doi.org/10.1002/adfm.201400279

Wang, Z., Cohen S. M., 2009. Postsynthetic modification of metal-organic frameworks. Chem. Soc. Rev. 38, 1315-1329. https://doi.org/10.1039/b802258p

Weissleder, R., 2001. A clearer vision for in vivo imaging. Nat. Biotechnol. 19, 316-317. https://doi.org/10.1038/86684

Whitfield, T. R., Wang X. Q., Liu L. M., Jacobson A. J., 2005. Metal-organic frameworks based on iron oxide octahedral chains connected by benzenedicarboxylate dianions. Solid State Sciences. 7, 1096-1103. https://doi.org/10.1016/j.solidstatesciences.2005.03.007

Wu, D., Xu X., 2018. Exploring cutting-edge hydrogel technologies and their biomedical applications. Bioact. Mater. 3, 446-447. https://doi.org/10.1016/j.bioactmat.2018.08.001
Wu, G., Fang Y. Z., Yang S., Lupton J. R., Turner N. D., 2004. Glutathione metabolism and its implications for health. J. Nutr. 134, 489-492. https://doi.org/10.1093/jn/134.3.489
Wu, M., Meng Q., Chen Y., Zhang L., Li M., Cai X., Li Y., Yu P., Zhang L., Shi J., 2016. Large Pore-Sized Hollow Mesoporous Organosilica for Redox-Responsive Gene Delivery and Synergistic Cancer Chemotherapy. Adv. Mater. 28, 1963-1969. https://doi.org/10.1002/adma.201505524
Wu, M. X., Gao J., Wang F., Yang J., Song N., Jin X. Y., Mi P., Tian J., Luo J. Y., Liang F., Yang Y. W., 2018. Multistimuli Responsive Core-Shell Nanoplatform Constructed from Fe3O4@MOF Equipped with Pillar 6 arene Nanovalves. Small. 14, https://doi.org/10.1002/smll.201704440
Wu, M. X., Yan H. J., Gao J., Cheng Y., Yang J., Wu J. R., Gong B. J., Zhang H. Y., Yang Y. W., 2018. Multifunctional Supramolecular Materials Constructed from Polypyrrole@UiO-66 Nanohybrids and Pillararene Nanovalves for Targeted Chemophotothermal Therapy. ACS Appl. Mater. Inter. 10, 34655-34663. https://doi.org/10.1021/acsami.8b13758
Wu, M. X., Yang Y. W., 2017. Metal-Organic Framework (MOF)-Based Drug/Cargo Delivery and Cancer Therapy. Adv. Mater. 29, https://doi.org/10.1002/adma.201606134
Wu, Y. N., Zhou M., Li S., Li Z., Li J., Wu B., Li G., Li F., Guan X., 2014. Magnetic metal-organic frameworks: gamma-Fe2O3@MOFs via confined in situ pyrolysis method for drug delivery. Small. 10, 2927-2936. https://doi.org/10.1002/smll.201400362
Wu, Z., Tang L. J., Zhang X. B., Jiang J. H., Tan W., 2011. Aptamer-modified nanodrug delivery systems. ACS Nano. 5, 7696-7699. https://doi.org/10.1021/nn2037384
Xiang, Z., Cao D., Lan J., Wang W., Broom D. P., 2010. Multiscale simulation and modelling of adsorptive processes for energy gas storage and carbon dioxide capture in porous coordination frameworks. Energy Environ. Sci. 3, https://doi.org/10.1039/c0ee00049c
Xu, R., Yang J., Qian Y., Deng H., Wang Z., Ma S., Wei Y., Yang N., Shen Q., 2021. Ferroptosis/pyroptosis dual-inductive combinational anti-cancer therapy achieved by transferrin decorated nanoMOF. Nanoscale Horiz. 6, 348-356. https://doi.org/10.1039/d0nh00674b
Xu, X., Liu C., Wang Y., Koivisto O., Zhou J., Shu Y., Zhang H., 2021. Nanotechnology-based delivery of CRISPR/Cas9 for cancer treatment. Adv. Drug Del. Rev. 113891. https://doi.org/10.1016/j.addr.2021.113891
Yaghi, O. M., Li G. M., Li H. L., 1995. Selective binding and removal of guests in a microporous metal–organic framework. Nature. 378, 703-706. https://doi.org/10.1038/378703a0
Yan, J., Liu C., Wu Q., Zhou J., Xu X., Zhang L., Wang D., Yang F., Zhang H., 2020. Mineralization of pH-Sensitive Doxorubicin Prodrug in ZIF-8 to Enable Targeted Delivery to Solid Tumors. Anal. Chem. 92, 11453-11461. https://doi.org/10.1021/acs.analchem.0c02599
Yan, Q., Guo X. L., Huang X. L., Meng X., Liu F., Dai P. P., Wang Z., Zhao Y. J., 2019. Gated Mesoporous Silica Nanocarriers for Hypoxia-Responsive Cargo Release. ACS Appl. Mater. Inter. 11, 24377-24385. https://doi.org/10.1021/acsami.9b04142
Yan, Y., Telepeni I., Yang S., Lin X., Kockelmann W., Dailly A., Blake A. J., Lewis W., Walker G. S., Allan D. R., Barnett S. A., Champness N. R., Schroder M., 2010. Metal-organic polyhedral frameworks: high h(2) adsorption capacities and neutron powder diffraction studies. J. Am. Chem. Soc. 132, 4092-4094. https://doi.org/10.1021/ja1001407
Yang, L., Alexandridis P., 2000. Physicochemical aspects of drug

delivery and release from polymer-based colloids. Current Opinion in Colloid & Interface Science. 5, 132-143. https://doi.org/10.1016/s1359-0294(00)00046-7

Yang, P., Li D., Jin S., Ding J., Guo J., Shi W., Wang C., 2014. Stimuli-responsive biodegradable poly(methacrylic acid) based nanocapsules for ultrasound traced and triggered drug delivery system. Biomaterials. 35, 2079-2088. https://doi.org/10.1016/j.biomaterials.2013.11.057

Yang, Q., Wang S. H., Fan P. W., Wang L. F., Di Y., Lin K. F., Xiao F. S., 2005. pH-responsive carrier system based on carboxylic acid modified mesoporous silica and polyelectrolyte for drug delivery. Chem. Mater. 17, 5999-6003. https://doi.org/10.1021/cm051198v

Yang, X., He D. G., He X. X., Wang K. M., Zou Z., Li X. C., Shi H., Luo J. R., Yang X. X., 2015. Glutathione-Mediated Degradation of Surface-Capped MnO2 for Drug Release from Mesoporous Silica Nanoparticles to Cancer Cells. Part. Part. Syst. Char. 32, 205-212. https://doi.org/10.1002/ppsc.201400092

Yang, X., Li L., He D., Hai L., Tang J., Li H., He X., Wang K., 2017. A metal-organic framework based nanocomposite with co-encapsulation of Pd@Au nanoparticles and doxorubicin for pH- and NIR-triggered synergistic chemo-photothermal treatment of cancer cells. J. Mater. Chem. B. 5, 4648-4659. https://doi.org/10.1039/c7tb00715a

Yang, Y., Hu Q., Zhang Q., Jiang K., Lin W., Yang Y., Cui Y., Qian G., 2016. A Large Capacity Cationic Metal-Organic Framework Nanocarrier for Physiological pH Responsive Drug Delivery. Mol. Pharm. 13, 2782-2786. https://doi.org/10.1021/acs.molpharmaceut.6b00374

Yao, J. Z., Liu Y., Wang J. W., Jiang Q., She D. J., Guo H. S., Sun N. R., Pang Z. Q., Deng C. H., Yang W. L., Shen S., 2019. On-demand CO release for amplification of chemotherapy by MOF functionalized magnetic carbon nanoparticles with NIR irradiation. Biomaterials. 195, 51-62. https://doi.org/10.1016/j.biomaterials.2018.12.029

You, Y. Z., Kalebaila K. K., Brock S. L., Oupicky D., 2008. Temperature-controlled uptake and release in PNIPAM-modified porous silica nanoparticles. Chem. Mater. 20, 3354-3359. https://doi.org/10.1021/cm703363w

Zhang, A. T., Jung K., Li A. H., Liu J. Q., Boyer C., 2019. Recent advances in stimuli-responsive polymer systems for remotely controlled drug release. Prog. Polym. Sci. 99, https://doi.org/10.1016/j.progpolymsci.2019.101164

Zhang, J., Mou L., Jiang X., 2020. Surface chemistry of gold nanoparticles for health-related applications. Chem. Sci. 11, 923-936. https://doi.org/10.1039/c9sc06497d

Zhang, J., Wu D., Li M. F., Feng J., 2015. Multifunctional Mesoporous Silica Nanoparticles Based on Charge-Reversal Plug-Gate Nanovalves and Acid-Decomposable ZnO Quantum Dots for Intracellular Drug Delivery. ACS Appl. Mater. Inter. 7, 26666-26673. https://doi.org/10.1021/acsami.5b08460

Zhang, K., Meng X. D., Cao Y., Yang Z., Dong H. F., Zhang Y. D., Lu H. T., Shi Z. J., Zhang X. J., 2018. Metal-Organic Framework Nanoshuttle for Synergistic Photodynamic and Low-Temperature Photothermal Therapy. Adv. Funct. Mater. 28, https://doi.org/10.1002/adfm.201804634

Zhang, L., Gu F. X., Chan J. M., Wang A. Z., Langer R. S., Farokhzad O. C., 2008. Nanoparticles in medicine: therapeutic applications and developments. Clin. Pharmacol. Ther. 83, 761-769. https://doi.org/10.1038/sj.clpt.6100400

Zhang, S. Y., Shi W., Cheng P., Zaworotko M. J., 2015. A Mixed-Crystal Lanthanide Zeolite-like Metal-Organic Framework as a Fluorescent Indicator for Lysophosphatidic Acid, a Cancer Biomarker. J. Am. Chem. Soc. 137, 12203-12206. https://doi.org/10.1021/jacs.5b06929

Zhao, D., Yuan D., Sun D., Zhou H. C., 2009. Stabilization of metal-organic frameworks with high surface areas by the incorporation of mesocavities with

microwindows. J. Am. Chem. Soc. 131, 9186-9188. https://doi.org/10.1021/ja901109t

Zhao, J., Yang Y., Han X., Liang C., Liu J., Song X., Ge Z., Liu Z., 2017. Redox-Sensitive Nanoscale Coordination Polymers for Drug Delivery and Cancer Theranostics. ACS Appl. Mater. Inter. 9, 23555-23563. https://doi.org/10.1021/acsami.7b07535

Zhao, M., Li J., Ji H., Chen D., Hu H., 2019. A versatile endosome acidity-induced sheddable gene delivery system: increased tumor targeting and enhanced transfection efficiency. Int. J. Nanomed. 14, 6519-6538. https://doi.org/10.2147/IJN.S215250

Zheng, C., Wang Y., Phua S. Z. F., Lim W. Q., Zhao Y., 2017. ZnO-DOX@ZIF-8 Core-Shell Nanoparticles for pH-Responsive Drug Delivery. ACS Biomater. Sci. Eng. 3, 2223-2229. https://doi.org/10.1021/acsbiomaterials.7b00435

Zheng, H., Zhang Y., Liu L., Wan W., Guo P., Nystrom A. M., Zou X., 2016. One-pot Synthesis of Metal-Organic Frameworks with Encapsulated Target Molecules and Their Applications for Controlled Drug Delivery. J. Am. Chem. Soc. 138, 962-968. https://doi.org/10.1021/jacs.5b11720

Zheng, H., Zhang Y., Liu L., Wan W., Guo P., Nystrom A. M., Zou X., 2016. One-pot Synthesis of Metal-Organic Frameworks with Encapsulated Target Molecules and Their Applications for Controlled Drug Delivery. J. Am. Chem. Soc. 138, 962-968. https://doi.org/10.1021/jacs.5b11720

Zheng, M., Liu S., Guan X., Xie Z., 2015. One-Step Synthesis of Nanoscale Zeolitic Imidazolate Frameworks with High Curcumin Loading for Treatment of Cervical Cancer. ACS Appl. Mater. Inter. 7, 22181-22187. https://doi.org/10.1021/acsami.5b04315

Zhou, H. C., Long J. R., Yaghi O. M., 2012. Introduction to metal-organic frameworks. Chem. Rev. 112, 673-674. https://doi.org/10.1021/cr300014x

Zhou, M., Zhang R., Huang M., Lu W., Song S., Melancon M. P., Tian M., Liang D., Li C., 2010. A chelator-free multifunctional [64Cu]CuS nanoparticle platform for simultaneous micro-PET/CT imaging and photothermal ablation therapy. J. Am. Chem. Soc. 132, 15351-15358. https://doi.org/10.1021/ja106855m

Zhou, Q., Zhang L., Yang T. H., Wu H., 2018. Stimuli-responsive polymeric micelles for drug delivery and cancer therapy. Int. J. Nanomed. 13, 2921-2942. https://doi.org/10.2147/ijn.s158696

Zhu, C.-L., Song X.-Y., Zhou W.-H., Yang H.-H., Wen Y.-H., Wang X.-R., 2009. An efficient cell-targeting and intracellular controlled-release drug delivery system based on MSN-PEM-aptamer conjugates. J. Mater. Chem. 19, https://doi.org/10.1039/b907978e

Zhu, Y. D., Chen S. P., Zhao H., Yang Y., Chen X. Q., Sun J., Fan H. S., Zhang X. D., 2016. PPy@MIL-100 Nanoparticles as a pH- and Near-IR-Irradiation-Responsive Drug Carrier for Simultaneous Photothermal Therapy and Chemotherapy of Cancer Cells. ACS Appl. Mater. Inter. 8, 34209-34217. https://doi.org/10.1021/acsami.6b11378

ISBN 978-952-12-4145-1